

AWARD NUMBER: W81XWH-12-1-0571

TITLE: Environment-Mediated Drug Resistance in Neuroblastoma

PRINCIPAL INVESTIGATOR: Yves A. DeClerck, Hua Yu

CONTRACTING ORGANIZATION: Children's Hospital Los Angeles  
Los Angeles, CA 90027

REPORT DATE: December 2015

TYPE OF REPORT: Final

PREPARED FOR: U.S. Army Medical Research and Materiel Command  
Fort Detrick, Maryland 21702-5012

DISTRIBUTION STATEMENT: Approved for Public Release;  
Distribution Unlimited

The views, opinions and/or findings contained in this report are those of the author(s) and should not be construed as an official Department of the Army position, policy or decision unless so designated by other documentation.

<b>REPORT DOCUMENTATION PAGE</b>			<i>Form Approved</i> <i>OMB No. 0704-0188</i>		
Public reporting burden for this collection of information is estimated to average 1 hour per response, including the time for reviewing instructions, searching existing data sources, gathering and maintaining the data needed, and completing and reviewing this collection of information. Send comments regarding this burden estimate or any other aspect of this collection of information, including suggestions for reducing this burden to Department of Defense, Washington Headquarters Services, Directorate for Information Operations and Reports (0704-0188), 1215 Jefferson Davis Highway, Suite 1204, Arlington, VA 22202-4302. Respondents should be aware that notwithstanding any other provision of law, no person shall be subject to any penalty for failing to comply with a collection of information if it does not display a currently valid OMB control number. <b>PLEASE DO NOT RETURN YOUR FORM TO THE ABOVE ADDRESS.</b>					
<b>1. REPORT DATE</b> December 2015		<b>2. REPORT TYPE</b> Final		<b>3. DATES COVERED</b> 30 Sept 2012 – 29 Sept 2015	
<b>4. TITLE AND SUBTITLE</b> Environment-Mediated Drug Resistance in Neuroblastoma			<b>5a. CONTRACT NUMBER</b>		
			<b>5b. GRANT NUMBER</b> W81XWH-12-1-0571		
			<b>5c. PROGRAM ELEMENT NUMBER</b>		
<b>6. AUTHOR(S)</b> Yves A. DeClerck, Hua Yu  E-Mail: declerck@usc.edu			<b>5d. PROJECT NUMBER</b>		
			<b>5e. TASK NUMBER</b>		
			<b>5f. WORK UNIT NUMBER</b>		
<b>7. PERFORMING ORGANIZATION NAME(S) AND ADDRESS(ES)</b>  Children's Hospital Los Angeles 4650 Sunset Blvd. Los Angeles, CA 90027			<b>8. PERFORMING ORGANIZATION REPORT NUMBER</b>		
<b>9. SPONSORING / MONITORING AGENCY NAME(S) AND ADDRESS(ES)</b> U.S. Army Medical Research and Materiel Command Fort Detrick, Maryland 21702-5012			<b>10. SPONSOR/MONITOR'S ACRONYM(S)</b>		
			<b>11. SPONSOR/MONITOR'S REPORT NUMBER(S)</b>		
<b>12. DISTRIBUTION / AVAILABILITY STATEMENT</b> Approved for Public Release; Distribution Unlimited					
<b>13. SUPPLEMENTARY NOTES</b>					
<b>14. ABSTRACT</b> During the past three funding years, collaborative experiments have demonstrated that monocytes collaborate with MSC in inducing STAT3-dependent drug resistance in neuroblastoma (Task 1), that S1P/S1PR1 contributes to a sustainable STAT3 activation leading toward increased survival (Task 2), and that Jak2 deletion/inhibition prevents drug resistance (Task 3). Experiments aimed at examining the effect of small pathway inhibitors suggest that inhibition of Jak2, MEK and S1PR1 all contribute to prevent drug resistance, but that inhibition of multiple pathways may be required (Task 4). Experiments aimed at examining the role of IL-6 clearly demonstrate that although IL-6 is involved in STAT3-mediated drug resistance, it is not necessary as STAT3 is activated in IL-6 KO mice and tumors develop in IL-6 KO mice crossed with NB-Tag mice (Task 5). As a result Task 6, which focused on targeting IL-6, has been abandoned. We show <i>in vitro</i> and in neuroblastoma human xenograft models that treatment with FTY720, an antagonist of S1PR1, dramatically sensitizes drug-resistant neuroblastoma cells to etoposide, indicating that S1PR1 is a critical target for reducing both EMDR and acquired chemo-resistance (Task 7).					
<b>15. SUBJECT TERMS</b> Drug resistance, tumor microenvironment, neuroblastoma, JAK2, STAT3					
<b>16. SECURITY CLASSIFICATION OF:</b>			<b>17. LIMITATION OF ABSTRACT</b>	<b>18. NUMBER OF PAGES</b>	<b>19a. NAME OF RESPONSIBLE PERSON</b>
<b>a. REPORT</b> U	<b>b. ABSTRACT</b> U	<b>c. THIS PAGE</b> U			USAMRMC
			UU	70	<b>19b. TELEPHONE NUMBER</b> (include area code)

## Table of Contents

	<u>Page</u>
1. Introduction.....	2
2. Keywords.....	4
3. Accomplishments.....	4
4. Impact.....	12
5. Changes/Problems.....	13
6. Products.....	13
7. Participants & Other Collaborating Organizations.....	14
8. Special Reporting Requirements.....	14
9. Appendices.....	14

## 1. INTRODUCTION:

Neuroblastoma is the most common extracranial solid tumor of childhood. Approximately 45% of children with neuroblastoma have aggressive tumors, nearly all of which are metastatic when diagnosed. This group includes patients with metastatic disease who are diagnosed at any age with MYCN-A tumors and patients older than 18 months of age with MYCN-non amplified (NA) tumors. During the past 20 years, long-term survival has steadily improved to 40% with increasing intensity of non-specific cytotoxic induction and consolidation therapy, followed by 13-cis-retinoic acid and anti-GD2 antibody immunotherapy of residual disease. It has become increasingly clear that tumor cells that may not be able intrinsically to resist therapeutic insults can acquire these properties as the result of specific interactions with the microenvironment. Although initially transient and reversible, this type of therapeutic resistance promotes the selection of surviving cells that have acquired permanent resistance. In 2005, the DeClerck laboratory identified the production of IL-6 by bone marrow mesenchymal stem cells as a major mechanism promoting osteolytic bone metastasis in neuroblastoma. In 2009 the laboratory demonstrated that in addition to promoting bone metastasis, IL-6 also promotes neuroblastoma cell survival and resistance to cytotoxic drugs. In collaboration, Drs. Seeger, Asgharzadeh and DeClerck demonstrated that not only MSC but also monocytes are a source of IL-6 in the tumor microenvironment of primary neuroblastoma tumors. In collaboration with Dr. Yu, partnering PI on this application, the DeClerck laboratory obtained data demonstrating that STAT3 and S1PR1 play a pivotal role in IL-6-mediated drug resistance in neuroblastoma.

**2. KEYWORDS:** Neuroblastoma, Drug Resistance, Tumor Microenvironment, Signal Transduction and Activation of Transcription, Sphingosine-1 Phosphate

## 3. ACCOMPLISHMENTS:

### Major goals of the project

Task	Sp. Aim	Subtask	Performed by	Site
1. Cooperation between monocytes and tumor cells in IL-6/sIL-6R/STAT3-induced EMDR	1a	Drug sensitivity screen in co-cultures with monocytes	DeClerck/Seeger	CHLA
	1a	Effect of inhibitors of IL-6R/Jak2/STAT3 inhibitors	DeClerck/Seeger	CHLA
	1a	Analysis of survival and apoptotic proteins by Western blot, FACS	DeClerck/Seeger	CHLA
	1a	Co-cultures of fresh neuroblastoma cells-fresh bone marrow monocytes	Seeger	CHLA
2. Role of S1P on STAT3 activation and drug resistance	1b	Effect of IL-6, sIL-6R, and S1P on STAT3 activation, survival and drug resistance	Yu	COH
3. Determine the impact of S1PR1/JAK2/STAT3 signaling in monocytes to drug resistance	1c	Murine NBT2 neuroblastoma cells and human NB cells co-cultured with mouse and human monocytes in which S1PR1 is KO or KD	Yu/DeClerck	COH/CHLA
4. Determine whether S1PR1 and JKA2 are effective targets to block tumor cell-monocyte crosstalk	1d	Co-cultures of NB cells and monocytes in the presence of inhibitors of IL-6, JAK2 and S1PR1 and tested for drug resistance	Yu/DeClerck	COH/CHLA
5. Effect of IL-6 in tumor and host cells on response to chemotherapy	2a	Breeding to obtain double transgenic homozygous IL-6 null	Asgharzadeh	CHLA
	2a	Imaging and monitoring for tumor development and tumor analysis by histology and TLDA microarrays	Asgharzadeh	CHLA
	2a	Treating NB-Tag mice and NB-Tag/IL-6 KO with cyclophosphamide and topotecan.	Asgharzadeh	CHLA

6. Contribution of bone marrow-derived IL-6 to response to therapy	2b	Transplantation of NB-Tag IL-6 $-/-$ mice with WT bone marrow	Yu/Asgharzadeh	COH/CHLA
	2b	Transplantation into NB-Tag mice, treatment with Poly I:C and monitoring of tumor development	Yu/Asgharzadeh	COH/CHLA
	2b	Effect on drug response: mice will be treated with cyclophosphamide/topotecan and monitored for response	Yu/Asgharzadeh	COH/CHLA
7. Develop strategies that can be translated into clinical trials to overcome EMDR	3a	Testing tocilizumab in SCID mice implanted with human NB cells and monocytes	DeClerck/Seeger	CHLA
	3a	Testing AZD 1480 in SCID mice implanted with human NB cells and monocytes	DeClerck/Seeger/Yu	CHLA/COH

## ACCOMPLISHMENTS UNDER THESE GOALS:

**Task 1. Cooperation between monocytes and tumor cells in IL-6/sIL-6R/STAT3-induced EMDR:** This task was completed last year and the manuscript published in *Cancer Research* in 2013 (Ara *et al.* 2013, in appendix).

**Task 2. Role of S1P on STAT3 activation and drug resistance:** This task has been performed by our collaborator at City of Hope, Dr. Hua Yu. She has shown the importance of S1PR1-STAT3 in EMDR in neuroblastoma. In a published manuscript (Yang *et al.*, *Cancer Biology & Therapy* 2012), she demonstrated that sorafenib inhibits endogenous and IL-6/S1P-induced JAK2-STAT3 signaling in human neuroblastoma, associated with growth suppression and apoptosis. In order to understand the mechanism of drug resistance and to develop targeted strategies for combating drug resistance, she has generated etoposide-resistant human neuroblastoma cells and demonstrated that etoposide-resistant human cells have highly elevated S1PR1 expression and STAT3 activity. In 2013, she showed that endogenous and IL-6/S1P induced JAK2-STAT3 signaling in human neuroblastoma is associated with growth suppression and apoptosis (Yang, Yu and Jove *et al.* 2012). In order to understand the mechanism of drug resistance and to develop targeted strategies for combating drug resistance, we have generated etoposide-resistant human neuroblastoma cells. We demonstrated that etoposide-resistant human cells have highly elevated S1PR1 expression and STAT3 activity (Fig. 1).

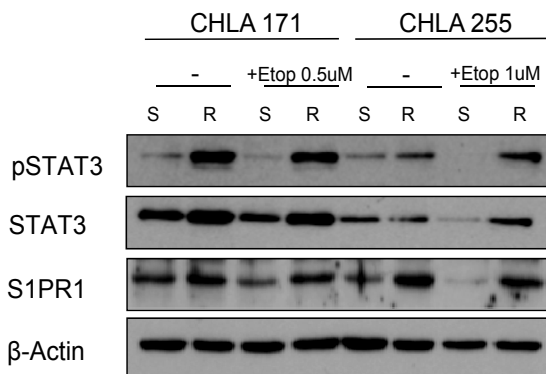


**Figure 1. Elevated S1PR1 expression and STAT3 activation in etoposide-resistant human neuroblastoma cells.** For selection of drug-resistant cell sublines, human neuroblastoma cells (CHLA-171 and CHLA-255) were continuously exposed to increasing concentrations of etoposide for at least 2 months. Representative Western blot of sensitive (S) and resistant (R) cells treated with etoposide for 48 h at indicated concentration.

They also showed that blocking S1PR1/JAK2/STAT3 pathway by downregulation of S1PR1 expression decreases STAT3 activity and causes apoptosis in neuroblastoma cells *in vitro* (Fig. 2).

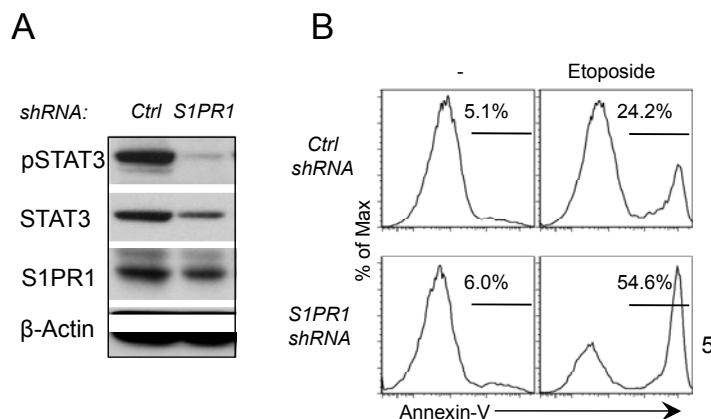


**Figure 2. Specific targeting of S1PR1 gene expression decreases STAT3-mediated survival of neuroblastoma cells.** CHLA-255 cells were transfected with both control and S1PR1 shRNA expressing lentiviruses. (A) Western blot analysis of protein expression levels of pSTAT3, STAT3 and S1PR1 in control and S1PR1 shRNA knockdown cells. (B) 24 h following etoposide treatment (2

$\mu\text{M}$ ) the cells were examined for apoptosis by Annexin V staining.

In 2014 and 2015, to further confirm the importance of S1PR1 in drug resistance, Dr. Yu's laboratory transduced CHLA-255 and CHLA-171 NB cell lines with MSCV-S1pr1-expressing lentiviruses. Overexpression of S1pr1 led to increased levels of pSTAT3 in both cell lines as detected by Western blotting (Fig. 3A). Furthermore, overexpression of S1pr1 caused resistance to etoposide in both CHLA-255 and CHLA-171 NB cells (Fig. 3B, C; Fig. 4A, B). Cross-resistance of S1pr1 transfectants to another common anticancer drug such as topotecan (topoisomerase I inhibitor) was also observed (Fig. 2B, C). Furthermore, S1pr1 overexpression reduced etoposide treatment-associated expression of the apoptosis markers, cleaved caspase-3 and cleaved PARP-1 (Fig. 3D, Fig. 4C).

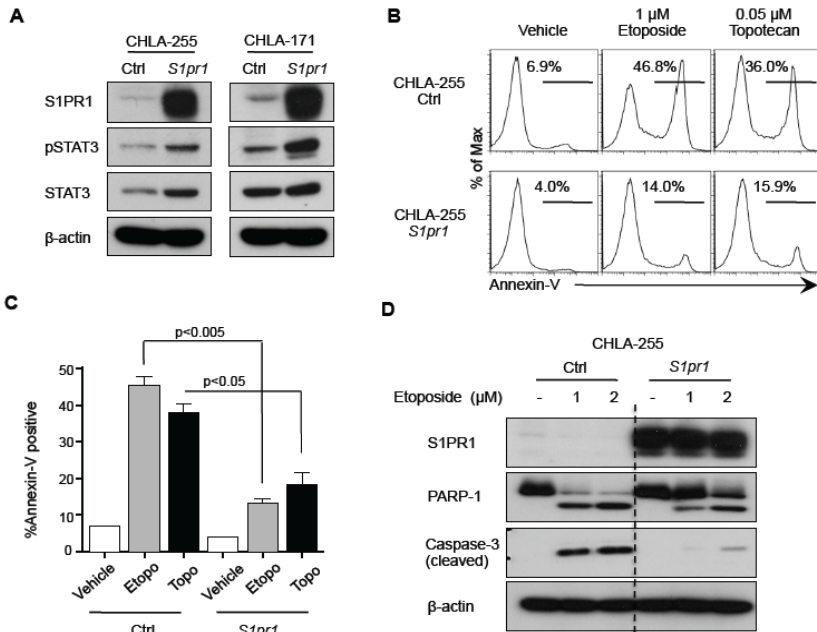


**Figure 3. S1PR1 promotes STAT3 activation and chemoresistance in NB cells.** (A) Western blot shows S1PR1, pSTAT3 and STAT3 expression levels in control and MSCV-S1pr1-overexpressing CHLA-255 and CHLA-171 cells. (B) Flow cytometry analysis of control and S1pr1 overexpressing CHLA-255 cells treated with 1  $\mu\text{M}$  etoposide or 0.05  $\mu\text{M}$  topotecan for 24 h and then stained with Annexin V and PI. (C) Bar chart showing percentages of apoptotic cells in control and S1pr1 overexpressing cells after adding the indicated drugs. Data were mean  $\pm$  SEM of 3 independent experiments. (D) Western blot analysis of full and cleaved PARP-1 and cleaved caspase-3 in control and S1pr1 overexpressing CHLA-255 cells following exposure to the indicated concentrations of etoposide for 24 h.

Our previous work showed that JAK2 is critical for S1PR1-induced STAT3 activation and tumor survival (Lee, Deng *et al.* 2010). We next tested the effects of the JAK inhibitor, AZD1480, on S1PR1-mediated NB-drug resistance, and found that JAK signaling blockade abrogated S1pr1-mediated protection of NB cells against etoposide-induced apoptosis (Fig. 4D). Collectively these data thus far demonstrate a clear role for S1PR1 in regulating EMDR, and show that JAK/STAT3 signaling is an important driver of S1PR1-induced EMDR in NB cells.

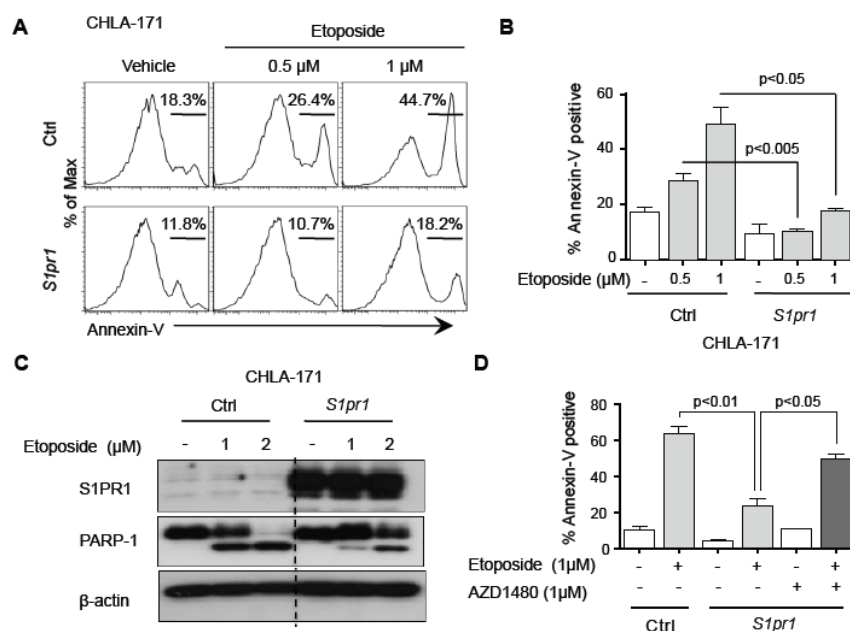


**Figure 4. Overexpression of S1PR1 in CHLA-171 cells activates STAT3 and renders cells resistant to etoposide via JAK2/STAT3 signaling.** (A) Flow cytometry analysis of control and S1pr1 overexpressing CHLA-171 cells treated with 0.5  $\mu\text{M}$  or 1  $\mu\text{M}$  etoposide for 24 h and then stained with Annexin V and PI. (B) Bar chart showing increased proportion of apoptotic cells after etoposide administration in control cells as compared to S1pr1 overexpressing cells. Data were mean  $\pm$  SEM of 3 independent experiments. (C) Western blot analysis of full and cleaved PARP-1 in control and S1pr1 overexpressing cells following exposure to the indicated concentrations of etoposide for 24 h. (D) Quantification of Annexin-V/PI staining analyzed by flow cytometry of control and S1pr1 overexpressing CHLA-171 cells pretreated with 1  $\mu\text{M}$  AZD1480 for 2 h, followed treatment with 1  $\mu\text{M}$  etoposide for

24 h. Shown are the mean  $\pm$  SEM of three independent experiments, each performed in duplicate.

A manuscript (Lifshitz, Priceman and Li *et al.*, *S1PR1-STAT3 signaling is critical for neuroblastoma chemoresistance*) has been reviewed and now is under revision.

**Task 3. Determine the impact of S1PR1/JAK2/STAT3 signaling in monocytes/MSC to drug resistance:**

In 2014 we generated three strains of mice homozygous floxed for the gene of interest (S1PR1, JAK2 or STAT3), and hemizygous for Rosa26-CreERT2 (Cre recombinase-estrogen receptor T2). We have begun to test the impact of S1PR1/JAK2/STAT3 signaling in myeloid lineage to drug resistance using co-culture of murine NBT2 neuroblastoma cells and murine S1PR1 and JAK2 knockout bone marrow-derived monocytes. Preliminary data indicates that co-culture of NBT2 cells with JAK2 deficient BM-derived myeloid cells potentiates the cytotoxicity of etoposide and decreases levels of pSTAT3 and S1PR1 expression in tumor cells (Fig. 5A, B). Besides monocytes, mesenchymal stem cells (MSC) are a critical cellular component in the tumor microenvironment involved in tumor progression and drug resistance. Thus in 2015 we further tested if S1PR1 also regulates interaction between tumor cells and MSC to promote EMDR. We found that human bone marrow-mesenchymal stromal cells induce expression of sphingosine-1-phosphate receptor-1 (S1PR1) in neuroblastoma cells leading to their resistance to chemotherapy (Fig. 5C, D).

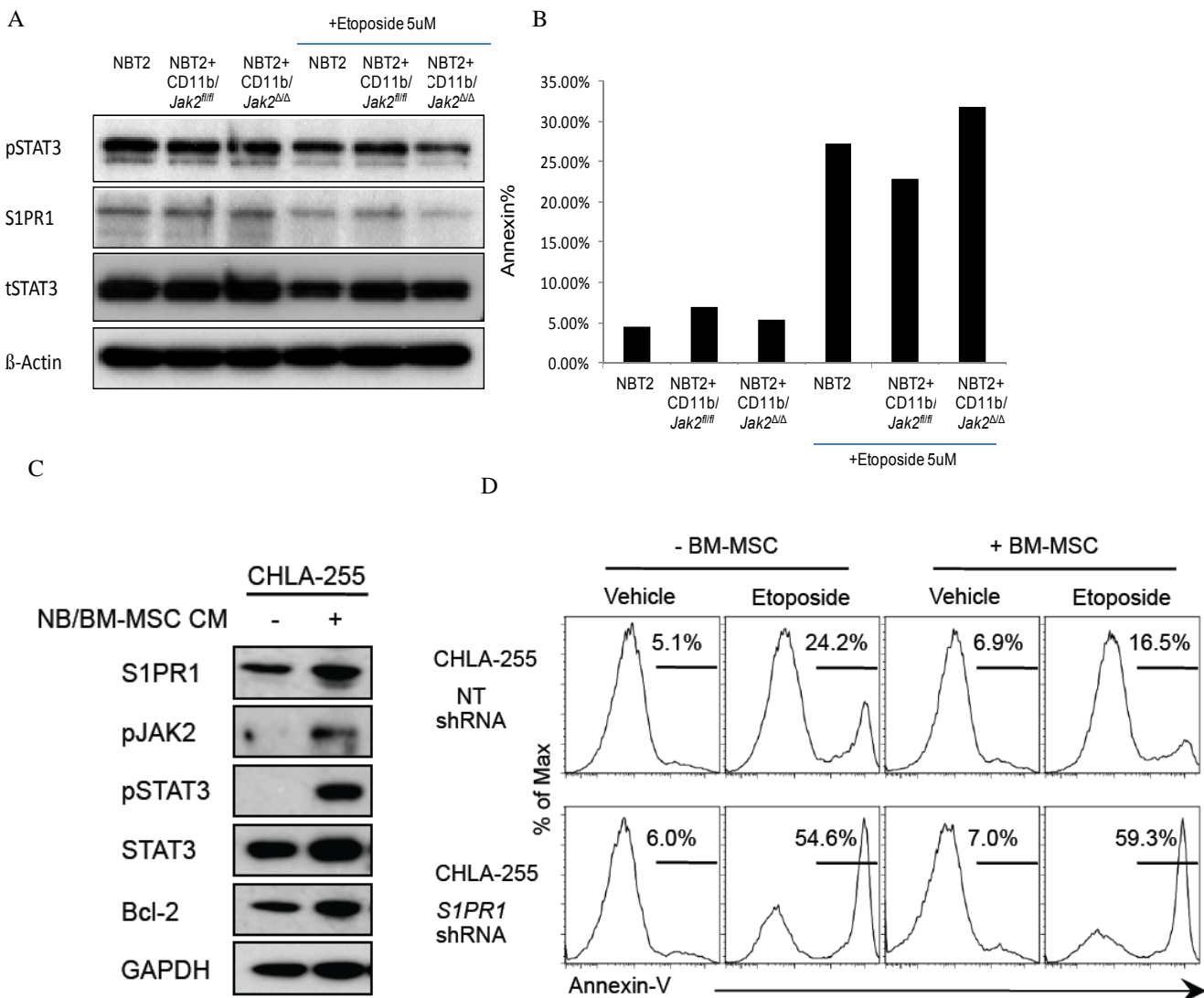


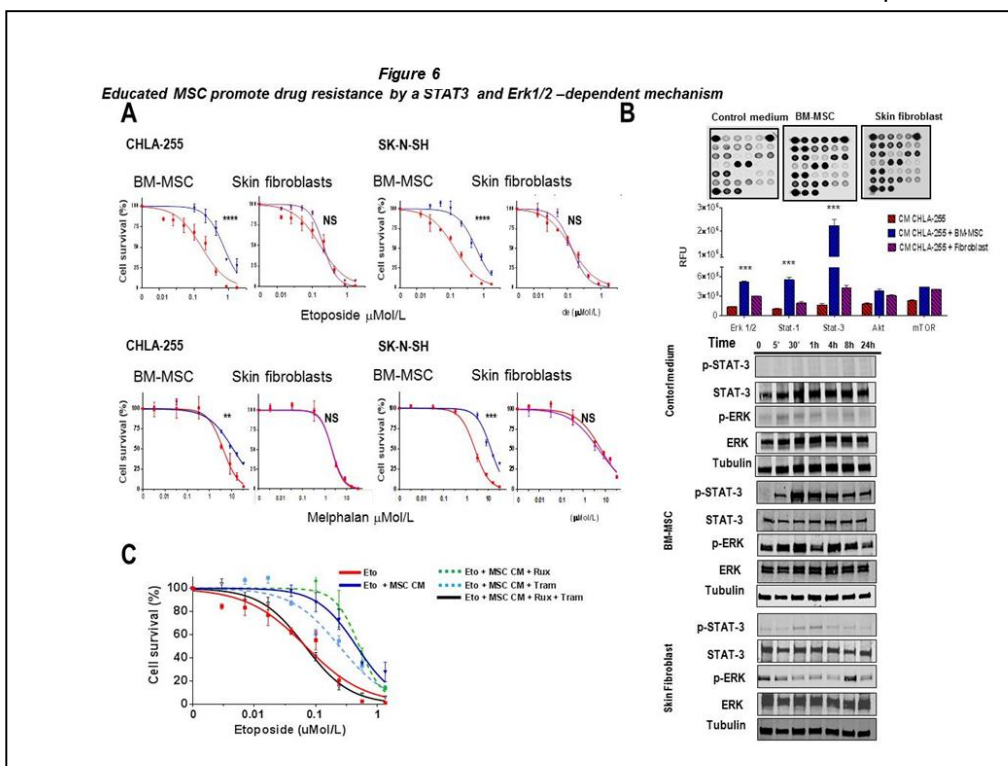
**Figure 5. Deletion of JAK2 in BM-derived myeloid cells decreases STAT3-mediated survival of neuroblastoma cells.** (A) Representative western blot of pSTAT3 and S1PR1 as detected in NBT2 cells co-cultured with BM-derived myeloid cells derived from *Jak2<sup>fl/fl</sup>* or *JAK2<sup>fl/fl</sup>CreERT2* mice. (B) The co-cultures were treated with etoposide (5  $\mu$ M) for 24 h. Apoptosis was determined by Annexin V staining and FACS analysis. (C) Western blotting showing increased expression of S1PR1, pJAK2, pSTAT3, STAT3 and Bcl-2 in CHLA-255 cells upregulated by conditioned medium prepared from BM-MSC cells of NB patients (NB/BM-MSC CM). GAPDH served as a

loading control. (D) Representative flow cytometry profiles of Annexin V-labeled CHLA-255 cells expressing NT or S1PR1 shRNA co-cultured with BM-MSC followed by exposure to 1  $\mu$ M etoposide.

**Task 4. Determine whether S1PR1 and JAK2 are effective targets to block tumor cell-monocyte crosstalk.** In 2014 we began to test the effect of STAT3 blocking on drug resistance induced in co-cultures of human tumor cells and mesenchymal stromal cells. We have used a combination of inhibitors of Jak2 and ERK1/2 as we found activation of both pathways when neuroblastoma cells were exposed to the conditioned medium of co-cultures of human MSC and NB cells. We tested ruxolitinib (a Jak2 inhibitor) and trametinib (an MEK inhibitor). In these experiments NB cells were cultured either in the presence of their own medium or in the presence of conditioned medium obtained from 48 h of co-cultures of NB and MSC (or skin fibroblasts as control). The data demonstrated that MSC increase the resistance of NB cells to chemotherapeutic agents like etoposide or melphalan (Fig. 6A) and stimulate in NB cells the activation of not only STAT3 as previously reported {Ara, 2013 #6449} but also ERK1/2 (Fig. 6B). We then tested the effect of ruxolitinib (a Jak2 inhibitor as Jak2 activation is upstream of STAT3 activation), and trametinib (GSK 2118436), a selective MEK inhibitor, for their effect on drug sensitivity. This experiment (Fig. 6C) indicated that the addition of ruxolitinib or trametinib alone had no inhibitory effect on the activity of the CM of educated MSC in increasing resistance to etoposide as the right shift of the dose-response curve for etoposide was maintained whereas the curve shifted back to the left when trametinib and ruxolitinib were both added at 1  $\mu$ M, a concentration where they had little

or no toxicity on their own (not shown). The data thus indicate that both STAT3 and ERK1/2 contribute to EMDR induced by MSC drug resistance.

**Figure 6. A combination of Jak2/STAT3 and MEK/ERK1/2 inhibition restores the sensitivity of NB cells to etoposide in the presence of MSC CM.** (A) CHLA-255 and SK-N-SH NB-cells cultured in the presence of CM from their own medium (reconstituted 50/50 with fresh medium; Red line) or medium from educated MSC or skin fibroblasts (Blue line), were treated with etoposide or melphalan at the indicated concentrations. After 48 h, cells were examined for viability by CellTiter-Glo bioluminescence. The data represent the mean ( $\pm$ SD)



percentage of luminescence from control in two experiments conducted in triplicate. (B) CHLA-255 cells were cultured in conditions described in (A) but after 1 h cells were lysed and examined for the presence of phosphorylated proteins by phosphor dot-blot (Top) or Western blot analysis (Bottom). (C) CHLA-255 were cultured in the presence of CM from educated MSC (blue line) or their own medium (red line) and treated with indicated concentrations of ruxolitinib (dotted green) or trametinib (dotted blue) or the combination (solid black) before being exposed to etoposide. Cells were examined after 48 h for viability by CellTiter-Glo (Promega). The data represent the mean percent luciferase activity from control of triplicate samples.

*In vitro* data showed anti-tumor therapeutic effect in NBT2 cells treated with S1PR1 and JAK2 inhibitors (FTY720 and AZD1480, respectively) (Fig. 7).

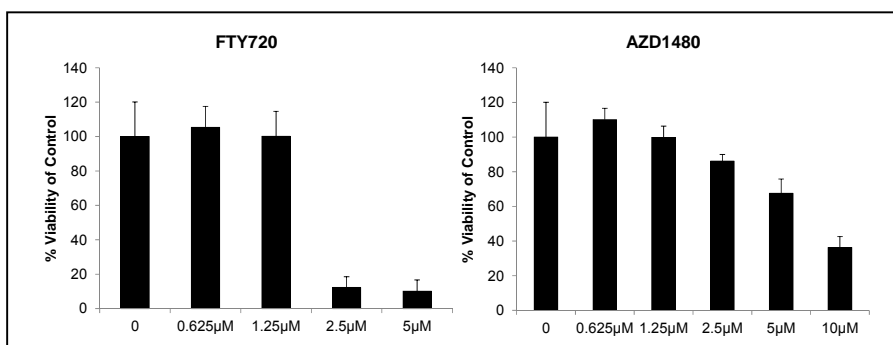


**Figure 7. Effects of specific inhibition of S1PR1 and JAK2 in NBT2 cell line.** Cell viability was assayed with an MTS

assay (Promega) 24 h post treatment with the indicated concentrations of FTY 720 and AZD1480.

In 2015, we further tested the anti-tumor therapeutic effect in chemotherapy sensitive or resistant human neuroblastoma cells treated with S1PR1 and JAK2 inhibitors (FTY720 and AZD1480, respectively) with or without chemotherapy drug (Fig. 8).

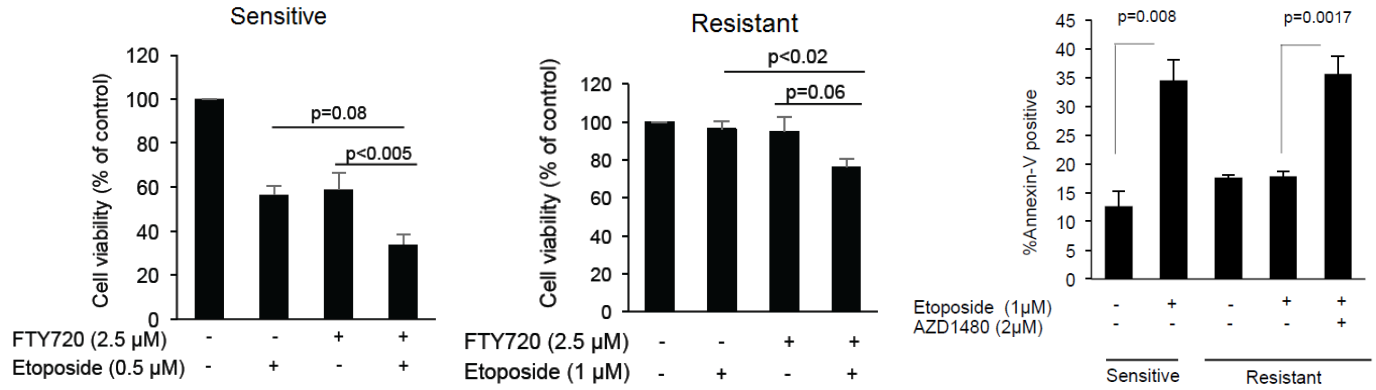
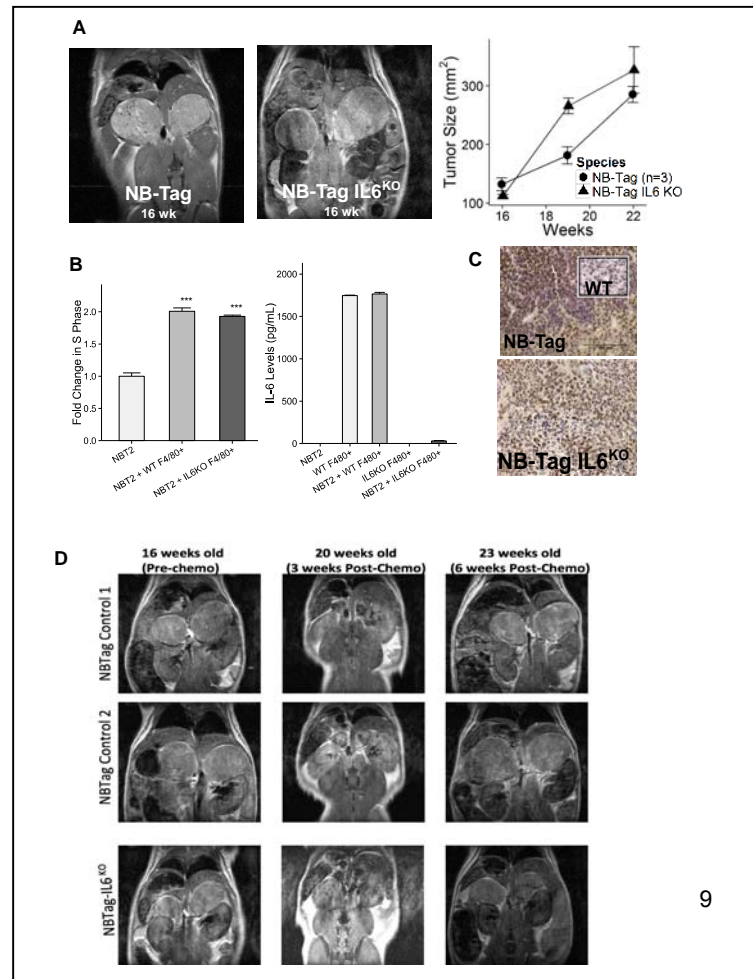


**Figure 8. Effects of combined administration of chemotherapeutic agent with specific inhibition of S1PR1 or JAK2 in NBT2 cell line.** Cell viability was assayed with flow cytometry 24 h post treatment with the indicated concentrations of FTY 720 and AZD1480 with or without chemotherapy drug.

**Task 5. Effect of IL-6 in tumor and host cells on response to chemotherapy:** Our collaborator, Dr. Asgharzadeh, has generated NB-Tag mice in an IL-6 KO background. He found that NB tumors in these mice develop at the anticipated rate seen in WT NB-Tag mice, indicating that lack of IL-6 does not affect tumor initiation and growth (Fig. 9A). While IL-6 production in these tumors has been demonstrated to occur during tumor growth and produced by macrophages, the growth promoting effects of these macrophages are evident even in the absence of IL-6 (Fig. 9B). Interestingly, an analysis of these tumors for pSTAT3 by Western blot and immunohistochemistry revealed the presence of pSTAT3, suggesting the presence of alternate pathways of activation.



The loss of IL-6 also does not alter the response of tumors to treatment with chemotherapy regimen (5 days of cyclophosphamide and topotecan), and time to regrowth is similar in both WT and IL-6 KO animals (Fig. 9D). A manuscript (in appendix) on this work has been submitted for publication to Cancer Discovery in March 2016 (Michael D. Hadjidaniel, Sakunthala Muthugounder, Long Hung, Soheila Shirinbak, Randall Chan, Rie Nakata, Lucia Borriello, Rebekah J. Kennedy, Michael Sheard, Hiroshi Iwakura, Takashi Akamizu, Hiroyuki Shimada, Richard Sposto, Yves A. DeClerck, Shahab Asgharzadeh. Tumor-associated macrophages activate STAT3 and MYC in neuroblastomas independently of IL6).

**Figure 9: Effect of IL-6 knockout crossing with NB-Tag mice.** (A) MRI of abdominal cavity of representative mice from NB-Tag and NB-TagxIL-6<sup>KO</sup> at 16 weeks of age, and growth rate of the two models over time (n=3-4 mice per group) (B) Proliferation index as measure by BrdU incorporation shows no difference between tumors co-cultured with WT or IL-6<sup>KO</sup> macrophages. The co-culture experiments also demonstrated a lack of IL-6

production in co-cultures between NB-Tag cell line and IL-6<sup>KO</sup> macrophages. (C) Immunohistochemical analysis of adrenal gland reveals no pSTAT3 expression while both NB-Tag and NB-TagxIL-6<sup>KO</sup> express pSTAT3 suggesting alternative pathways of activation independent of IL-6 production. (D) Representative MRI images of NB-Tag and NB-Tag/IL-6<sup>KO</sup> pre-chemotherapy, post 3 and 6 weeks of chemotherapy.

**Task 6. Contribution of bone marrow-derived IL-6 to response to therapy:** Based on findings from Task 5, it would be illogical to perform wild-type bone marrow transplantation into NB-Tag/IL-6 KO mice, as we have demonstrated a growth pattern similar to WT NB-Tag mice. However, our data also provided insight into the possibility that multiple pathways may converge to phosphorylate STAT3, and removal of IL-6 alone may be insufficient to overcome EMDR. Future experiments for this task will assess the significance of STAT3 in this model following similar strategies outlined in Task 5 and 6.

**Task 7. Develop strategies that can be translated into clinical trials to overcome EMDR:** In 2013, we tested the effect of tocilizumab in mice implanted with human NB tumor cells and human monocytes. These experiments were not conclusive and although they initially showed some effects, repeated experiments failed to show a statistically significant effect. This approach was abandoned. Then in 2014, *in vitro* data showed anti-tumor therapeutic effect in CHLA-255 cells induced by S1PR1 inhibitor (FTY720) alone or in combination with etoposide (Fig. 9A). We tested this approach *in vivo* and preliminary data showed significant decrease in tumor weight in NSG mice injected with CHLA-255 Fluc cells following FTY720 treatment (Fig. 9B).

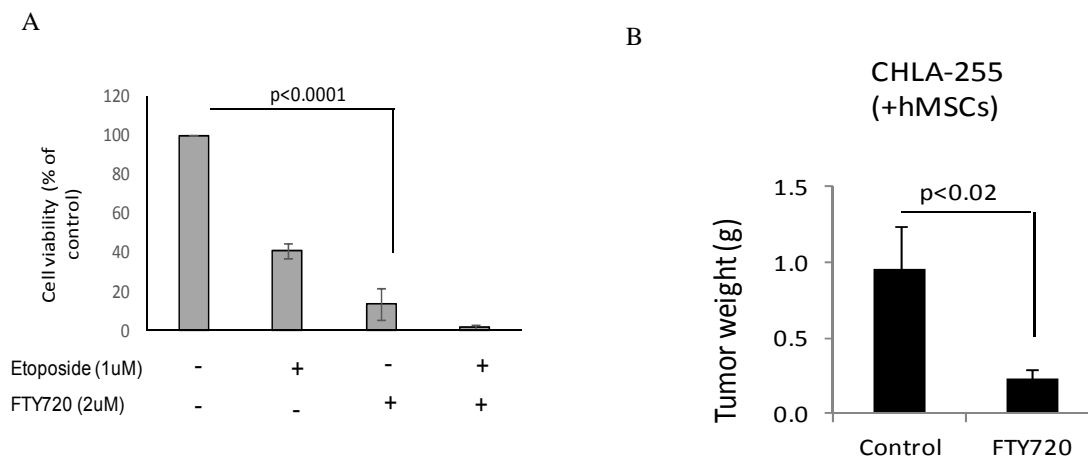


**Figure 10. Effect of S1PR1 antagonist FTY720 on human neuroblastoma cells. (A)** CHLA-255 neuroblastoma cell line was pretreated with FTY720 (2  $\mu$ M) following etoposide (1  $\mu$ M) treatment for 24 h. Cell viability was determined using MTS assays. Shown are the mean of three independent experiments, each performed in triplicates. **(B)** NSG mice were injected subcutaneously with CHLA-255 cells and hBM-MSC (100:1). A week after implantation, mice were treated with 5 mg/kg FTY720 or vehicle control by intraperitoneal injection daily. After 12 days tumors were excised, measured and weighed. Data are mean  $\pm$  SEM.

In 2015, we further examined the effects of FTY720 on NB etoposide resistance in a human NB xenograft model in NSG mice by co-injecting human NB/BM-MSC and CHLA-255 NB cells. Both FTY720 and etoposide inhibited tumor growth, but a combination of the two compounds inhibited tumor growth more significantly than each compound alone (Fig. 10A). Furthermore, the combinatorial treatment resulted in a significant increase in apoptotic cells within the tumor as shown by the increased presence of cells staining positive for cleaved caspase-3 (Fig. 10B). Finally, we evaluated whether FTY720 could sensitize drug-resistant NB cells to etoposide in a human NB xenograft model. This experiment demonstrated that although etoposide and FTY720 monotherapy failed to effectively control the growth of drug-resistant NB tumors, a significant growth inhibition was observed when FTY720 was added to etoposide treatment (Fig. 10C). Consistently, the combination of FTY720 and etoposide caused an increased apoptotic response, as shown by an increase in cells positive for cleaved caspase-3 in tumors (Fig. 10D).

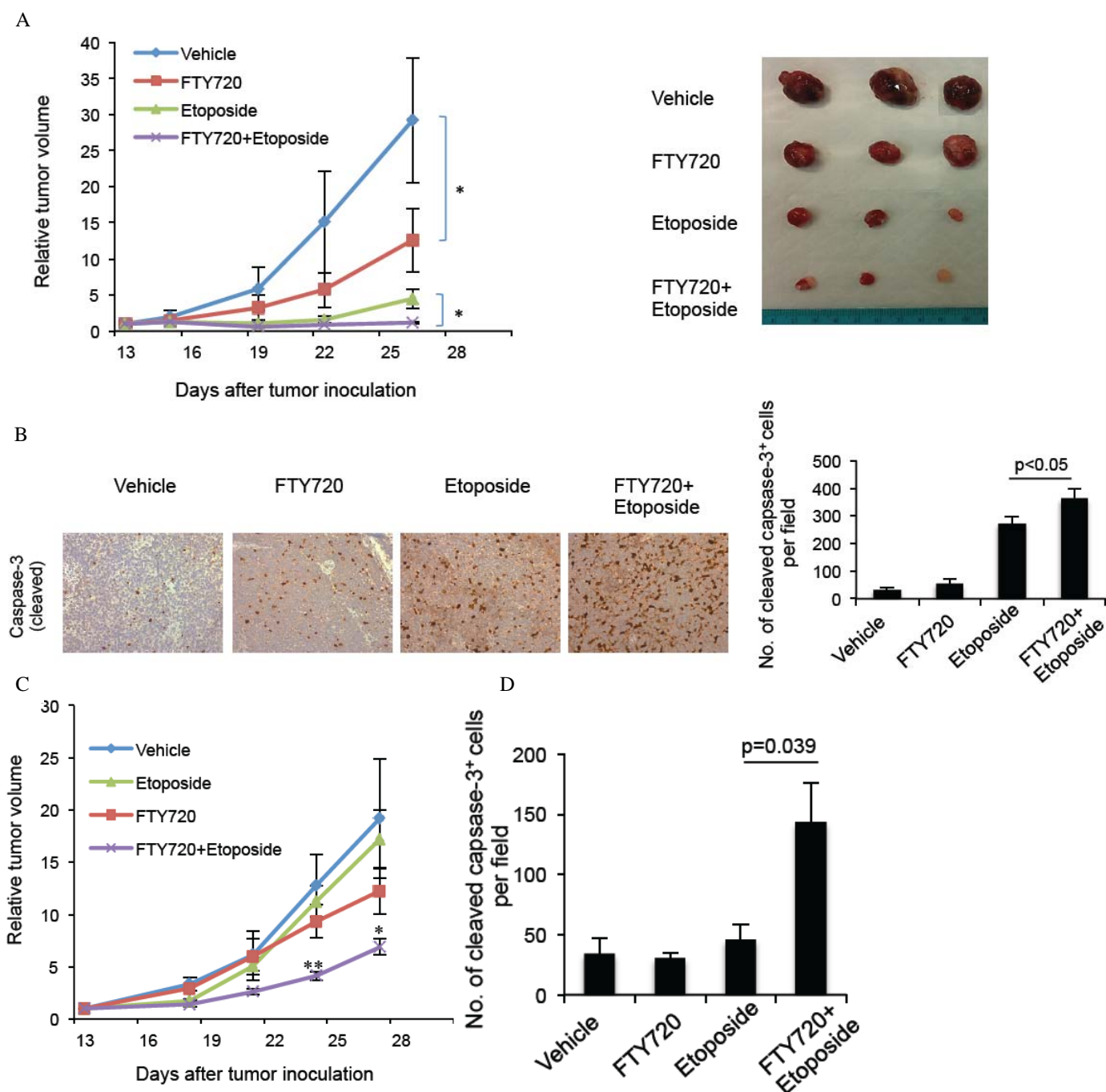


**Figure 11. Effect of S1PR1 antagonist FTY720 on human neuroblastoma cells.** (A) Growth of NB xenografts in mice treated with vehicle, FTY720, etoposide or FTY720 plus etoposide. Mean relative tumor volume (RTV) with SEM is shown as a function of time ( $n=5-7$ ,  $*p<0.05$ ). Right panel, tumors from Fig. 3A excised at the conclusion of the study (day 26) and photographed. (B) Representative immunohistochemistry images for cleaved caspase 3 staining in tumor tissue sections (original magnification,  $\times 20$ ). Right panel, quantification of IHC staining-positive cells in tumor tissues. The data were analyzed by ImageJ software. (C) Growth of etoposide resistant NB xenografts in mice treated with vehicle, FTY720, etoposide or FTY720 plus etoposide. Mean relative tumor volume with SEM is shown as a function of time. ( $n=5-7$ ,  $**p<0.01$  and  $*p<0.05$  versus FTY720-treated mice). (D) Quantification of IHC staining-positive cells in tumor tissues. The data were analyzed by ImageJ software.

We have also initiated a series of experiments testing the therapeutic impact of targeting S1PR1 to overcome EMDR in mouse models of neuroblastoma (NB-Tag mice). Donor BMC from CreERT2/S1PR1<sup>-/-</sup> and appropriate littermate controls were harvested from femurs and tibias, and injected intravenously in lethally irradiated NB-Tag recipient mice. The preliminary data showed no significant difference in tumor size (after 5 weeks) in both of the groups. We are planning to repeat this experiment in combination with chemotherapeutic agents. In another set of experiments we will overexpress S1PR1 in NBT2 cells and inject them into

CreERT2/S1PR1<sup>-/-</sup> mice (our preliminary data showed that NBT2 cells either failed to engraft or regressed in CreERT2/S1PR1<sup>-/-</sup> mice).

#### **TRAINING OPPORTUNITIES:**

The project has provided training opportunities for several post-doctoral trainees who worked on the project, were associated with publications (names underlined in publication list) and who participated in regular meetings held by the investigators. Dr. S. Priceman is now an assistant research professor at City of Hope.

#### **CONCLUSIONS:**

Over the last year we have generated data that brought additional light to the mechanisms by which the TME protects tumor cells from drug-induced apoptosis. In particular we show:

1. That MSC and monocytes collaborate in part by activating STAT3 and ERK1/2 in tumor cells and promote survival and drug resistance.
2. STAT3 activation—although downstream of IL-6—is activated by other pathways including S1PR1 mediated signaling.
3. Inhibitors of S1PR1 such as FTY720 prevent EMDR *in vitro* and have anti-tumor activity *in vivo*. More importantly, S1PR1 inhibitor could disrupt EMDR and thus sensitize tumor cells to chemotherapy *in vivo*.

#### **REFERENCES:**

Lee, H., J. Deng, M. Kujawski, C. Yang, Y. Liu, A. Herrmann, M. Kortylewski, D. Horne, G. Somlo, S. Forman, R. Jove and H. Yu (2010). "STAT3-induced S1PR1 expression is crucial for persistent STAT3 activation in tumors." Nat Med **16**(12):1421-1428.

Yang, F., V. Jove, R. Buettner, H. Xin, J. Wu, Y. Wang, S. Nam, Y. Xu, T. Ara, Y. A. DeClerck, R. Seeger, H. Yu and R. Jove (2012). "Sorafenib inhibits endogenous and IL-6/S1P induced JAK2-STAT3 signaling in human neuroblastoma, associated with growth suppression and apoptosis." Cancer Biol Ther **13**(7): 534-541.

#### **DISSEMINATION OF RESULTS TO THE COMMUNITY:**

See publications in

**FUTURE PLANS:** Nothing to report (final report)

We have obtained a no cost extension of our grant till September 29, 2016 in order to complete some of the experiments needed for the completion of manuscripts listed above.

#### **4. IMPACT:**

**4.1 Impact on neuroblastoma:** The early work led to a phase I clinical trial of sorafenib in combination with cyclophosphamide and topotecan in children with recurrent neuroblastoma by the New Advance in Neuroblastoma Therapy Consortium (NANT N2013-02 A Phase I Study of Sorafenib and Cyclophosphamide/Topotecan in Patients With Relapsed and Refractory Neuroblastoma NCT02298348) that opened for patient recruitment in 2015. The more recent results will lead to a proposal to combine a STS3 inhibitor (ruxolitinib) and a S1PR1 inhibitor in combination with chemotherapy pending of preclinical data in mice models.

**4.2 Impact on other disciplines:** Nothing to report

**4.3 Impact on technology transfer:** Nothing to report

**4.4 Impact on society beyond science and technology:** See 4.1

#### **5. CHANGES/PROBLEMS**

**5.1 Change to approach:** As described, Task 6 was not continued as the data indicated that in IL-6 KO mice, STAT3 was still activated.

**5.2 Impact on expenditures:** Nothing to report

**5.3 Changes in use of human subjects, animals, biohazards ... :** Nothing to report

#### **6. PRODUCTS**

## 6.1 Publications, review papers and presentations

### 6.1.1 Manuscript published:

Ara, T., Nakata, R, Shimada, H, Buettner, R., Groshen, SG, Ji, L, Sheard, M, Yu, H, Jove, R, Seeger, RC and DeClerck, YA. Critical role of STAT3 in interleukin-6-mediated drug resistance in human neuroblastoma. *Cancer Res*, 73:3852-3864, 2013.

### 6.1.2 Manuscripts under revision or submitted:

Veronica Lifshitz, Saul J. Priceman, Wenzhao Li, Gregory Cherryholmes, Heehyoung Lee, Adar Makovski-Silverstein, Yves A. DeClerck, Hua Yu. S1PR1-STAT3 signaling is critical for neuroblastoma chemo-resistance.

Michael D. Hadjidaniel, Sakunthala Muthugounder, Long Hung, Soheila Shirinbak, Randall Chan, Rie Nakata, Lucia Borriello, Rebekah J. Kennedy, Michael Sheard, Hiroshi Iwakura, Takashi Akamizu, Hiroyuki Shimada, Richard Sposto, Yves A. DeClerck, Shahab Asgharzadeh. Tumor-associated macrophages activate STAT3 and MYC in neuroblastomas independently of IL6.

### 6.1.3 Manuscript in preparation:

Lucia Borriello, Rie Nakata, G. Esteban Fernandez, Hiroyuki Shimada, Shahab Asgharzadeh, Vasu Punj, Richard Sposto, Laurence Blavier, Robert C. Seeger, Yves A. DeClerck. Mesenchymal stromal cells promote a pro-tumorigenic environment in primary neuroblastoma via STAT3 and ERK1/2 signaling pathways.

### 6.1.4 Review article:

Lucia Borriello, Robert C. Seeger, Shahab Asgharzadeh, Yves A. DeClerck. More than the genes, the tumor microenvironment in neuroblastoma. *Cancer Lett*, Nov 17, 2015

### 6.1.5 Presentations at meetings: (last year)

“Mesenchymal stem cells, the bone marrow niche and drug resistance.” The Stem Cell Niche and Cancer Microenvironment Symposium, Regenerative Medicine Institute and Samuel Oschin Comprehensive Cancer Institute, Cedars-Sinai Medical Center, Los Angeles, CA. November 12-14, 2015.

“The bone marrow niche and environment-mediated drug resistance.” 6<sup>th</sup> Annual NCI Tumor Microenvironment Network Junior Investigator Meeting, Children’s Hospital Los Angeles. June 23-25, 2015.

“The tumor microenvironment of high risk neuroblastoma: from discovery to therapy.” Center for Cell and Gene Therapy, Baylor College of Medicine, Houston. October 17, 2014.

**6.2 Website:** Nothing to report

**6.3 Inventions, patents:** Nothing to report

**6.4 Other products:** Nothing to report

7. **PARTICIPANTS:** Nothing to report

8. **SPECIAL REPORTING REQUIREMENTS:** None

9. **APPENDICES:**

Ara, T., Nakata, R, Shimada, H, Buettner, R, Groshen, SG, Ji, L, Sheard, M, Yu, H, Jove, R, Seeger, RC, DeClerck, YA. Critical role of STAT3 in interleukin-6-mediated drug resistance in human neuroblastoma. *Cancer Res*, 73:3852-3864, 2013.

Lucia Borriello, Robert C. Seeger, Shahab Asgharzadeh, Yves A. DeClerck. More than the genes, the tumor microenvironment in neuroblastoma. *Cancer Lett*, Nov 17, 2015.

Michael D. Hadjidaniel, Sakunthala Muthugounder, Long Hung, Soheila Shirinbak, Randall Chan, Rie Nakata, Lucia Borriello, Rebekah J. Kennedy, Michael Sheard, Hiroshi Iwakura, Takashi Akamizu, Hiroyuki Shimada, Richard Sposto, Yves A. DeClerck, Shahab Asgharzadeh. Tumor-associated macrophages activate STAT3 and MYC in neuroblastomas independently of IL6.

BLANK PAGE

## Critical Role of STAT3 in IL-6–Mediated Drug Resistance in Human Neuroblastoma

Tasnim Ara<sup>1,5</sup>, Rie Nakata<sup>1,5</sup>, Michael A. Sheard<sup>1,5</sup>, Hiroyuki Shimada<sup>2,5</sup>, Ralf Buettner<sup>6</sup>, Susan G. Groshen<sup>4</sup>, Lingyun Ji<sup>4</sup>, Hua Yu<sup>6</sup>, Richard Jove<sup>6</sup>, Robert C. Seeger<sup>1,5</sup>, and Yves A. DeClerck<sup>1,3,5</sup>

### Abstract

Drug resistance is a major cause of treatment failure in cancer. Here, we have evaluated the role of STAT3 in environment-mediated drug resistance (EMDR) in human neuroblastoma. We determined that STAT3 was not constitutively active in most neuroblastoma cell lines but was rapidly activated upon treatment with interleukin (IL)-6 alone and in combination with the soluble IL-6 receptor (sIL-6R). Treatment of neuroblastoma cells with IL-6 protected them from drug-induced apoptosis in a STAT3-dependent manner because the protective effect of IL-6 was abrogated in the presence of a STAT3 inhibitor and upon STAT3 knockdown. STAT3 was necessary for the upregulation of several survival factors such as survivin (BIRC5) and Bcl-xL (BCL2L1) when cells were exposed to IL-6. Importantly, IL-6–mediated STAT3 activation was enhanced by sIL-6R produced by human monocytes, pointing to an important function of monocytes in promoting IL-6–mediated EMDR. Our data also point to the presence of reciprocal activation of STAT3 between tumor cells and bone marrow stromal cells including not only monocytes but also regulatory T cells (Treg) and nonmyeloid stromal cells. Thus, the data identify an IL-6/sIL-6R/STAT3 interactive pathway between neuroblastoma cells and their microenvironment that contributes to drug resistance. *Cancer Res*; 73(13); 3852–64. ©2013 AACR.

### Introduction

Over the last 10 years, it has become increasingly appreciated that tumor cells that lack the intrinsic ability to initiate an angiogenic response, to resist the injury of therapies or to metastasize, can acquire such properties through the influence of the microenvironment (1). The acquisition of these properties occurs through complex interactions between tumor cells and a variety of stromal cells such as carcinoma-associated fibroblasts, endothelial cells, adipocytes, myofibroblasts, mesenchymal cells, and innate and adaptive immune cells (2–5). The identification of pathways involved in these interactions has therefore been the subject of intensive investigation over the recent years with the anticipation that these pathways will be novel targets for anticancer therapy (6). Among the characteristics that tumor cells acquire through their interaction with the microenvironment is drug resistance, a major cause of failure to eradicate cancer. The acquisition of drug

resistance through interactions between tumor cells and their environment, known as "environment-mediated drug resistance" (EMDR; ref. 7), is an important contributor to the emergence of minimal residual disease in cancer. EMDR occurs through complex adhesion-dependent and -independent interactions between tumor cells and the extracellular matrix (ECM) and stromal cells (8, 9). The bone marrow microenvironment plays a particularly important role in EMDR as it is an abundant source of ECM proteins, cytokines, and growth factors produced by mesenchymal and hematopoietic stem cells and their progeny that promote homing and survival (10).

The bone marrow is also the most frequent site of metastasis in neuroblastoma, a tumor derived from the neural crest that is the second most common solid malignancy affecting children (11, 12). It is a source of multiple chemokines, cytokines, and growth factors including interleukin (IL)-6. We have previously shown that in the case of neuroblastoma, IL-6 is not produced by tumor cells but by bone marrow-derived mesenchymal stem cells (BMMSC) and tumor-associated macrophages (TAM; refs. 13–15). The paracrine production of IL-6 by BMMSC plays a dual role in neuroblastoma bone marrow and bone metastasis. It activates osteoclasts, promoting the formation of osteolytic lesions and stimulates the growth and survival of neuroblastoma cells (16). Among the signaling pathways activated by IL-6, is the signal transducer and activator of transcription (STAT3) that plays a central role in the communication between tumor cells and immune cells (17). STAT3 was initially discovered as a transcription factor induced by IFN- $\gamma$  (18). It is considered an oncogene as it is required for the oncogenic transformation activity of v-Src (19). It has multiple protumorigenic functions including the

**Authors' Affiliations:** <sup>1</sup>Division of Hematology-Oncology, Department of Pediatrics, Departments of <sup>2</sup>Pathology, <sup>3</sup>Biochemistry & Molecular Biology, and <sup>4</sup>Preventive Medicine, Keck School of Medicine, University of Southern California, Los Angeles; <sup>5</sup>The Saban Research Institute, Children's Hospital Los Angeles, Los Angeles; and <sup>6</sup>Department of Immunology and Cancer Biology, Beckman Research Institute, City of Hope, Duarte, California

**Note:** Supplementary data for this article are available at Cancer Research Online (<http://cancerres.aacrjournals.org/>).

**Corresponding Author:** Yves A. DeClerck, Children's Hospital Los Angeles, 4650 Sunset Boulevard, MS#54, Los Angeles, CA 90027. Phone: 323-361-2150; Fax: 323-361-4902; E-mail: [declerck@usc.edu](mailto:declerck@usc.edu)

doi: 10.1158/0008-5472.CAN-12-2353

©2013 American Association for Cancer Research.

promotion of tumor cell proliferation, survival, invasion, metastasis, and angiogenesis (20–22). In addition, STAT3 is a major contributor to inflammation (23) and has been shown to promote the acquisition of chemo- and radioresistance (24, 25). In most cancers STAT3 is constitutively active, but its activation can also occur through the influences of the micro-environment and in particular IL-6 (26). IL-6 binds to a heterodimeric receptor made of 2 subunits, the gp80  $\alpha$  subunit (IL-6R) that is the ligand-binding unit and the gp130  $\beta$  subunit that is the signal-transducing unit, which via phosphorylation of Janus-activated kinases (JAK), activates STAT3 (27). The gp80 unit is also present in a soluble form [soluble IL-6 receptor (sIL-6R)] that has an agonistic effect through its trans signaling function (28). Here, we have explored the role of STAT3 activation by IL-6 and sIL-6R in EMDR in human neuroblastoma.

## Materials and Methods

### Cell culture

Human neuroblastoma cell lines were cultured as previously reported (16). The cells were authenticated by genotype analysis using AmpFISTR Identifier PCR kit and GeneMapper ID v. 3.2 (Applied Biosystems). Human BMMSC were purchased from AllCells LLC. Monocytes of normal healthy donors were obtained from peripheral blood and separated by Ficoll density gradient centrifugation using a human monocyte isolation kit (Miltenyi Biotech).

### Reagents

Rabbit polyclonal antibodies against pY<sup>705</sup> STAT3, STAT3, survivin, Bcl-xL XIAP, Bcl-2, Mcl-1, uncleaved and cleaved caspase-3 and -9, and cytochrome C and Alexa Fluor 488–conjugated antibodies against survivin and Bcl-xL were purchased from Cell Signaling Technology, Inc. A rabbit polyclonal antibody against actin and a mouse monoclonal antibody (mAb) against  $\beta$ -actin were purchased from Sigma-Aldrich. A mouse polyclonal antibody against STAT3 was purchased from Cell Signaling Technology, Inc. The following secondary antibodies were used for Western blot analyses, immunocyto-fluorescence, and immunohistochemistry: biotinylated anti-rabbit immunoglobulin G (IgG; H+L; Vector Labs), donkey anti-rabbit IRDye 800CW, donkey anti-mouse IRDye 680 (LI-COR Biosciences), goat horseradish peroxidase (HRP)–conjugated anti-rabbit Streptavidin Dylight 488 (Jackson ImmunoResearch), goat anti-mouse Alexa Fluor 555 (Invitrogen), and donkey anti-rabbit IgG (Thermo Scientific). Antibodies against the following markers were from BD Biosciences: CD14-V450, phospho-Stat3 (pY705)-PE, CD4-APC-H7, CD25-PE-Cy7, FoxP3-PerCP-Cy5.5, and GD2-APC. Anti-CD3-Alexa Fluor 488 was from BioLegend. Anti-CD163-Alexa Fluor 700 was from R&D Systems. Anti-CD45-Krome Orange was from Life Technologies. Human FcR blocking agent was from Miltenyi Biotec. BD Fix I Buffer and BD Perm III Buffer were from BD Biosciences. Etoposide (Ben Venue Laboratories, Inc.) and melphalan (Sigma-Aldrich) were dissolved in acidified-ethanol at a stock concentration of 64  $\mu$ g/mL. The STAT3 inhibitor stattic (29) was purchased from Calbiochem and solubilized in dimethyl sulfoxide (DMSO) at a stock concentration of

60 mmol/L. Recombinant human IL-6 and sIL-6R were purchased from R&D Systems. A humanized mouse monoclonal function–blocking antibody against IL-6R (tocilizumab; ref. 30) was purchased from Genentech, Inc.

### Western blot analysis

Western blot analyses were conducted as previously described (16). Cells were lysed in radioimmunoprecipitation assay (RIPA) buffer supplemented with 1 tablet of complete mini-EDTA protease inhibitor cocktail (Roche Diagnostics) or halt protease and phosphatase inhibitor cocktail (Thermo Scientific). The detection of immune complexes and their quantification was conducted using either the Odyssey Infrared Imaging Systems (LI-COR Biosciences) or chemiluminescence with an HRP antibody detection kit (Denville) and the NIH ImageJ software for analysis.

### Cell viability assay

Cell viability in the presence of cytotoxic drugs was determined by fluorescence-based cytotoxicity assay using digital imaging microscopy (DIMSCAN; ref. 31).

### Flow cytometry

For JC-1 stain, cultured cells were detached in cell dissociation buffer (Invitrogen) and stained for 30 minutes in the presence of JC-1 dye (10 mg/mL; MitoProbe JC-1 Assay Kit; Invitrogen) before being analyzed by flow cytometry. For Annexin V stain, cultured cells were resuspended in 1 $\times$  Annexin V–binding buffer. Annexin V and propidium iodide (PI) staining were conducted using an Annexin V–fluorescein isothiocyanate (FITC) apoptosis detection kit II according to the manufacturer's instructions (BD Pharmingen).

### Enzyme-linked immunosorbent assay (ELISA)

The levels of human IL-6 and sIL-6R in serum-free conditioned medium of cultured cells were determined by ELISA using the Quantikine Immunoassay Kit or DuoSet ELISA Development Kit from R&D Systems.

### siRNA-based gene knockdown

Downregulation of the expression of STAT3 was done using the Signal Silence STAT3 siRNA Kit (Cell Signaling Technology, Inc.). Cells plated in 6-well plates ( $2.5 \times 10^5$  cells) were transfected with scrambled siRNA or STAT3 siRNA and a fluorescein-conjugated siRNA (to verify transfection efficiency) using the Lipofectamine RNAi MAX reagent (Invitrogen). The downregulation of the protein (STAT3) was verified by Western blot analysis on cell lysates obtained 72 hours after transfection. The following siRNA sequences were used from SignalSilence: STAT3 siRNA I, cat. no. 6582 and STAT3 siRNA I, cat. no. 6580.

### Immunohistochemistry and immunofluorescence

Paraffin-embedded sections (4  $\mu$ m) of bone marrow biopsies were obtained through the Children's Oncology Group Biorepository by H.S. These samples were acquired after informed consent was obtained and upon approval of Children's Hospital Los Angeles (CHLA) Institutional Review Board. Antigen

unmasking was conducted by proteinase K treatment (20  $\mu$ g/mL for 10 minutes at 25°C). The slides were incubated overnight at 4°C in the presence of the following primary antibodies: a rabbit anti-human pY705 STAT3, survivin, or Bcl-xL, a mouse anti-CD68 or a rabbit antityrosine hydroxylase mAb (dilutions 1:100). After washing 3 $\times$  with 0.1% Triton-X 100 in PBS, the slides were incubated in the presence of one of the following secondary antibodies: an Alexa Fluor 488-conjugated goat anti-mouse IgG or anti-mouse IgG antibody (dilution 1:50) for 1 hour at room temperature. For immunofluorescence, slides were mounted in 4',6-diamidino-2-phenylindole (DAPI) containing Vectashield medium. For dual immunohistochemistry, the Bond Polymer Refine Detection (Leica Biosystems Newcastle Ltd.) was used. Slides were heated at pH 6 for 20 minutes before being processed. The biotin-free polymeric HRP linker (DS 9800) was used for the detection of pSTAT3 and the biotin-free polymeric alkaline phosphatase linker (DS 9390) was used for the detection of Protein Gene Product (PGP) 9.5 and CD45. As primary antibodies, we used a mouse anti-human PGP 9.5 from Leica (PA0286) undiluted, a mouse anti-CD45 mAb from Abcam (ab8216) at a 1:25 dilution, and a rabbit anti-pSTAT3 (Tyr705) polyclonal antibody from Cell Signaling Technology, Inc. (9131) at a 1:25 dilution. Primary and secondary antibodies were incubated for 30 minutes.

#### Immunocytofluorescence

Cells were cultured in Lab-Tek II 8 chamber slides for 48 hours ( $2 \times 10^4$  and  $10 \times 10^4$  cells/well). Cells were then washed, treated with IL-6 and sIL-6R for 30 minutes, and then fixed with 4% formaldehyde in PBS for 10 minutes and permeabilized with 0.1% Triton-X100 in 15% FBS in PBS for 5 minutes, before being incubated in the presence of an anti-human pSTAT3 or STAT3 antibody overnight at 4°C.

#### Statistical analysis

For the analyses of cell viability, the luciferase or fluorescence activity readings were assumed to have a lognormal distribution and were transformed to the  $\log_{10}$  scale before analyses were conducted. ANOVA was used to examine the differences in mean cell viability among groups and the Student (two-tailed) test was used to compare 2 groups in the apoptotic assays. All *P* values reported were two-sided. A *P* value of less than 0.05 was considered significant. Data were analyzed with software STATA version 11.2 (StataCorp LP).

### Results

#### IL-6 and sIL-6R activate STAT3 in neuroblastoma cells

We had previously reported that with a few exceptions most human neuroblastoma cells do not produce significant amounts of IL-6 and do not secrete sIL-6R, but express the 2 IL-6R subunits (16). To determine the status of STAT3 activation in neuroblastoma, we initially examined 8 human tumor cell lines for the expression of STAT3 and phospho Y<sup>705</sup> STAT3 (pSTAT3) by Western blot analysis under baseline conditions and upon treatment with IL-6, sIL-6R, and their combination. This analysis revealed a low amount of pSTAT3 in most untreated cells (except in SK-N-SH and CHLA-90 cells), indicating a general absence of constitutive activation of

STAT3 in neuroblastoma (Fig. 1A). However, when cells were treated with IL-6 alone and in particular in combination with sIL-6R, we observed a significant increase in pSTAT3 after 30 minutes in all cell lines. Activation of STAT3 in CHLA-255 and CHLA-90 cells was confirmed by immunocytofluorescence (Fig. 1B). This analysis revealed the presence of cytoplasmic STAT3 in both cell lines. In CHLA-255 cells, pSTAT3 was not detected in the absence of IL-6 but became detectable in the nucleus upon treatment with IL-6 alone or in combination with sIL-6R. In contrast, nuclear pSTAT3 was detected in CHLA-90 cells with or without treatment with IL-6 and sIL-6R. To confirm the role of IL-6 in STAT3 activation, we showed that incubation of CHLA-255 cells with a mAb against human IL-6R (tocilizumab) before treatment with IL-6 and IL-6 plus sIL-6R suppressed STAT3 phosphorylation (Supplementary Fig. S1A) and the binding of STAT3 to DNA as determined by electrophoretic mobility shift assay (EMSA; Supplementary Fig. S1B). We also showed that CHLA-255 cells transiently transfected with a STAT3 responsive promoter construct driving the firefly luciferase reporter gene (*STAT3Luc*) and a renilla luciferase vector had a 4-fold increase in firefly/*Renilla* luciferase activity when treated with IL-6 plus sIL-6R, and that this increase in activity was suppressed in the presence of tocilizumab (Supplementary Fig. S1C). Thus, altogether the data showed that IL-6 is an effective and specific activator of STAT3 in human neuroblastoma, in particular in the presence of sIL-6R.

#### IL-6 and sIL-6R protect neuroblastoma cells from drug-induced apoptosis

To show the role of IL-6 in chemoresistance, we selected 2 drug-sensitive neuroblastoma cell lines (CHLA-255 and SK-N-SH) and tested the effect of IL-6 and sIL-6R on their survival in the presence of etoposide and melphalan (32, 33). This analysis revealed a dose-dependent decrease in the survival fraction in both cell lines upon exposure to etoposide or melphalan for 24 hours (Fig. 2A–D). However, when cells were pretreated with IL-6 (alone and with sIL-6R) and then exposed to the drug, we observed a significant increase in the survival fraction when compared with the drug alone. As anticipated, the addition of sIL-6R alone in the absence of IL-6 failed to protect neuroblastoma cells from etoposide-induced apoptosis (Supplementary Fig. S3A). We next examined the effect of IL-6 and sIL-6R pretreatment on mitochondrial membrane depolarization and caspase-3 and -9 activation in cells treated with etoposide or melphalan (Fig. 3). The data showed that pretreatment of CHLA-255 cells with IL-6 alone or with sIL-6R resulted in less mitochondrial membrane depolarization (Fig. 3A and B). IL-6 also inhibited the cytoplasmic release of cytochrome C upon treatment with etoposide (Fig. 3C). Consistently, pretreatment of CHLA-255 cells with IL-6 inhibited the cleavage of caspase-3 and -9 in the presence of increased concentrations of etoposide or melphalan (Fig. 3D and E). Altogether, the data thus indicated that IL-6 had a protective effect on drug-induced intrinsic apoptosis.

#### STAT3 is necessary for IL-6-mediated drug resistance

We next asked the question whether STAT3 activation was necessary for the protective effect of IL-6 on drug-induced

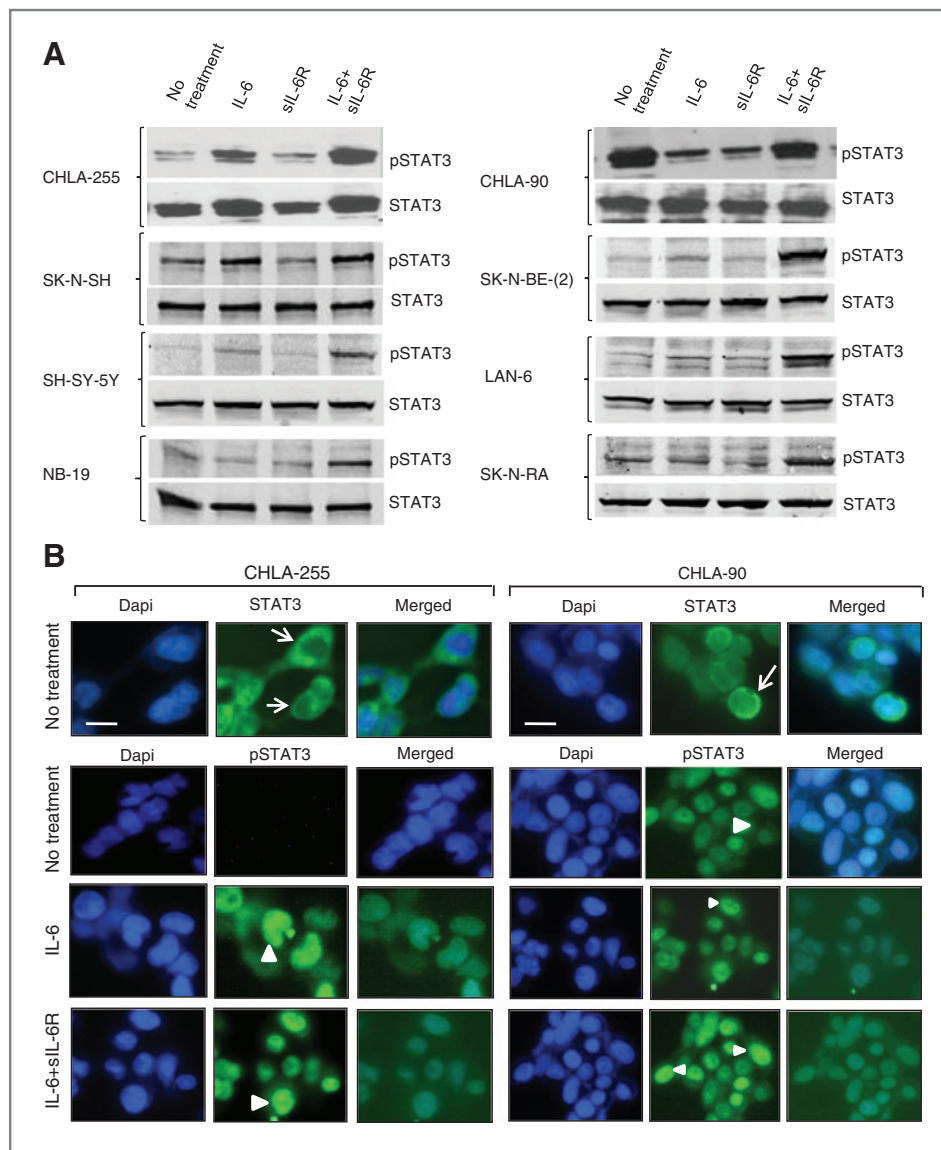


**Figure 1.** IL-6 and siL-6R activate STAT3 in human neuroblastoma cells. **A**, the presence of phosphorylated pY<sup>705</sup> STAT3 and STAT3 was detected by Western blot analysis in total cell lysates from 8 neuroblastoma cell lines. When indicated, cells were treated with IL-6 (10 ng/mL) and siL-6R (25 ng/mL). Lysates were obtained 30 minutes after treatment. The data are representative of 2 to 3 separate experiments showing similar results. **B**, the presence of STAT3 and pY<sup>705</sup> STAT3 in cultured CHLA-255 (left) and CHLA-90 (right) cells untreated or treated for 30 minutes with IL-6 alone or with siL-6R as described earlier was examined by immunocytofluorescence. Arrow, cytoplasmic STAT3. Arrowhead, nuclear pSTAT3 (scale bar, 20  $\mu$ m).

apoptosis. We first used stattic, a small-molecule inhibitor of STAT3 activation (29) and showed that treatment of CHLA-255 cells with stattic (0.5 to 20  $\mu$ mol/L) prevented STAT3 activation by IL-6 plus siL-6R (Fig. 4A). We then examined the effect of stattic (at 2.5  $\mu$ mol/L, to maintain 80% cell viability) on apoptosis induced by etoposide in CHLA-255 cells pretreated with IL-6 and siL-6R. The data indicated that stattic restored etoposide-induced apoptosis in the presence of IL-6 and IL-6 plus siL-6R to levels observed in the absence of IL-6 and stattic (Fig. 4B).

The necessary role of STAT3 in IL-6-mediated drug resistance was confirmed by examining the effect of

siRNA-mediated STAT3 knockdown on neuroblastoma cell sensitivity to etoposide in the presence of IL-6 and siL-6R. The data indicated that transfection of CHLA-255 cells with a combination of 2 siRNA sequences resulted in an 80% STAT3 knockdown and a complete suppression of STAT3 activation upon treatment with IL-6 alone or with siL-6R when compared with a scramble siRNA sequence (Fig. 4C). STAT3 knockdown in CHLA-255 cells restored their sensitivity to etoposide in the presence of IL-6 and siL-6R to levels close to the level of apoptosis observed in the absence of IL-6 (Fig. 4D). The knockdown of STAT3 in SK-N-SH cells had a similar effect on the sensitivity of these cells to etoposide in

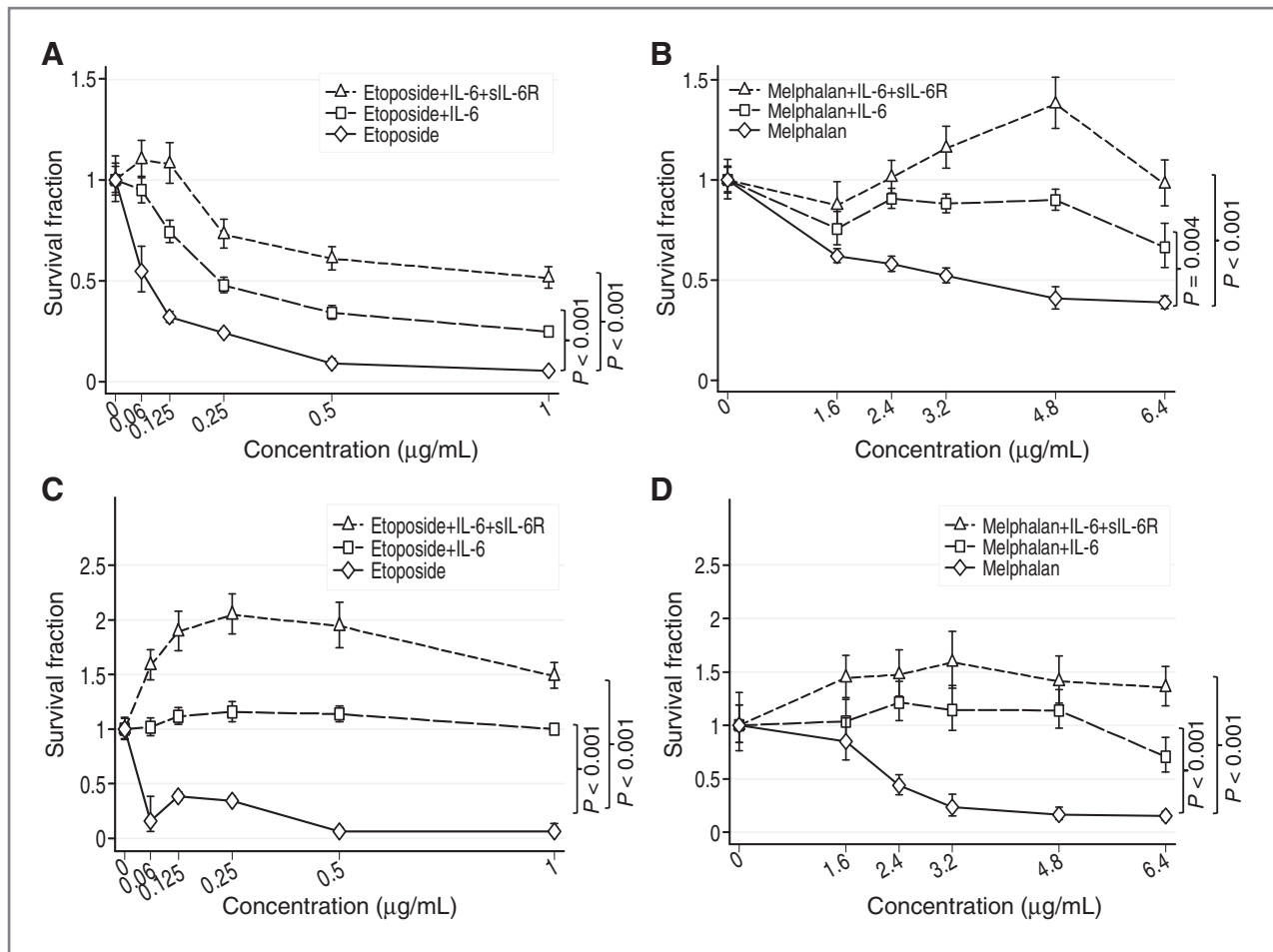


**Figure 2.** IL-6 and sIL-6R protect neuroblastoma cells from drug toxicity. CHLA-255 (A and B) and SK-N-SH cells (C and D) were treated with IL-6 (10 ng/mL) alone or with sIL-6R (25 ng/mL) for 24 hours before being exposed to etoposide (A and C) or melphalan (B and D) at indicated concentrations. Cell viability was determined after 24 hours of drug exposure by DIMSCAN analysis. The data represent the mean ( $\pm$ SD) survival fraction with a minimum of 10 replicates for each experimental condition.

the presence of IL-6 and sIL-6R (Supplementary Fig. S2A and S2B). The data thus showed that the protective effect of IL-6 on drug-induced apoptosis in neuroblastoma was STAT3 activation-dependent.

#### Upregulation of survival proteins by IL-6 is STAT3 dependent

We investigated the effect of IL-6 on the expression of survival proteins in CHLA-255 cells. The data indicated an increase in the expression of survivin, Mcl-1, XIAP-1, and Bcl-xL (Fig. 5A). An upregulation of survivin and Bcl-xL (to a lesser extent) was also observed in SK-N-SH cells treated with IL-6 (Supplementary Fig. S2C). We then showed that the upregulation of some of these survival proteins was STAT3 dependent by showing that statin inhibited the nuclear expression of survivin in CHLA-255 cells treated with IL-6 and IL-6 + sIL-6R (Fig. 5B) and by documenting a marked decrease in survivin expression and an absence of Bcl-xL expression upon STAT3 knockdown in cells treated with IL-6 and IL-6 plus sIL-6R (Fig. 5C). The data suggested that STAT3-dependent upregulation

of survival factors such as survivin and Bcl-xL was a mechanism by which IL-6 protected neuroblastoma cells from apoptosis.

#### BMSC and monocytes cooperate to sensitize neuroblastoma cells to IL-6-mediated STAT3 activation

Our *in vitro* data consistently showed that IL-6 was more active on neuroblastoma cells in the presence of sIL-6R. This suggested that sIL-6R sensitized neuroblastoma cells to STAT3 activation by IL-6. To test this hypothesis, we examined whether the addition of sIL-6R at a concentration of 25 ng/mL, which is within the range of the levels detected in the blood of patients with neuroblastoma (10–90 ng/mL; refs. 34, 35), would result in STAT3 activation in the presence of concentrations of IL-6 in the (0.1 to 10) ng/mL range. These experiments showed that when IL-6 was used alone, a concentration of 10 ng/mL was necessary to activate STAT3, whereas when used in combination with sIL-6R (25 ng/mL), a concentration of 0.1 ng/mL of IL-6 was sufficient for STAT3 activation (Fig. 6A). We then tested whether activation of

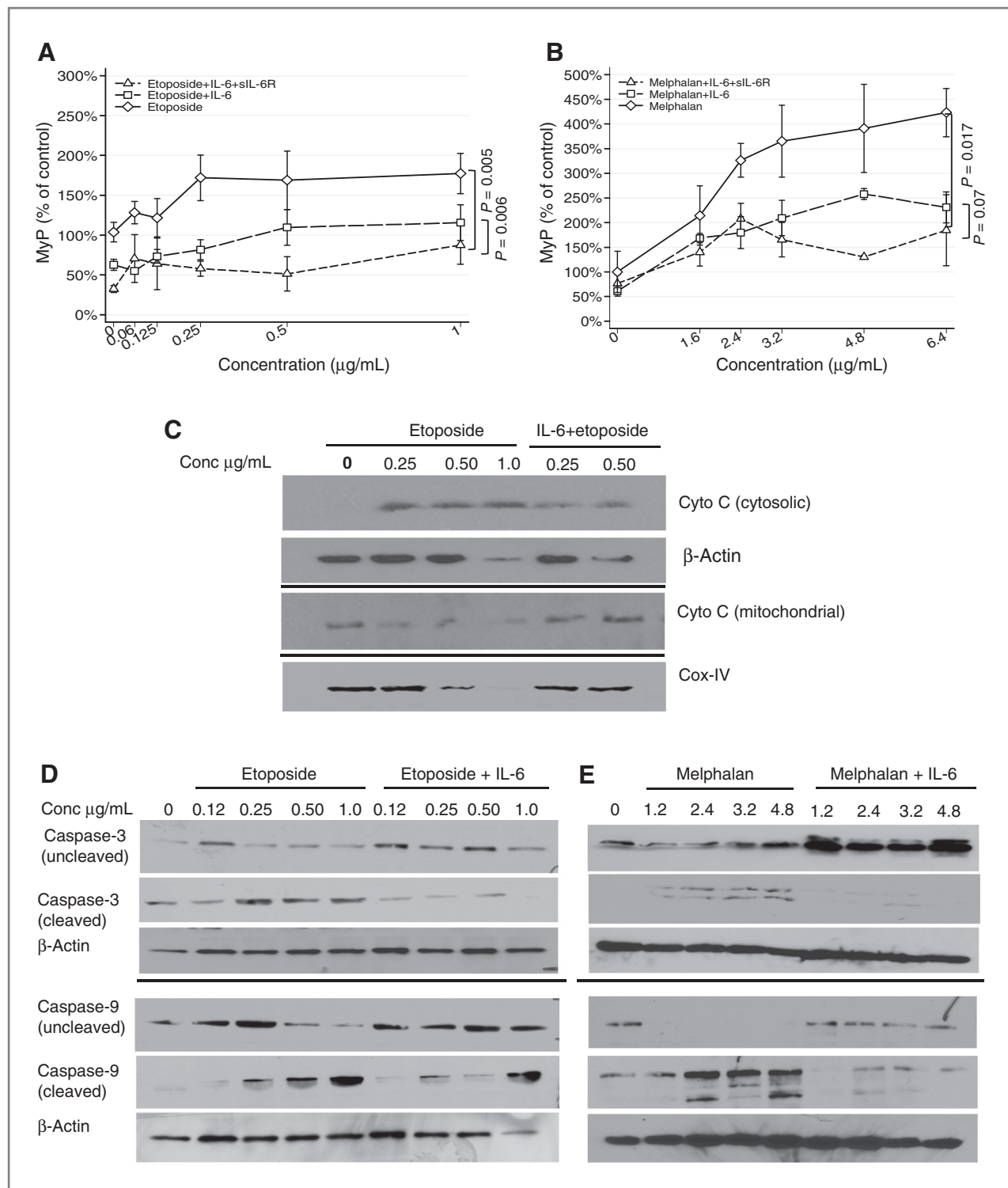


**Figure 3.** IL-6 and sIL-6R protect neuroblastoma cells from drug-induced apoptosis. **A** and **B**, CHLA-255 cells were treated as in Fig. 2. After 24 hours, mitochondrial membrane depolarization (M $\psi$ P) was examined by JC-1 staining by flow cytometry. The data represent the mean ( $\pm$ SE) percentage change in depolarization from control cells (untreated with cytotoxic drugs). **C**, CHLA-255 cells were treated as indicated earlier. After 24 hours, cytosolic and mitochondrial extracts were examined for the presence of cytochrome C by Western blot analysis. The data are representative of 2 separate experiments showing similar results. Cox-IV and  $\beta$ -actin were used as loading control for mitochondrial and cytosolic fractions, respectively. **D** and **E**, CHLA-255 cells were treated with IL-6 and etoposide or melphalan. After 24 hours of drug exposure, cell lysates were examined for the expression of full length and cleaved caspase-3 and -9. The data are representative of 2 separate experiments showing similar results. In all gels (C–E), separation lines indicate different gels loaded with the same amount of cell lysate.

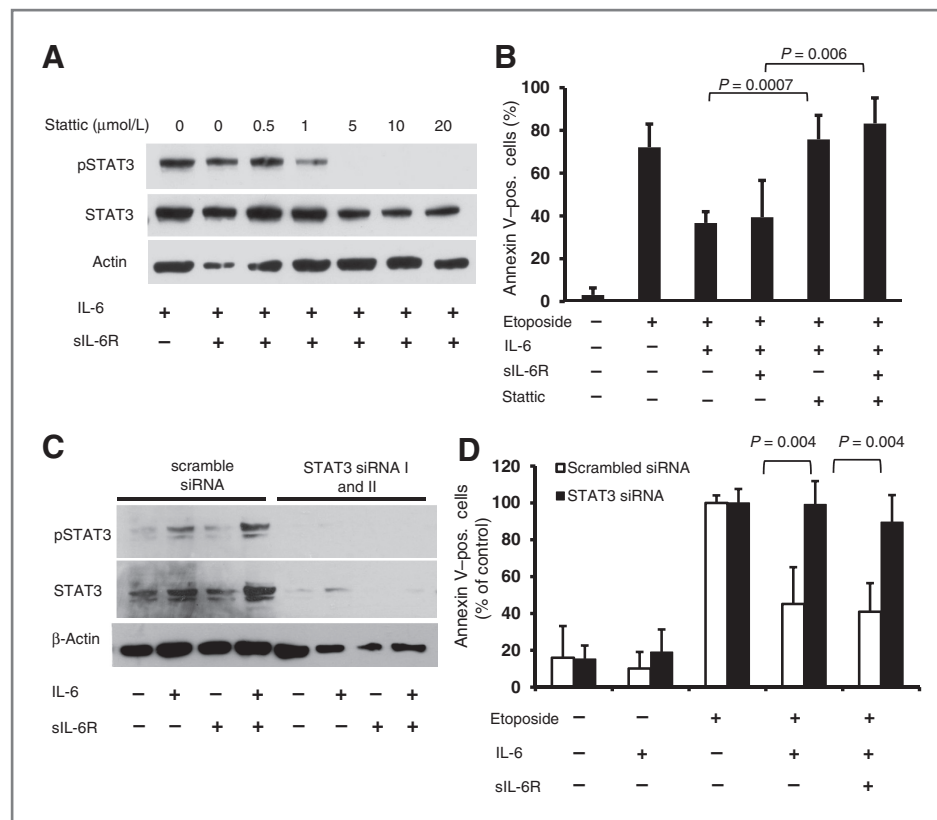
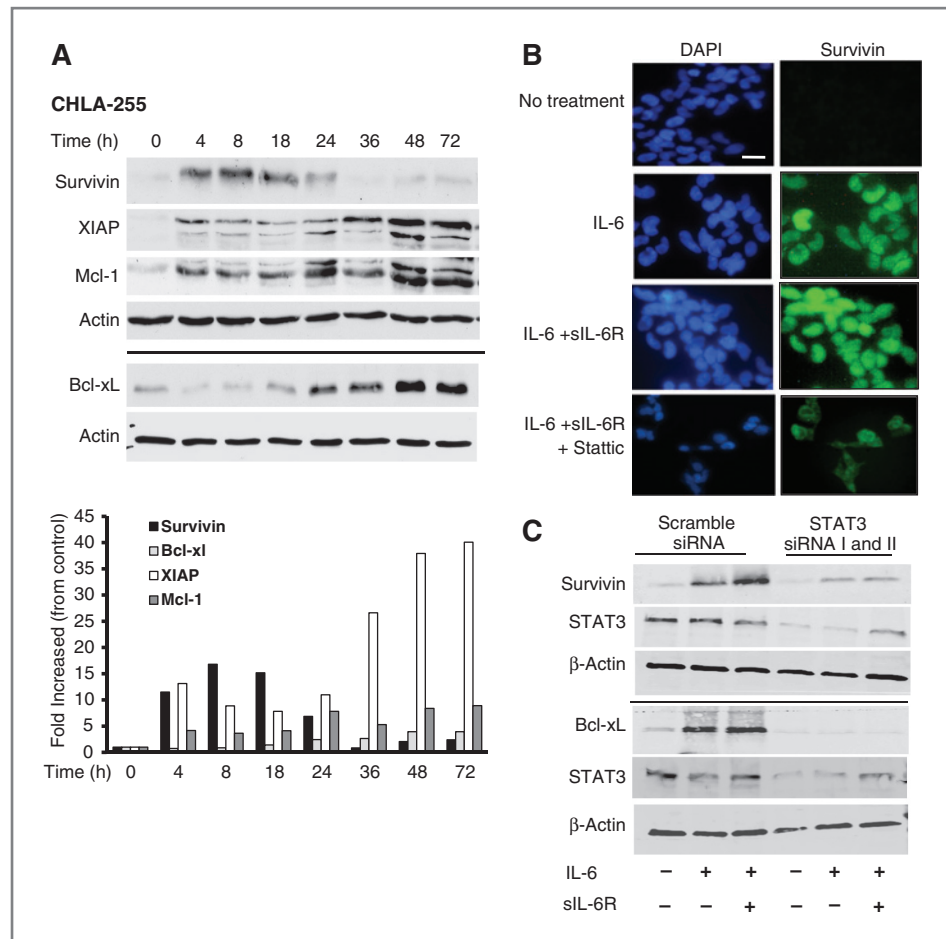


**Figure 4.** STAT3 is necessary for IL-6-mediated drug resistance. **A**, CHLA-255 cells were treated with IL-6 (10 ng/mL) and sIL-6R (25 ng/mL) for 30 minutes in the presence of static at indicated concentrations. Cell lysates were examined for pSTAT3 and STAT3 expression by Western blot analysis. **B**, CHLA-255 cells were treated with static (2.5 μmol/L) and IL-6 and sIL-6R for 24 hours before being exposed to etoposide (0.25 μg/mL). After 24 hours, cells were examined for Annexin V expression by flow cytometry. The data represent the mean percentage (±SD) of Annexin V-positive cells from 4 samples obtained in 3 independent experiments. **C**, CHLA-255 cells were transfected with STAT3 siRNA or with a scramble sequence. After 72 hours, cells were treated with IL-6 and sIL-6R for 30 minutes and cell lysates were examined for pSTAT3 and STAT3 expression by Western blot analysis. The data are representative of 3 separate experiments showing similar results. **D**, siRNA-transfected CHLA-255 cells were treated with IL-6 and sIL-6R for 24 hours before being exposed to etoposide (0.25 μg/mL) and examined for the presence of Annexin V at the cell surface. The data represent the mean percentage (±SD) of Annexin V-positive cells compared with control (cells treated with etoposide alone) from 4 samples obtained from 3 independent experiments.

STAT3 in the presence of 10 ng/mL of IL-6 could be potentiated by lower concentrations of sIL-6R. The data (Fig. 6B) showed an increase in pSTAT3 activation in the presence of 10 ng/mL of sIL-6R and above but not at lower concentrations (0.1 and 1.0 ng/mL). These sIL-6R concentrations are found in the blood of patients with cancer (35). Because neuroblastoma cells do not produce sIL-6R and are thus dependent of a paracrine source (16), we examined whether it was produced by normal cells in the tumor microenvironment. We first tested BMMSC that we had previously shown to be a source of IL-6 (13). The data showed an anticipated increase in the production of IL-6 (to 1,600 pg/mL) when BMMSC were cocultured with CHLA-255 cells and low amount of sIL-6R (mean  $32.5 \pm 14.8$  pg/mL; Fig. 6C, top). We then tested human monocytes that we had also shown to be a source of IL-6 (14). This experiment revealed that monocytes produced IL-6 and sIL-6R in culture and that their production was significantly increased in the presence of CHLA-255 cells. The amount of sIL-6R produced (mean  $149.5 \pm 8.6$  pg/mL) in the presence of CHLA-255 was

5-fold higher than BMMSC in similar conditions (Fig. 6C, bottom). Although this concentration is lower than the concentration required to enhance STAT3 activation *in vitro* (Fig. 6B), we showed that when human monocytes were cocultured with CHLA-255 cells, STAT3 became activated in the tumor cells even in the presence of low amounts of IL-6 (20 pg/mL) and that activation was in part IL-6R-dependent as it was partially inhibited in the presence of tocilizumab (Fig. 6D). The data thus point to the important contributory function of monocytes to STAT3 activation that is in part mediated by IL-6 and sIL-6R but could involve other activators. We also asked whether STAT3 would be activated in monocytes when cultured in the presence of neuroblastoma cells. In this experiment, CHLA-255 cells and human monocytes were cultured alone or in contact for 24 hours and the mixture of cells was analyzed for the presence of nuclear pSTAT3 and cell surface CD14 (monocytes) and CD56 (neuroblastoma). The data (Fig. 6E and Supplementary Fig. S3B) indicated an absence of pSTAT3 in cells cultured alone but a significant increase in pSTAT3 in both tumor cells and

**Figure 5.** IL-6 upregulates the expression of antiapoptotic proteins. A, CHLA-255 cells were treated with IL-6 (10 ng/mL) and cells were lysed at indicated time points (hours). Total cell lysates (20  $\mu$ g/lane) were then examined by Western blot analysis for the expression of indicated antiapoptotic proteins. Actin was used as loading control. The data are representative of 3 separate experiments showing similar results. The bar graph represents the fold increase compared with control after the ratios of antiapoptotic protein: actin were normalized for the ratio at 0 hour. B, CHLA-255 cells were treated with IL-6 and siL-6R and examined for survivin expression by immunofluorescence. Static (2.5 mmol/L) was added 4 hours before IL-6 and siL-6R when indicated (scale bar, 20  $\mu$ m). C, siRNA-transfected CHLA-255 cells treated as described earlier were examined for STAT3, survivin, and Bcl-xL expression by Western blot analysis after 24 hours of stimulation with IL-6 and siL-6R. The data are representative of 3 experiments showing similar results.



monocytes after 24 hours of coculture, indicating the presence of a reciprocal STAT3 activation loop between neuroblastoma cells and monocytes.

### STAT3 is activated in the bone marrow microenvironment in patients with metastatic neuroblastoma

To provide evidence for a role of STAT3 in patients with metastatic neuroblastoma, we examined STAT3 activation in a series of 10 bone marrow biopsies obtained from children with neuroblastoma. Five specimens were classified as positive for tumor involvement in the marrow (as assessed by the presence of tyrosine hydroxylase-positive cells by immunohistochemistry; ref 36) and 5 were classified as negative for tumor cells. An analysis of the presence of nuclear pSTAT3-positive cells in these samples revealed a higher percentage ( $22.3\% \pm 6.06\%$ ) of nuclear pSTAT3 in samples with tumor cells and a lower percentage ( $7.9\% \pm 1.8\%$ ;  $P = 0.002$ ) in samples negative for tumor cells (Fig. 7A). There was also a higher number of survivin-positive cells in samples infiltrated with tumor cells than in samples without tumor cells ( $122 \pm 69$  vs.  $10 \pm 14$ , respectively) and a higher level of Bcl-xL expression (Supplementary Fig. S3C). Because our *in vitro* coculture experiments on tumor cells and monocytes indicated a reciprocal activation of pSTAT3 (Fig. 6D and E), we then asked the question whether

STAT3 was activated in tumor cells and stromal cells in the bone marrow of patients with neuroblastoma. An analysis of pSTAT3 and CD45 by double immunohistochemistry on a bone marrow biopsy sample containing more than 90% tumor cells (Fig. 7B) indicated that 93% of PGP9.5<sup>+</sup> tumor cells were also pSTAT3-positive and that 42% of CD45<sup>+</sup> myeloid cells were also positive for pSTAT3. By double immunofluorescence with an anti-CD68 antibody, we then showed the presence of nuclear pSTAT3 in CD68<sup>+</sup> monocytes/macrophages. The data are consistent with our *in vitro* coculture experiment (Fig. 6E) and indicate that STAT3 in the bone marrow microenvironment is not only activated in tumor cells but also in myeloid cells including monocytes/macrophages (Fig. 7C). To better define subpopulations of these pSTAT3-positive myeloid cells, we examined by flow cytometry an additional 8 fresh bone marrow samples from patients with neuroblastoma for the presence of nuclear pSTAT3 (Supplementary Fig. S4A). Using a combination of 6 surface markers (CD3, CD4, CD14, CD25, CD45, and GD2) and 1 nuclear marker (FoxP3), we identified 6 populations of cells with CD45<sup>-</sup>/GD2<sup>-</sup> (nonmyeloid), CD45<sup>+</sup>/CD14<sup>-</sup> (myeloid nonmonocytic), and CD45<sup>+</sup>/CD14<sup>+</sup> (monocytic) being the most (>10% of total mononuclear cells) abundant (Supplementary Fig. S4B). An analysis of pSTAT3 in these different populations indicated a greater than 10% positive cells in 4 subpopulations,

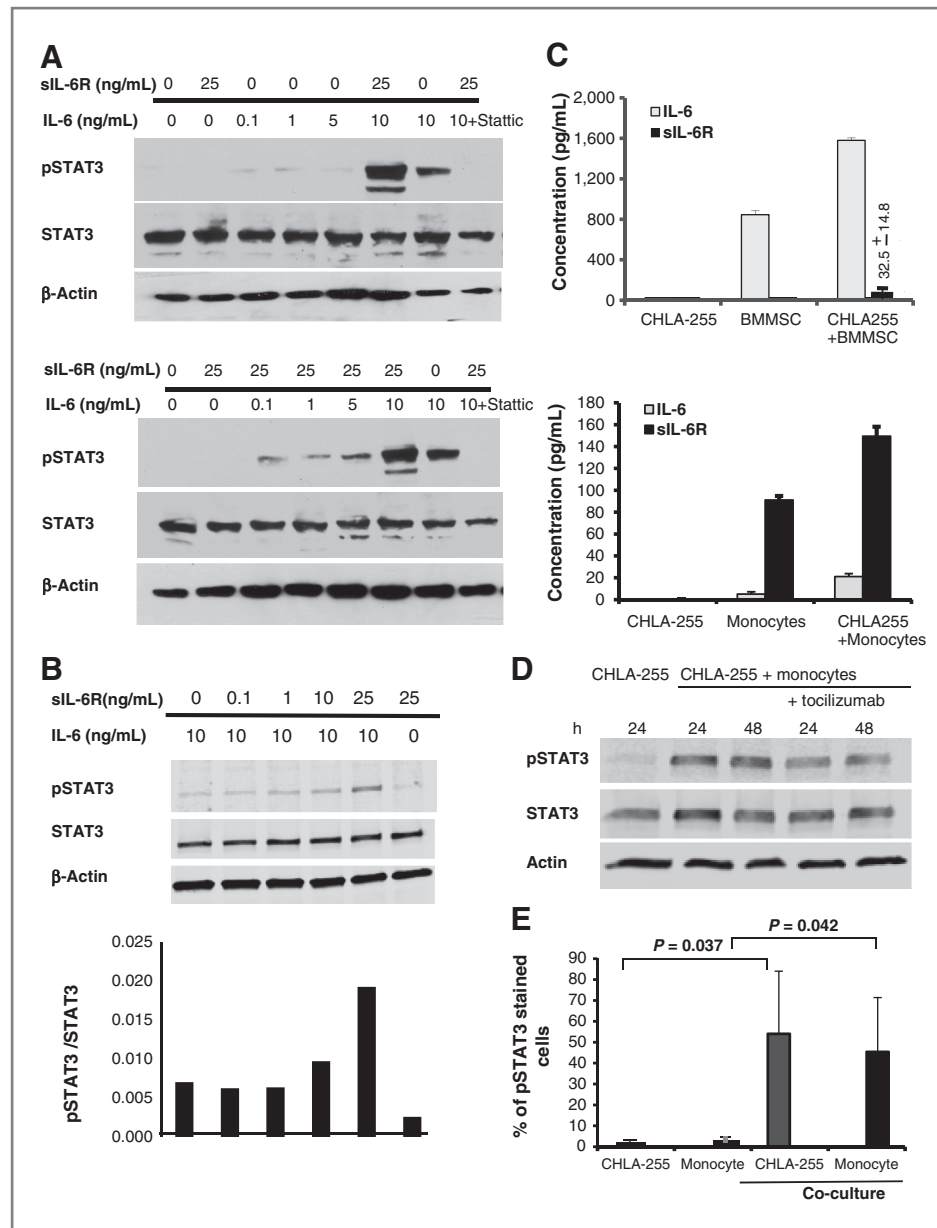
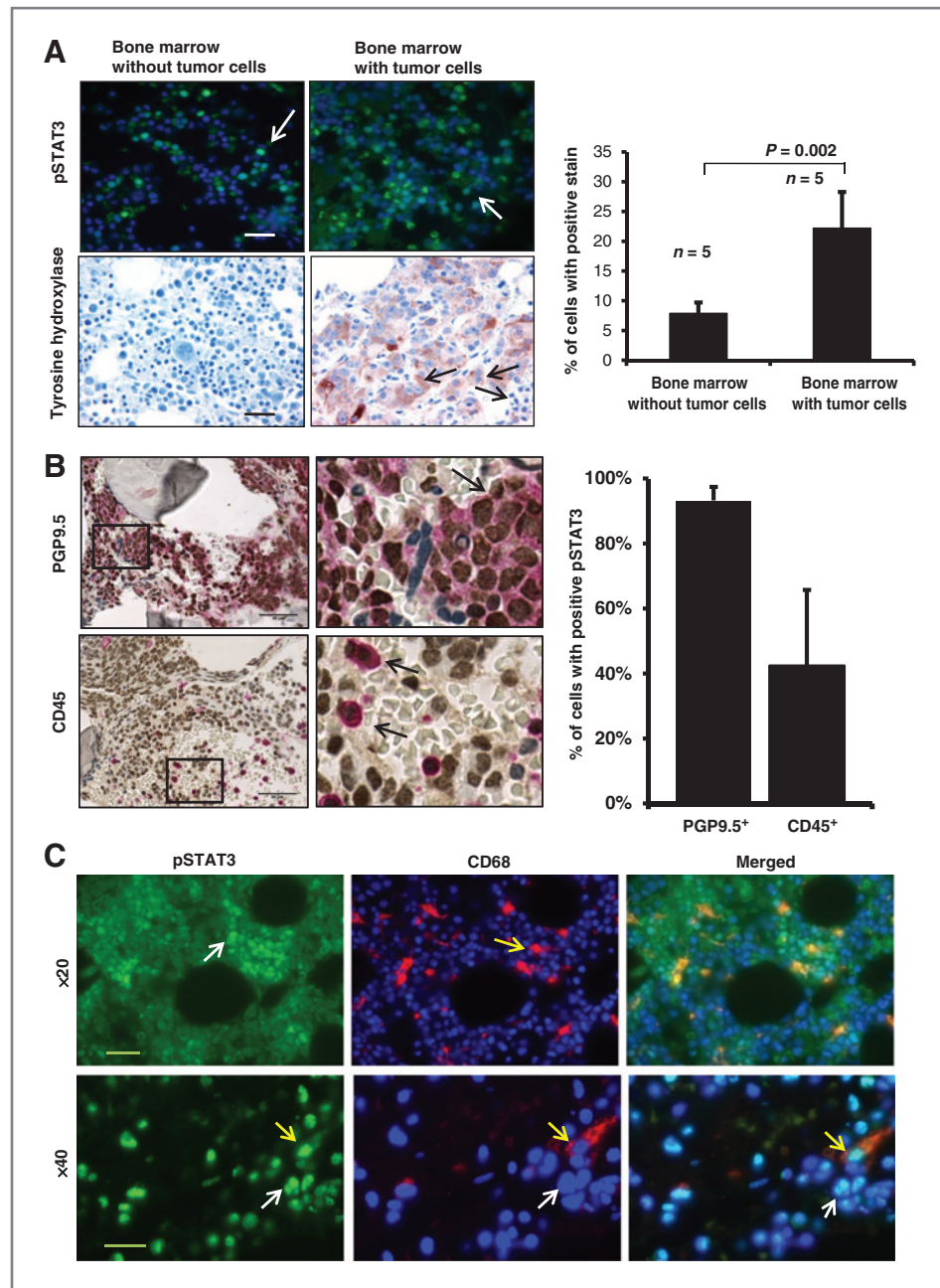


**Figure 6.** sIL-6R produced by monocytes sensitizes neuroblastoma cells to IL-6-mediated STAT3 activation. **A**, CHLA-255 cells were treated with IL-6 at indicated concentrations in the absence (top) or presence (bottom) of sIL-6R (25 ng/mL) for 30 minutes. The cell lysates were examined for expression of pSTAT3 and STAT3 by Western blot analysis. **B**, CHLA-255 cells were treated with IL-6 alone (10 ng/mL) and in the presence of increased concentrations of sIL-6R (0.1–25 ng/mL) for 30 minutes. The cell lysates were then examined for expression of pSTAT3 and STAT3 by Western blot analysis. The bar diagram represents the ratio pSTAT3/STAT3 obtained by scanning of the blot. **C**, CHLA-255 ( $4.5 \times 10^5$ ) and human BMMSC or monocytes ( $4.5 \times 10^5$ ) were cultured either alone or together in Transwell plates for 48 hours. The culture medium was collected and the concentrations of IL-6 and sIL-6R were determined by ELISA. The data represent the mean concentration ( $\pm$ SD) of duplicate (top) and triplicate (bottom) samples. **D**, CHLA-255 cells were cocultured with monocytes in Transwell plates in the absence or presence of an anti-IL-6R antibody (tocilizumab). After 48 hours, cell lysates were examined for pSTAT3 and STAT3 by Western blot analysis. **E**, monocytes isolated from the peripheral blood of patients with neuroblastoma and CHLA-255 cells were cultured alone or in contact (ratio tumor cells:monocytes 4:1) for 24 hours. Cells were then harvested and examined by flow cytometry for the presence of nuclear pSTAT3 and expression of cell surface CD56 and CD14 to separate tumor cells from monocytes. The data represent the average percentage of pSTAT3-positive cells ( $\pm$ SD) from 3 separate samples.

CD45<sup>-</sup>/GD2<sup>-</sup> nonmyeloid, nontumor cells, CD45<sup>-</sup>/GD2<sup>+</sup> tumor cells, CD45<sup>+</sup>/CD14<sup>+</sup> monocytes, and CD45<sup>+</sup>/CD3<sup>+</sup>/CD4<sup>+</sup>/CD25<sup>+</sup>/FoxP3<sup>+</sup> regulatory T cells (Treg), indicating that in addition to monocytes, Treg and nonmyeloid cells

could be part of the reciprocal loop of STAT3 activation between tumor cells and bone marrow-derived cells. Thus our data identify an IL-6/sIL-6R/STAT3 interactive pathway between neuroblastoma cells and the tumor

**Figure 7.** STAT3 is activated in the bone marrow microenvironment in patients with metastatic neuroblastoma. **A**, left, paraffin-embedded sections of bone marrow biopsies from patients ( $n = 10$ ) with neuroblastoma were examined by immunofluorescence for the presence of nuclear pSTAT3 (white arrow) and by immunohistochemistry for the presence of tyrosine hydroxylase-positive tumor cells (black arrow; bar, 50  $\mu$ m). Right, the data represent the mean percentage ( $\pm$ SD) of positive nuclei determined in 5 high magnification ( $\times 40$ ) fields per sample. **B**, bone marrow biopsy infiltrated with more than 90% of neuroblastoma cells was examined by dual immunohistochemistry as described in Materials and Methods for the presence of pSTAT3 in PGP9.5<sup>+</sup> tumor cells (top) or CD45<sup>+</sup> myeloid cells (bottom; arrows indicate dual positive cells). The histogram on the right side represents the mean ( $\pm$ SD) percentage of PGP9.5<sup>+</sup> and CD45<sup>+</sup> cells that were also positive for pSTAT3 from 5 high-power field areas (scale bar, 50  $\mu$ m). **C**, the presence of pSTAT3-positive and CD68<sup>+</sup> cells in bone marrow samples was examined by dual immunofluorescence (white arrows indicate nuclear localization of pSTAT3 in tumor cells and yellow arrows in CD68<sup>+</sup>; scale bar, 50  $\mu$ m at  $\times 20$  and 20  $\mu$ m at  $\times 40$ ).



microenvironment that contributes to drug resistance and in which STAT3 has a necessary function.

## Discussion

Overexpression of IL-6 by BMMSC has a dual protumorigenic function on neuroblastoma cells by promoting osteoclast activation (13) and tumor cell proliferation and survival (16). Here, we show the presence of an IL-6/sIL-6R/STAT3 paracrine pathway of interaction between tumor cells and the microenvironment that provides tumor cells with the ability to counteract the apoptotic effect of cytotoxic agents. Constitutive activation of STAT3 by oncogenes

such as Src, Fes, Sis, PyMT, Ros, or Eyk has been reported (37) but not by MYC-N, which is often amplified in neuroblastoma (38). Among the 8 cell lines examined, one, SK-N-BE (2), exhibited amplification of the MYC-N oncogene and in this cell line—as in most other cell lines without MYC-N amplification—STAT3 was not constitutively active. Our data indicate that in contrast to many other types of cancer, STAT3 activation is rarely constitutive in neuroblastoma but seems dependent on the tumor microenvironment. Although our data specifically point to a role for IL-6 as activator of STAT3, they do not rule out the possibility that other cytokines and growth factors could also contribute.

Our data identify a central function for the IL-6/sIL-6R/STAT3 pathway in conferring drug resistance to neuroblastoma cells. This effect involves the upregulation of several antiapoptotic proteins in particular survivin, Bcl-xL, Mcl-1, and XIAP that are known transcriptional targets of STAT3 (25, 39, 40). The observation that survivin is downstream of STAT3 signaling is relevant as high levels of survivin in neuroblastoma have also been associated with poorer clinical outcome (41). It has been previously reported that IL-6-mediated STAT3 activation plays a role in EMDR in myeloma (42), however, the mechanisms involved seem different between the 2 types of cancer. In myeloma, activation of STAT3 by IL-6 is primarily mediated by  $\beta$ 1 integrin-dependent adhesion of myeloma cells to bone marrow stromal cells (8). In contrast, in neuroblastoma, the expression of IL-6 in the bone marrow stroma is primarily regulated by soluble factors produced by tumor cells including prostaglandin E2 (16) and galectin-3-binding protein (43) among others.

Our data provide a new insight into the contributory role of monocytes to STAT3 activation by showing that monocytes produce sIL-6R and that sIL-6R enhances the sensitivity of neuroblastoma cells to IL-6-mediated STAT3 activation. The importance of sIL-6R in IL-6/gp130 signaling in autoimmunity, inflammation and cancer has been recently emphasized (44). Elevated levels of sIL-6R have been reported in the blood of patients with cancer including neuroblastoma and myeloma, and are typically a marker of unfavorable clinical outcome (34, 35, 45). These blood levels (ng/mL) are higher by 100-fold than the *in vitro* concentration of sIL-6R observed in cocultures of neuroblastoma cells and human monocytes. Although the reason for this discrepancy is not entirely clear, our data show a strong activation of STAT3 in cocultures of neuroblastoma cells and monocytes that is in part suppressed by a blocking antibody against IL-6R supporting a potentiating effect also at lower concentrations in coculture when IL-6 and sIL-6R are constantly produced and secreted. The data nevertheless do not rule out the possibility of other interactive pathways of activation. For example, a reciprocal activation of STAT3 between tumor cells and bone marrow-derived cells has recently been described and shown to be mediated by the sphingosine-1 phosphate receptor 1 (S1PR1), a member of the G protein-coupled receptor family of the lysophospholipids that sustains STAT3 activation by IL-6 (46). Whether S1PR1 plays such a role in sustaining STAT3 activation in neuroblastoma is presently investigated by our laboratories. Our data point to the important role that monocytes could play in EMDR in cancer, a new function recently showed in a mouse model of mammary carcinoma by Denardo and colleagues, who showed that suppression of macrophage infiltration in tumors increases response to chemotherapy (47). A similar protective role of monocytes in cis-platinum-induced apoptosis in colon and lung cancer-initiating cells has also been recently reported (48).

Interestingly, our analysis of pSTAT3 expression in bone marrow samples of patients with neuroblastoma revealed the presence of pSTAT3 not only in tumor cells and in CD45<sup>+</sup> myeloid cells including CD68<sup>+</sup> monocytes/macrophages, but also in a CD25<sup>+</sup>, FoxP3<sup>+</sup> Treg cells. Activation of pSTAT3 in

Treg cells has been shown to be mediated by IL-23 produced by TAM under STAT3 activation, which leads to the expression of FoxP3 and the secretion of the immunosuppressive cytokines IL-10 by Treg (49). Finally, we also observed a subpopulation of CD45<sup>-</sup>/GD2<sup>-</sup> bone marrow cells that expressed pSTAT3. Although these cells were not fully characterized at this point, they could represent in part mesenchymal cells that we have shown to play a critical intermediary role in bone invasion in neuroblastoma (13).

Ultimately, our data raise the question whether inhibition of IL-6-mediated STAT3 activation in neuroblastoma could play a role in therapy by preventing EMDR. Several humanized mAbs against soluble and membrane bound IL-6R (tocilizumab, REGN88) or against IL-6 (siltuximab and sirukumab) are currently in clinical trials for Castleman's disease, rheumatoid arthritis, and several types of cancer (44). Other potentially active agents include small-molecule inhibitors of JAK, some of them being currently tested in clinical trials (50, 51). Our data suggest that in neuroblastoma, these inhibitors may be most effective in combination with cytotoxic agents to prevent EMDR.

In summary, we provide here a new mechanistic insight on the contributory role of the bone marrow microenvironment in promoting drug resistance in neuroblastoma, as we show that by being a source of IL-6 and sIL-6R, the bone marrow microenvironment provides tumor cells with the ability to resist the cytotoxic effects of chemotherapy through STAT3 activation.

#### Disclosure of Potential Conflicts of Interest

Y.A. DeClerck is a consultant/advisory board member of AACR/Editorial Board. No potential conflicts of interest were disclosed by the other authors.

#### Authors' Contributions

**Conception and design:** T. Ara, R. Nakata, R. Buettner, S.G. Groshen, H. Yu, R. Jove, Y.A. DeClerck

**Development of methodology:** T. Ara, R. Nakata, R. Buettner, R.C. Seeger, Y.A. DeClerck

**Acquisition of data (provided animals, acquired and managed patients, provided facilities, etc.):** T. Ara, R. Nakata, M.A. Sheard, H. Shimada, R. Buettner

**Analysis and interpretation of data (e.g., statistical analysis, biostatistics, computational analysis):** T. Ara, M.A. Sheard, H. Shimada, R. Buettner, S.G. Groshen, L. Ji, R.C. Seeger, Y.A. DeClerck

**Writing, review, and/or revision of the manuscript:** T. Ara, R. Nakata, H. Shimada, R. Buettner, S.G. Groshen, L. Ji, H. Yu, R. Jove, Y.A. DeClerck

**Administrative, technical, or material support (i.e., reporting or organizing data, constructing databases):** T. Ara, R. Buettner

**Study supervision:** Y.A. DeClerck

#### Acknowledgments

The authors thank J. Rosenberg for her excellent assistance in preparing the article.

#### Grant support

The work was supported by an NIH grant PO1 CA 84103 (R.C. Seeger and Y.A. DeClerck), a NIH grant U54 CA163117 (Y.A. DeClerck), and a ThinkCure grant (R.C. Seeger). T. Ara was the recipient of a grant from the Children's Cancer Research Fund and the Children's Neuroblastoma Cancer Foundation.

The costs of publication of this article were defrayed in part by the payment of page charges. This article must therefore be hereby marked *advertisement* in accordance with 18 U.S.C. Section 1734 solely to indicate this fact.

Received June 18, 2012; revised March 20, 2013; accepted April 3, 2013; published OnlineFirst April 30, 2013.

## References

- Hanahan D, Weinberg RA. Hallmarks of cancer: the next generation. *Cell* 2011;144:646–74.
- Denardo DG, Barreto JB, Andreu P, Vasquez L, Tawfik D, Kolhatkar N, et al. CD4(+) T cells regulate pulmonary metastasis of mammary carcinomas by enhancing protumor properties of macrophages. *Cancer Cell* 2009;16:91–102.
- Tlsty TD, Coussens LM. Tumor stroma and regulation of cancer development. *Annu Rev Pathol* 2006;1:119–50.
- Joyce JA, Pollard JW. Microenvironmental regulation of metastasis. *Nat Rev Cancer* 2009;9:239–52.
- Karnoub AE, Dash AB, Vo AP, Sullivan A, Brooks MW, Bell GW, et al. Mesenchymal stem cells within tumour stroma promote breast cancer metastasis. *Nature* 2007;449:557–63.
- Dalton WS, Hazlehurst L, Shain K, Landowski T, Alsina M. Targeting the bone marrow microenvironment in hematologic malignancies. *Semin Hematol* 2004;41:1–5.
- Meads MB, Gatenby RA, Dalton WS. Environment-mediated drug resistance: a major contributor to minimal residual disease. *Nat Rev Cancer* 2009;9:665–74.
- Shain KH, Yarde DN, Meads MB, Huang M, Jove R, Hazlehurst LA, et al. Beta1 integrin adhesion enhances IL-6-mediated STAT3 signaling in myeloma cells: implications for microenvironment influence on tumor survival and proliferation. *Cancer Res* 2009;69:1009–15.
- Nefedova Y, Landowski TH, Dalton WS. Bone marrow stromal-derived soluble factors and direct cell contact contribute to *de novo* drug resistance of myeloma cells by distinct mechanisms. *Leukemia* 2003;17:1175–82.
- Meads MB, Hazlehurst LA, Dalton WS. The bone marrow microenvironment as a tumor sanctuary and contributor to drug resistance. *Clin Cancer Res* 2008;14:2519–26.
- Maris JM, Hogarty MD, Bagatell R, Cohn SL. Neuroblastoma. *Lancet* 2007;369:2106–20.
- Dubois SG, Kalika Y, Lukens JN, Brodeur GM, Seeger RC, Atkinson JB, et al. Metastatic sites in stage IV and IVS neuroblastoma correlate with age, tumor biology, and survival. *J Pediatr Hematol Oncol* 1999;21:181–9.
- Sohara Y, Shimada H, Minkin C, Erdreich-Epstein A, Nolte JA, DeClerck YA. Bone marrow mesenchymal stem cells provide an alternate pathway of osteoclast activation and bone destruction by cancer cells. *Cancer Res* 2005;65:1129–35.
- Song L, Asgharzadeh S, Salo J, Engell K, Wu HW, Spoto R, et al. Valpha24-invariant NKT cells mediate antitumor activity via killing of tumor-associated macrophages. *J Clin Invest* 2009;119:1524–36.
- Song L, Ara T, Wu HW, Woo CW, Reynolds CP, Seeger RC, et al. Oncogene MYCN regulates localization of NKT cells to the site of disease in neuroblastoma. *J Clin Invest* 2007;117:2702–12.
- Ara T, Song L, Shimada H, Keshelava N, Russell HV, Metelitsa LS, et al. Interleukin-6 in the bone marrow microenvironment promotes the growth and survival of neuroblastoma cells. *Cancer Res* 2009;69:329–37.
- Yu H, Pardoll D, Jove R. STATs in cancer inflammation and immunity: a leading role for STAT3. *Nat Rev Cancer* 2009;9:798–809.
- Shuai K, Stark GR, Kerr IM, Darnell JE Jr. A single phosphotyrosine residue of Stat91 required for gene activation by interferon-gamma. *Science* 1993;261:1744–6.
- Turkson J, Bowman T, Adnane J, Zhang Y, Djeu JY, Sekharam M, et al. Requirement for Ras/Rac1-mediated p38 and c-Jun N-terminal kinase signaling in Stat3 transcriptional activity induced by the Src oncoprotein. *Mol Cell Biol* 1999;19:7519–28.
- Grivennikov S, Karin E, Terzic J, Mucida D, Yu GY, Vallabhapurapu S, et al. IL-6 and Stat3 are required for survival of intestinal epithelial cells and development of colitis-associated cancer. *Cancer Cell* 2009;15:103–13.
- Calo V, Migliavacca M, Bazan V, Macaluso M, Buscemi M, Gebbia N, et al. STAT proteins: from normal control of cellular events to tumorigenesis. *J Cell Physiol* 2003;197:157–68.
- Hirano T, Ishihara K, Hibi M. Roles of STAT3 in mediating the cell growth, differentiation and survival signals relayed through the IL-6 family of cytokine receptors. *Oncogene* 2000;19:2548–56.
- Aggarwal BB, Kunnumakkara AB, Harikumar KB, Gupta SR, Tharakan ST, Koca C, et al. Signal transducer and activator of transcription-3, inflammation, and cancer: how intimate is the relationship? *Ann N Y Acad Sci* 2009;1171:59–76.
- Bonner JA, Trummell HQ, Willey CD, Plants BA, Raisch KP. Inhibition of STAT-3 results in radiosensitization of human squamous cell carcinoma. *Radiother Oncol* 2009;92:339–44.
- Bewry NN, Nair RR, Emmons MF, Boulware D, Pinilla-Ibarz J, Hazlehurst LA. Stat3 contributes to resistance toward BCR-ABL inhibitors in a bone marrow microenvironment model of drug resistance. *Mol Cancer Ther* 2008;7:3169–75.
- Ara T, DeClerck YA. Interleukin-6 in bone metastasis and cancer progression. *Eur J Cancer* 2010;46:1223–31.
- Kishimoto T. Interleukin-6: discovery of a pleiotropic cytokine. *Arthritis Res Ther* 2006;8(Suppl 2):S2.
- Kallen KJ. The role of transsignaling via the agonistic soluble IL-6 receptor in human diseases. *Biochim Biophys Acta* 2002;1592:323–43.
- Schust J, Sperl B, Hollis A, Mayer TU, Berg T. Stattic: a small-molecule inhibitor of STAT3 activation and dimerization. *Chem Biol* 2006;13:1235–42.
- Nishimoto N. Humanized anti-human IL-6 receptor antibody, tocilizumab. *Nippon Rinsho* 2007;65:1218–25.
- Keshelava N, Frgala T, Krejsa J, Kalous O, Reynolds CP. DIMSCAN: a microcomputer fluorescence-based cytotoxicity assay for preclinical testing of combination chemotherapy. *Methods Mol Med* 2005;110:139–53.
- Simon T, Langler A, Harnischmacher U, Fruhwald MC, Jorch N, Claviez A, et al. Topotecan, cyclophosphamide, and etoposide (TCE) in the treatment of high-risk neuroblastoma. Results of a phase-II trial. *J Cancer Res Clin Oncol* 2007;133:653–61.
- Molina B, Alonso L, Gonzalez-Vicent M, Andion M, Hernandez C, Lassaletta A, et al. High-dose busulfan and melphalan as conditioning regimen for autologous peripheral blood progenitor cell transplantation in high-risk neuroblastoma patients. *Pediatr Hematol Oncol* 2011;28:115–23.
- Egler RA, Burlingame SM, Nuchtern JG, Russell HV. Interleukin-6 and soluble interleukin-6 receptor levels as markers of disease extent and prognosis in neuroblastoma. *Clin Cancer Res* 2008;14:7028–34.
- Russell HV, Groshen SG, Ara T, DeClerck YA, Hawkins R, Jackson HA, et al. A phase I study of zoledronic acid and low-dose cyclophosphamide in recurrent/refractory neuroblastoma: a new approaches to neuroblastoma therapy (NANT) study. *Pediatr Blood Cancer* 2011;57:275–82.
- Iwase K, Nagasaka A, Nagatsu I, Kiuchi K, Nagatsu T, Funahashi H, et al. Tyrosine hydroxylase indicates cell differentiation of catecholamine biosynthesis in neuroendocrine tumors. *J Endocrinol Invest* 1994;17:235–9.
- Bowman T, Broome MA, Sinibaldi D, Wharton W, Pledger WJ, Sedivy JM, et al. Stat3-mediated Myc expression is required for Src transformation and PDGF-induced mitogenesis. *Proc Natl Acad Sci U S A* 2001;98:7319–24.
- Brodeur GM, Seeger RC, Schwab M, Varmus HE, Bishop JM. Amplification of N-myc in untreated human neuroblastomas correlates with advanced disease stage. *Science* 1984;224:1121–4.
- Gritsko T, Williams A, Turkson J, Kaneko S, Bowman T, Huang M, et al. Persistent activation of stat3 signaling induces survivin gene expression and confers resistance to apoptosis in human breast cancer cells. *Clin Cancer Res* 2006;12:11–9.
- Lassmann S, Schuster I, Walch A, Gobel H, Jutting U, Makowiec F, et al. STAT3 mRNA and protein expression in colorectal cancer: effects on STAT3-inducible targets linked to cell survival and proliferation. *J Clin Pathol* 2007;60:173–9.
- Miller MA, Ohashi K, Zhu X, McGrady P, London WB, Hogarty M, et al. Survivin mRNA levels are associated with biology of disease and patient survival in neuroblastoma: a report from the children's oncology group. *J Pediatr Hematol Oncol* 2006;28:412–7.
- Dalton WS. Drug resistance and drug development in multiple myeloma. *Semin Oncol* 2002;29:21–5.

43. Silverman AM, Nakata R, Shimada H, Sposto R, DeClerck YA. A galectin-3-dependent pathway upregulates interleukin-6 in the microenvironment of human neuroblastoma. *Cancer Res* 2012;72:2228–38.
44. Jones SA, Scheller J, Rose-John S. Therapeutic strategies for the clinical blockade of IL-6/gp130 signaling. *J Clin Invest* 2011;121:3375–83.
45. Stasi R, Brunetti M, Parma A, Di Giulio C, Terzoli E, Pagano A. The prognostic value of soluble interleukin-6 receptor in patients with multiple myeloma. *Cancer* 1998;82:1860–6.
46. Lee H, Deng J, Kujawski M, Yang C, Liu Y, Herrmann A, et al. STAT3-induced S1PR1 expression is crucial for persistent STAT3 activation in tumors. *Nat Med* 2010;16:1421–8.
47. Denardo DG, Brennan DJ, Rexhepaj E, Ruffell B, Shiao SL, Madden SF, et al. Leukocyte complexity predicts breast cancer survival and functionally regulates response to chemotherapy. *Cancer Discov* 2011;1:54–67.
48. Jinushi M, Chiba S, Yoshiyama H, Masutomi K, Kinoshita I, Dosaka-Akita H, et al. Tumor-associated macrophages regulate tumorigenicity and anticancer drug responses of cancer stem/initiating cells. *Proc Natl Acad Sci U S A* 2011;108:12425–30.
49. Kortylewski M, Xin H, Kujawski M, Lee H, Liu Y, Harris T, et al. Regulation of the IL-23 and IL-12 balance by Stat3 signaling in the tumor microenvironment. *Cancer Cell* 2009;114–23.
50. Jing N, Tweardy DJ. Targeting Stat3 in cancer therapy. *Anticancer Drugs* 2005;16:601–7.
51. Verstovsek S. Ruxolitinib: the first agent approved for myelofibrosis. *Clin Adv Hematol Oncol* 2012;10:111–3.

# Cancer Research

The Journal of Cancer Research (1916–1930) | The American Journal of Cancer (1931–1940)

## Critical Role of STAT3 in IL-6–Mediated Drug Resistance in Human Neuroblastoma

Tasnim Ara, Rie Nakata, Michael A. Sheard, et al.

*Cancer Res* 2013;73:3852-3864. Published OnlineFirst April 30, 2013.

**Updated version** Access the most recent version of this article at:  
doi:[10.1158/0008-5472.CAN-12-2353](https://doi.org/10.1158/0008-5472.CAN-12-2353)

**Supplementary Material** Access the most recent supplemental material at:  
<http://cancerres.aacrjournals.org/content/suppl/2013/04/30/0008-5472.CAN-12-2353.DC1.html>

**Cited articles** This article cites 49 articles, 15 of which you can access for free at:  
<http://cancerres.aacrjournals.org/content/73/13/3852.full.html#ref-list-1>

**Citing articles** This article has been cited by 9 HighWire-hosted articles. Access the articles at:  
<http://cancerres.aacrjournals.org/content/73/13/3852.full.html#related-urls>

**E-mail alerts** [Sign up to receive free email-alerts](#) related to this article or journal.

**Reprints and Subscriptions** To order reprints of this article or to subscribe to the journal, contact the AACR Publications Department at [pubs@aacr.org](mailto:pubs@aacr.org).

**Permissions** To request permission to re-use all or part of this article, contact the AACR Publications Department at [permissions@aacr.org](mailto:permissions@aacr.org).



ELSEVIER

Contents lists available at ScienceDirect

Cancer Letters

journal homepage: [www.elsevier.com/locate/canlet](http://www.elsevier.com/locate/canlet)

## Mini-review

## More than the genes, the tumor microenvironment in neuroblastoma

Lucia Borriello <sup>a,b,c</sup>, Robert C. Seeger <sup>a,b,c</sup>, Shahab Asgharzadeh <sup>a,b,c</sup>, Yves A. DeClerck <sup>a,b,c,d,\*</sup><sup>a</sup> Division of Hematology, Oncology and Blood and Marrow Transplantation, Children's Hospital Los Angeles, Los Angeles, CA 90027, USA<sup>b</sup> Department of Pediatrics, Keck School of Medicine of the University of Southern California, Los Angeles, CA, USA<sup>c</sup> The Saban Research Institute, Children's Hospital Los Angeles, Los Angeles, CA 90027, USA<sup>d</sup> Department of Biochemistry and Molecular Biology, Keck School of Medicine of the University of Southern California, Los Angeles, CA, USA

## ARTICLE INFO

## Keywords:

Neuroblastoma  
Tumor microenvironment  
Hallmarks of cancer  
Cell–cell communication

## ABSTRACT

Neuroblastoma is the second most common solid tumor in children. Since the seminal discovery of the role of amplification of the MYCN oncogene in the pathogenesis of neuroblastoma in the 1980s, much focus has been on the contribution of genetic alterations in the progression of this cancer. However it is now clear that not only genetic events play a role but that the tumor microenvironment (TME) substantially contributes to the biology of neuroblastoma. In this article, we present a comprehensive review of the literature on the contribution of the TME to the ten hallmarks of cancer in neuroblastoma and discuss the mechanisms of communication between neuroblastoma cells and the TME that underlie the influence of the TME on neuroblastoma progression. We end our review by discussing how the knowledge acquired over the last two decades in this field is now leading to new clinical trials targeting the TME.

© 2015 Elsevier Ireland Ltd. All rights reserved.

## Introduction: neuroblastoma, a cancer not solely driven by genetic events

Neuroblastoma is the second most common solid tumor in children and accounts for 8–10% of childhood cancers in the USA and Europe. This cancer derives from neuroepithelial cells that migrate from the neural crest to form the sympathetic nervous system [1]. Children affected with this disease typically present with a posterior, paraspinal mass in the adrenal gland or along the sympathetic chain in the chest or abdomen. In approximately 50% of children the disease presents as a locoregional tumor lacking amplification of the MYCN oncogene, and carries an excellent prognosis (>90% overall survival). However, the other half is considered clinically to be high-risk, either having tumors harboring MYCN amplification or being older (diagnosed in children older than 18 months of age) with metastatic disease irrespective of MYCN amplification. The children with high-risk disease have less than 50% chance of event-free long term survival despite an intensive therapy that combines myeloablative chemotherapy, radiation therapy, progenitor cell transplantation, surgery, isotretinoin and antibody-based immunotherapy [2,3]. The discovery in the early 1980s of a correlation between the amplification of the MYCN oncogene and advanced stage neuroblastoma [4–6] led to the anticipation of other genetic events. About

1–2% of patients with neuroblastoma have a family history of the disease and 2 specific genes, ALK and PHOX2B, have been shown to be mutated (gain of function in the case of ALK, loss of function in the case of PHOX2B) in 80% of the familial cases [7,8]. Genome-wide association studies further identified several gene polymorphisms associated with a low but significant risk of neuroblastoma, including BARD1, LMO1 and LIN28B [9]. However a recent genomic analysis of more than 200 neuroblastoma tumors revealed an unexpected low level of recurrent-driver mutations in neuroblastoma. These were mainly activation mutation and amplification of ALK (8% of the cases), activation mutations in PTPN11 (a tyrosine phosphatase), inactivating mutations in chromatin remodeling genes (ATRX and ARID1A) and activating mutations in NRAS in addition to amplification and activation mutations of MYCN [10–12]. A recent analysis in a subgroup of patients with MYCN non-amplified neuroblastoma revealed that metastatic neuroblastomas had higher infiltration of tumor-associated macrophages (TAM) than locoregional tumors. This analysis also revealed that metastatic tumors diagnosed in patients at age ≥18 months had higher expression of inflammation-related genes than those in patients diagnosed at age <18 months. Expression of genes representing TAMs (CD33/CD16/IL-10/FCGR3) in addition to IL-6 receptor (IL-6R) contributed to 25% of the accuracy of a novel 14-gene tumor classification score [13]. Infiltration with Th2-driven macrophages expressing CD163 and CD206 was also recently observed in a subset of high-risk neuroblastoma tumors with deletion of chromosome 11q and high levels of prostaglandin-synthase and elevated levels of PGE2 [14].

In this article we will review the multiple mechanisms by which the TME regulates tumor progression and metastasis in neuroblastoma, focusing on the contribution of innate (TAM, neutrophils, NK,

Abbreviations: TME, Tumor microenvironment; TAM, Tumor-associated macrophages; TAF, Tumor-associated fibroblasts; MSC, Mesenchymal stromal cells; BM, Bone marrow; ECM, Extracellular matrix.

\* Corresponding author. Tel.: +1 323 361 5648; fax: +1 323 361 4902.

E-mail address: [declerck@usc.edu](mailto:declerck@usc.edu) (Y.A. DeClerck).

<http://dx.doi.org/10.1016/j.canlet.2015.11.017>

0304-3835/© 2015 Elsevier Ireland Ltd. All rights reserved.

dendritic cells) and adaptive (T, B, and NKT) immune cells, tumor-associated fibroblasts (TAF), bone marrow-derived mesenchymal stromal cells (MSC), endothelial cells, Schwann cells, and the extracellular matrix (ECM). We will discuss various mechanisms of communication between neuroblastoma cells and the TME used by neuroblastoma cells to “educate” the TME and by TME cells to activate in neuroblastoma signaling pathways affecting their behavior. This review will conclude with a brief discussion on ongoing clinical trials in neuroblastoma patients that target the TME.

### Role of the TME in the hallmarks of neuroblastoma

In their article of 2011, Weinberg and Hanahan identified eight critical biological processes controlling cancer progression that they designated “Hallmarks” [15]. These include the ability (1) to sustain proliferative signals, (2) to evade growth-suppressors, (3) to invade and metastasize, (4) to enable replicative immortality, (5) to induce angiogenesis, (6) to resist cell death, (7) to escape immune destruction, and (8) to deregulate cellular metabolism. Genomic instability and tumor promoting inflammation were also recognized as two

enabling characteristics. The contribution of the TME to these ten fundamental characteristics of cancer is now evident [16]. It is reviewed in the case of neuroblastoma in this section (Fig. 1).

#### Ability to sustain proliferative signals

The growth of neuroblastoma cells is regulated by several growth factors that interact with specific receptor tyrosine kinases and non-receptor tyrosine kinases present at their surface. Among the most extensively studied are the neurotrophin receptors – TrkA/NTRK1, TrkB/NTRK2 and TrkC/NTRK3 – that bind to a family of cognate ligands including nerve growth factor (NGF), brain-derived neurotrophic factor (BDNF) and neurotrophin-3 (NT3), respectively [17]. These receptors have different effects on proliferation, and whereas the TrkA receptor limits proliferation and promotes differentiation, the TrkB receptor drives proliferation. Activation of these receptors can occur either by an autocrine mechanism by growth factors produced by neuroblastoma cells, by a paracrine mechanism or by autoactivation [18]. Much has been learned on how the TME could participate in the NGFs/NGFR pathway in controlling

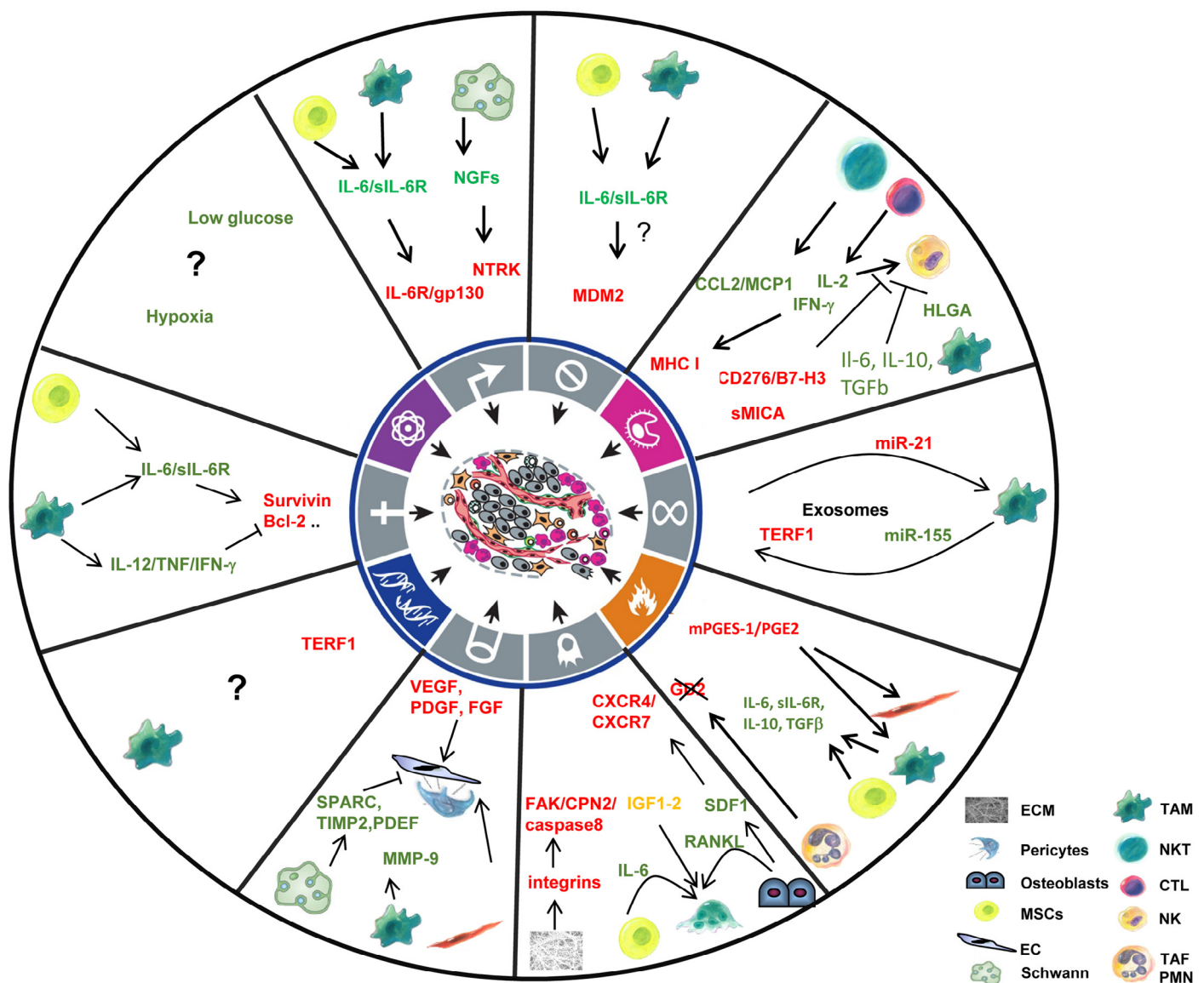


**Fig. 1.** Diagram summarizing the contribution of the cells and ECM in the TME to the ten hallmarks of cancer shown at the center of the wheel. The central graph was reproduced from Hanahan and Weinberg [15].

neuroblastoma cell proliferation from studies on spontaneous regression and differentiation of neuroblastoma tumors [19]. Many neuroblastoma tumors that spontaneously regress or differentiate like ganglioneuroblastoma have a stroma rich in Schwann cells, and although the origin of these cells remains controversial (normal cells that infiltrate the tumor vs. malignant cells sharing the same genetic abnormalities as tumor cells), these cells are an abundant source of NGF and other neurotrophins and cause immature MYCN-amplified (A) and non-amplified (NA) neuroblastoma cell lines to differentiate into benign ganglioneuroblastoma and ganglioneuroblastoma [20–22].

Another cytokine receptor whose function in neuroblastoma has been more recently elucidated is the receptor for interleukin-6 (IL-6R). High expression of this receptor in high-risk MYCN-NA human tumors was reported to be associated with poorer clinical outcomes [13]. Most human neuroblastoma cell lines (MYCN-A and NA) express both the gp130 and gp80 proteins that constitute the IL-6R [23]. They do not express the ligand IL-6 or the soluble agonistic IL-6 receptor (sIL-6R). However, MSC and TAM are an abundant source of IL-6 and sIL-6R in the TME and cooperate to activate signal transduction and activator of transcription (STAT)3 which promotes proliferation and survival in neuroblastoma cell lines [24].

The ECM also plays a role in controlling the growth of neuroblastoma cells. In most epithelial cancer an increased stiffness in the ECM (desmoplastic response) is associated with a stimulatory effect on cell proliferation [25], however it enhances neurogenesis, suppresses cell proliferation and reduces expression of MYCN in an MYCN-A cell line (SK-N-DZ), an effect that is enhanced by retinoic acid [26].

#### *Ability to evade growth-suppressors*

The major tumor suppressor pathway in neuroblastoma is p53. However, a striking feature is the low frequency (<2%) of TP53 mutations at diagnosis and even at recurrence [27]. In contrast, alteration of the MDM2 (a p53 inhibitor that promotes p53 degradation) pathway seems to be the mechanism allowing escape from tumor suppression [28]. Evidence that the TME can dysregulate this pathway is currently missing although there is evidence that IL-6 can upregulate MDM2 in transformed and non-transformed cells [29] but this has not been examined in neuroblastoma.

#### *Ability to enable replicative immortality*

Like most cancers, neuroblastoma tumors express high levels of telomerase, and such high levels are typically associated with MYCN amplification and poor outcome [30]. Although considered for long to be an intrinsic property of tumor cells, there has been recent evidence demonstrating that telomerase activity in human neuroblastoma cell lines could be controlled by the TME and in particular by inflammatory monocytes/macrophages. It has been shown that exosome-mediated transfer of miR-21 from neuroblastoma cells to monocytes induces the release of miR-155 containing exosomes captured by neuroblastoma cells. Once in neuroblastoma cells, miR-155 directly targets TERF1, an inhibitor of telomerase whose silencing increases telomerase activity promoting chemoresistance in xenograft tumors [31].

#### *Ability to invade and metastasize*

The bone marrow, bone and liver are the most common sites of distant metastasis in patients with stage 4 neuroblastoma [32]. Some of the mechanisms involved in bone marrow and bone metastasis have been unraveled. Most human neuroblastoma cell lines derived from patients with high-risk disease (MYCN-A and NA) express the CXCR4 and CXCR7 receptors for the chemokine CXCL12, also known as stromal-derived factor-1 (SDF-1) [33,34]. Expression of CXCR4

in primary tumors also correlates with bone and bone marrow metastasis [35]. CXCR4 expression is associated with highly aggressive undifferentiated tumors, while CXCR7 expression is present in more differentiated and mature tumors. Whereas CXCR4 overexpression in neuroblastoma cells favors dissemination to the liver and the lungs, CXCR7 strongly promotes homing to the adrenal gland and the liver, and co-expression of CXCR4 and CXCR7 receptors significantly and selectively increases neuroblastoma dissemination toward the bone marrow [36,37]. MSC and osteoblasts are a major source of CXCL12/SDF-1 and thus contribute to a microenvironment that promotes bone marrow and bone metastasis [38].

Bone metastasis in neuroblastoma is associated with a predominant osteolytic process led by activation of osteoclasts [39]. Here also the TME plays a critical role. In bone metastasis, secretion of IL-6 by MSC triggered by neuroblastoma cell lines is a major factor promoting osteoclast activation and bone degradation [40]. The production of insulin-like growth factors (IGF-) 1 and -2 by neuroblastoma cell lines and their release from the bone contribute to this process. IGF acts on type I growth factor receptor IGF-1R expressed by preosteoclasts and promotes their activation [41]. High expression of IGF-1R in neuroblastoma cell lines increases adherence and homing to bone and bone metastasis [42]. Preosteoclasts express the receptor activator of NFκB (RANK) which when interacting with RANK ligand (RANKL) produced by osteoblasts becomes activated and promotes osteoclast maturation and activity [43]. The mechanism of liver metastasis in neuroblastoma is much less understood although gastrin-releasing peptide receptor (GRP-R), expressed in metastatic neuroblastoma cells, may play a role. This receptor activates focal adhesion kinase (FAK), a critical downstream regulator of GRP-R that promotes liver metastasis. FAK expression correlates with GRP-R expression in tumors and cell lines (MYCN-A and NA) [44].

#### *Ability to promote tumor vascularization*

Both angiogenesis and vasculogenesis contribute to the vascularization of neuroblastoma tumors. As in most cancers, angiogenesis in neuroblastoma occurs through the production by tumor cells of several angiogenic factors such as vascular endothelial cell growth factor (VEGF), platelet-derived growth factor (PDGF) and fibroblast growth factor (FGF) whose expression correlates with MYCN amplification and other markers of aggressiveness [45,46]. MYC, being a master regulator of vascular remodeling, has an important paracrine function in angiogenesis [47,48]. MYC knock out in mice is embryonically lethal as a consequence of defective hematopoiesis and vasculogenesis and endogenous suppression of MYC in a pancreatic islet tumor model in mice causes tumor regression through vascular collapse [49]. In neuroblastoma, MYCN upregulates the expression of VEGF [50] and driving MYCN degradation with inhibitors of PI3K/mTOR inhibits tumor progression in TH-MYC transgenic mice, not only through MYCN downregulation but also through a paracrine blockade of angiogenesis [51]. There is also evidence that ALK controls angiogenesis via the production of VEGF as ALK knock-down in human neuroblastoma cell lines transduced with ALK mutant is associated with a marked reduction of VEGF secretion and blood vessel density in xenotransplanted tumors [52]. Although tumor cells are the main source of VEGF, murine and human neuroblastoma cell lines also stimulate the production of VEGF by MSC which promotes osteoblastogenesis through an intracrine mechanism [53]. Schwann cells, which are abundantly present in more differentiated stroma rich tumors, exert an anti-angiogenic function through the production of several inhibitors of angiogenesis such as tissue inhibitor of metalloproteinase 2 (TIMP-2), pigment-derived epithelial factor (PDEF) and secreted protein acidic rich in cysteine (SPARC) [54–56]. Whereas the presence of Schwann cells in tumors is typically associated with decreased vascularization, the

presence of TAF (also inversely related to the presence of Schwann cells) is associated with increased vascularity, thus suggesting that these 2 cell types control the balance of angiogenesis in neuroblastoma [57].

VEGFR2 expressing endothelial progenitor cells (EPC) are recruited to tumors from the bone marrow by a mechanism that is dependent on the production of matrix metalloproteinase-9 (MMP-9) by myeloid cells [58]. MMP-9 promotes the release of soluble c-kit ligand that is necessary for the transition of EPC from a quiescent to a proliferative state in the bone marrow. MMP-9 promotes the recruitment of pericytes into the vasculature [59,60].

#### *Ability to resist cell death*

Loss of caspase-8 expression by gene silencing or gene deletion is a common feature of aggressive and metastatic neuroblastoma cell lines and patient tumors which allows to avoid programmed cell death [61]. However, when present, caspase-8 has a second function that is regulated by the TME. Paradoxically caspase-8 can promote migration and metastasis in neuroblastoma cell lines (NB 5, 7 and 16) in a manner that is not dependent on its proteolytic and apoptotic activity but that is regulated by contact with the ECM. Upon integrin ligation to ECM proteins, caspase-8 forms a complex with FAK, calpain2/CPN2 and calpastatin which, by disrupting CPN2/calpastatin interaction, activates CPN2. Activation of CPN2 enhances the cleavage of focal adhesion substrates and migration of MYCN-A and MYCN-NA human neuroblastoma cells lines *in vitro* [62]. There is also evidence that the TME promotes survival in neuroblastoma cell lines by upregulating anti-apoptotic proteins. For example, activation of STAT3 by IL-6 and sIL-6R produced by MSC and TAM induces the expression of several pro-survival proteins like survivin, MCL-1 and Bcl-XL that cause resistance to chemotherapeutic agents [24]. In contrast, IL-12 produced by Th1-driven TAM increases apoptosis in orthotopic murine neuroblastoma tumor models via tumor necrosis (TNF)- $\alpha$  and interferon (IFN)- $\gamma$  which increase the expression of pro-apoptotic proteins, inhibit Akt phosphorylation and activate Bid [63].

#### *Ability to escape the immune system*

Neuroblastoma cells have developed multiple mechanisms to escape the immune system. Cell lines typically have low levels of expression of peptide presenting HLA class I molecules, which impairs target peptide recognition by cytotoxic T cells (CTL) [64–66]. The expression of major histocompatibility complex (MHC) I in neuroblastoma cell lines is controlled by the TME. For example, INF- $\gamma$  produced by NK, NKT and T cells increases the expression of MHC I [65,67] and activation of NTRK1/TrkA upon ligation with NGF leads to an increased immunogenicity by overexpression of MHC I proteins [68], whereas MYCN amplification causes a downregulation of MHC I [69]. Neuroblastoma cells also escape immune attack by CTL and NK cells by producing soluble MHC I related chain (sMICA) and by expressing CD276/B7-H3, a co-stimulatory protein, which inhibit activation of NK cells and T cells via interaction with their receptors. Downregulation of the NKG2D ligands observed in human primary tumors and cell lines also contributes to immune evasion [70,71]. Neuroblastoma cell lines (6 out of 12) express low levels of HLA-G but induce monocytes to release soluble HLA-G, a protein that induces immune tolerance during pregnancy and is a ligand for the NK cell inhibitory receptor KIR2DL4 [72]. TAM further contribute to this immunosuppressive environment because they are a source of secreted immunosuppressive cytokines including IL-6, IL-10, and transforming growth factor (TGF) $\beta$ 1. Despite this suppressive environment, NK cells, which in contrast to CTL do not depend on the expression of MHC I proteins on tumor cells, may be more effective although they still can be inhibited. Type 1 NKT

cells do not depend on CD1d expression in neuroblastoma cells to be active in tumors [73]. When activated by IL-2, NK cells secrete IFN- $\gamma$  and become cytotoxic via perforin-dependent and independent mechanisms [74]. Activated NKT cells secrete IL-2 which in turn activates NK cells [73] and eliminates TAM [75].

There is evidence that MYCN has a paracrine regulatory role on immune cells in the TME. For example, MYCN downregulates CCL2/MCP-1 (macrophage chemoattractant protein) which attracts NKT cells in tumors [76,77]. The contribution of immune check points such as PD-1/PD-L1 and CTLA-4/B7-1 to immunosuppression has just begun to be explored. In murine neuroblastoma models mAb targeting 4-1BB, CD40 and CTLA-4 induces tumor regression [78]. There is also pre-clinical evidence that PDL-1 blockade potentiates immunogenicity of human neuroblastoma cell lines [79].

#### *Ability to deregulate cellular metabolism*

Many cancers preferentially meet their energy requirements through the glycolytic pathway rather than via the more efficient oxidative phosphorylation pathway (the Warburg effect). Human neuroblastoma cell lines (MYCN-A and NA) *in vitro* preferentially use the glycolytic pathway in a way that is not dependent on MYCN [80]. The contribution of the TME to this effect has not been well explored and is thus poorly understood. There is some suggestion that dietary restriction leading toward low glucose concentration may inhibit the Warburg effect and increase cytotoxicity in neuroblastoma cell lines [81].

#### *Genomic instability*

Genomic instability has been extensively studied in neuroblastoma as discussed in our introduction. There is however little evidence so far that genomic instability can be affected by the TME. Considering that telomere-dependent chromosomal instability is highly prevalent in aggressive MYCN-NA neuroblastoma [82], it is conceivable that it could be affected by regulators of telomerase such as TERF1, whose expression in neuroblastoma cell lines has been shown to be dependent on an interactive loop between neuroblastoma cells and TAM [31].

#### *Induction of a pro-tumorigenic inflammation*

Innate immune cells such as monocytes/macrophages and neutrophils can create in neuroblastoma tumors an inflammatory environment that affects tumor progression and metastasis. There is evidence that neuroblastoma cells educate TAM toward a Th2-driven phenotype that supports their progression. The presence of macrophages in neuroblastoma tumors is an indicator of poor outcome and more aggressive disease in MYCN-NA high risk tumors [13,14], and blocking macrophage stimulatory factor (CSF-1) in CSF-1 negative xenotransplanted neuroblastoma tumors extends survival in tumor-bearing mice [83]. The presence of these macrophages is also associated with elevated levels of PGE2 and the presence of cancer-associated fibroblasts [14]. In contrast, neutrophils can be cytotoxic and inhibit the growth of human neuroblastoma cell lines (GD2 positive and negative) when in the presence of a chimeric anti-GD2 antibody but promote tumor cell growth in the absence of such antibody or if GD2 is not expressed [84,85].

There is thus growing evidence that the TME plays a regulatory role in neuroblastoma progression. The ultimate effect however is the result of dynamic and complex interactions between neuroblastoma cells and TME cells, leading toward an environment that is pro- or anti-tumorigenic. In the next section, we will review several mechanisms of communication between neuroblastoma cells and TME cells and the ECM that regulate these interactions (Fig. 2).

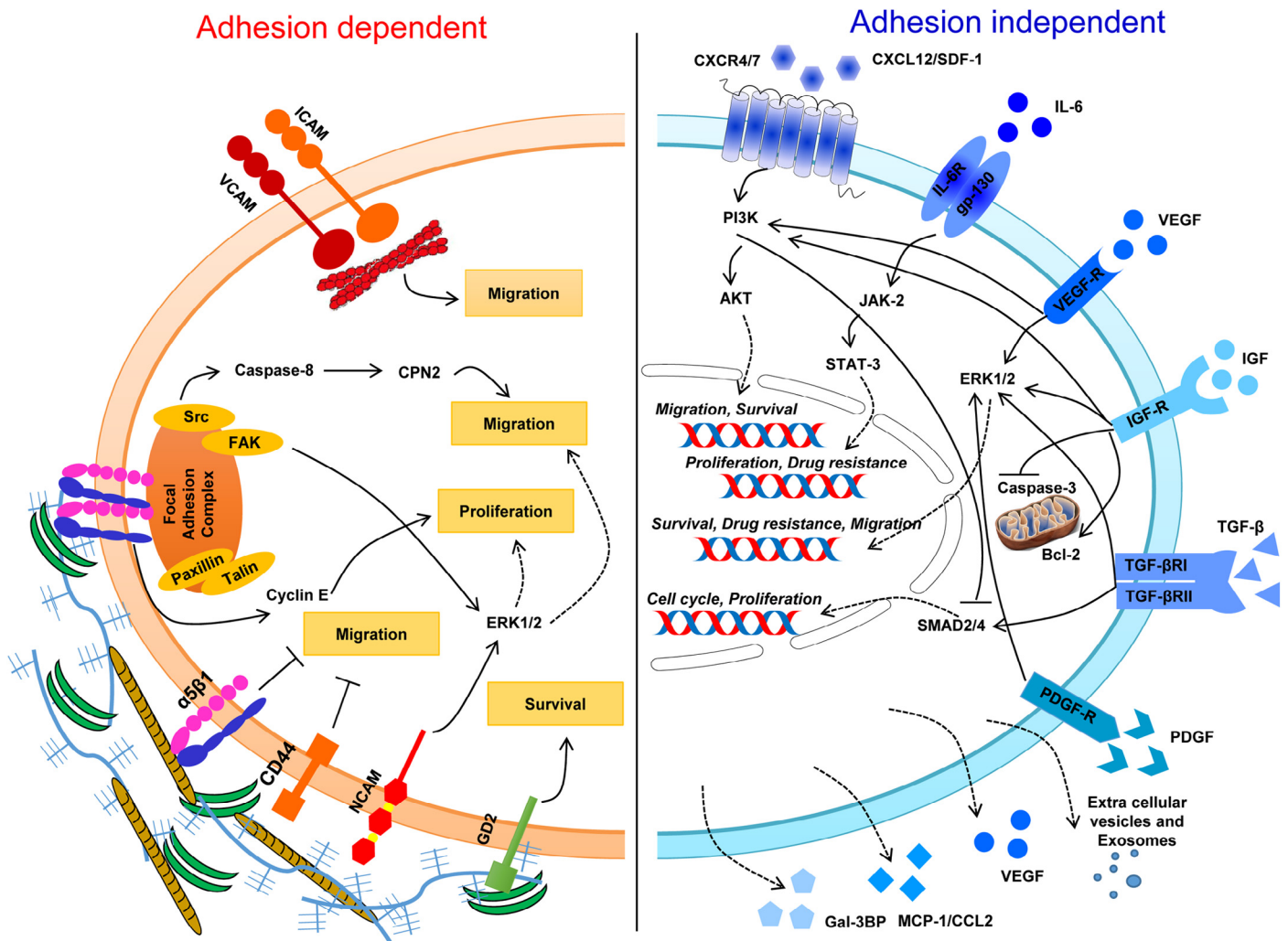


Fig. 2. Diagram summarizing the major mechanisms of communication between neuroblastoma cells and TME cells and the ECM and pathways they activate in neuroblastoma cells.

### Mechanisms of communication between neuroblastoma cells and TME cells

The reciprocal communication between neuroblastoma cells and the TME is based on 2 fundamental types of mechanism, (i) adhesion-dependent mechanisms that involve a contact between tumor cells and TME cells (cell-cell contact) or between tumor cells and components of the ECM (cell-ECM contact); and (ii) adhesion-independent mechanisms through the production of soluble products.

#### Adhesion-dependent mechanisms

##### Cell-TME contact

Neuroblastoma cell lines (SK-N-SH and LAN-1) are able to interact directly with endothelial cells [86] and leukocytes [87] as they express cell adhesion molecules (CAM) of the IgG superfamily like VCAM-1 and ICAM-1 which promote cell migration and metastasis. The expression of VCAM-1 and ICAM-1 in neuroblastoma cell lines (SK-N-SH and SK-N-MC) is upregulated by inflammatory cytokines, such as TNF- $\alpha$  and IFN- $\gamma$  [88].

Neuroblastoma cells express CD56/NCAM which mediates their interaction with CD56/NCAM positive NK cells. It has been suggested

that such interaction augments tumor cell lysis by NK cells but the importance of such function is not entirely clear [89-91].

##### Cell-ECM contact

Neuroblastoma cells interact with the ECM through the expression of several integrins. The effect that integrins have on neuroblastoma progression depends on the type of integrin expressed and the type of ECM protein involved. For example, the integrin  $\alpha 5 \beta 1$  that mediates adhesion to collagen and fibronectin has an inhibitory function on migration. *In vitro* substrate adherent (S-type) neuroblastoma cells with high levels of  $\alpha 5 \beta 1$  are less migratory and tumorigenic, whereas neuroblastic (N-type) neuroblastoma cells with low levels of integrin  $\alpha 5 \beta 1$  do not attach to fibronectin and collagen IV, and are more migratory and tumorigenic. Consistently, blocking of  $\alpha 5 \beta 1$  integrin in S-type cells promotes migration and the overexpression of  $\alpha 5 \beta 1$  integrin into N-type cells increases their attachment to fibronectin and collagen IV and inhibits migration [92,93]. IGF-1R stimulation decreases  $\beta 1$ -integrin promoting cell migration and invasion [94]. There is also a reverse correlation between  $\beta 1$  integrin and MYCN expression and progression in neuroblastoma cell lines and xenografts. Over-expression of MYCN in transfected SK-N-SH cells downregulates the expression of  $\beta 1$  integrin [95,96]. Consistently, human neuroblastoma

tumors with good prognosis have a high expression of  $\alpha 5\beta 1$  integrin, whereas in tumors that originate from patients with metastatic disease there is a lack of  $\alpha 5\beta 1$  integrin expression and high level of  $\alpha v\beta 3$  integrin [97].

Other integrins promote migration. This is the case of  $\alpha 3\beta 1$  and  $\alpha 1\beta 1$  integrins that interact with laminin promoting migration but also neurite outgrowth in the N-type SH-SY5Y human neuroblastoma cell line in a manner that is dependent on O-mannosyl-linked glycosylation events [98,99]. Binding of integrins to ECM proteins activates FAK and Src [100]. FAK-Src activation stimulates neuroblastoma cell motility but also recruits several adapter proteins such as talin and paxillin as well as the protease CPN2/calpain [101]. As previously discussed, caspase-8 is also recruited in this complex, is inactivated by Src-dependent phosphorylation of Tyr380 and activates CPN2, which promotes cell migration in apoptosis resistant cells [62,102,103]. Binding of integrins to fibronectin in mouse neuroblastoma cell lines also promotes the activation of cyclin E and cell proliferation [104].  $\alpha 4$  integrin is more frequently expressed in MYCN-NA human neuroblastoma cell lines and is selectively associated with a poorer outcome in MYCN-NA tumors. It interacts with an alternatively spliced variant of fibronectin, as well as with VCAM-1 promoting migration *in vitro* and metastasis *in vivo* [105].

CD44, a transmembrane glycoprotein that mediates cell adhesion to hyaluronan, is expressed by neuroblastoma cells. Its expression correlates with a non-metastatic phenotype and is commonly seen in MYCN-NA neuroblastoma tumors [106,107]. MYCN-A neuroblastoma cell lines (SHEP and ACN) do not express CD44 or express a non-functional variant of CD44 that does not bind to hyaluronan [108].

Disialoganglioside (GD2), a surface glycolipid present on neurons, peripheral nerve fibers, and skin melanocytes, is highly expressed in primary neuroblastoma tumors and is a target for immunotherapy [109]. GD2 facilitates the attachment of tumor cells to ECM proteins such as collagen, vitronectin, laminin, and fibronectin [110,111], which is blocked by the anti-GD2 mAb 14G2a leading to cell death [112].

#### Adhesion-independent mechanisms

The reciprocal communication between neuroblastoma cells and TME cells also involves soluble products providing paracrine and distant mechanisms of communication. Whereas much of the focus has been on the contribution of proteins there has been recent evidence that extracellular vesicles (EV) carrying not only proteins but also DNA and RNA could play an important role [31]. In this section, we will focus on some of the major chemokines, cytokines and growth factors specifically involved in paracrine interaction between neuroblastoma cells and stromal cells, illustrating how they are used by TME cells to activate specific signaling pathways in tumor cells and how they are used by tumor cells to “educate” the TME.

#### Axes of communication from TME cells to tumor cells

**CXCL12/CXCR4/Akt axis.** As previously discussed, the chemokine CXCL12/SDF-1, produced by MSC and osteoblasts in the bone marrow niche, plays an important role in the establishment of distant metastasis by attracting neuroblastoma cells that express CXCR4 and CXCR7 [38]. Interaction between CXCL12/SDF-1 with its receptor CXCR4 induces cell migration, proliferation and survival in an Akt-dependent mechanism that is inhibited by dipeptidyl peptidase IV, a cell surface serine protease present in some neuroblastoma cell lines [113].

**IL-6/IL-6R/STAT3 axis.** Neuroblastoma cell lines do not make IL-6, but upregulate its expression by MSC and TAM. In addition to activating osteoclasts and promoting osteolytic bone metastasis [40],

IL-6 binding to its receptor IL-6R expressed by neuroblastoma cell lines exerts a pro-tumorigenic effect on tumor cells, enhancing growth, survival and drug resistance in a STAT3-dependent mechanism [23,24].

**VEGF/VEGFR/Akt and ERK1/2 axis.** Among the growth factors involved in the interaction between neuroblastoma cells and stromal cells is VEGF. Neuroblastoma cell lines, in particular MYCN-A, produce large amounts of VEGF but also stimulate its production in TME cells. Several studies reported the expression of VEGF receptors, primarily neuropilin-1 and 2, in neuroblastoma cell lines and some expression of VEGFR1 and VEGFR2 mRNA in state III tumors [114–117]. VEGF promotes cell survival of neuroblastoma cells via the PI3K/Akt pathway [118] and resistance to etoposide by activating ERK1/2 and upregulating BCL-2 [119].

**IGF-1/IGFR/ERK1/2 and PI3K/Akt axis.** IGF-1 is secreted by many cells including MSC [120] and endothelial cells [121]. It is also released from the bone matrix during osteolysis [122]. N-type neuroblastoma cell lines express the IGF-1 receptor (IGF-1R) [42]. Binding of IGF-1 to its receptor activates ERK1/2 and PI3K/Akt and promotes cell migration [94,123–125] and homing in the bone marrow [42]. It also stimulates neuroblastoma cell survival in SHEP cells and protects them from apoptosis through the upregulation of BCL-2 and inhibition of caspase-3 [126]. This effect could be particularly significant in MYCN-A neuroblastoma cell lines since there is an increased expression of IGF-1R in MYCN-transfected cells [127].

**TGF- $\beta$ /TGFB $\beta$ /SMAD axis.** TGF- $\beta$  is secreted by many TME cells such as MSC and TAM, and is also released in the bone environment upon bone degradation [128–131]. In addition to being a potent inhibitor of the immune system, TGF- $\beta$  directly acts on neuroblastoma cells by affecting proliferation and differentiation in a way that depends on the receptors expressed. Neuroblastoma cells express various levels of TGFB $\beta$  (I, II and III) with expression of TGFB $\beta$ II and III being inversely correlated with poor outcome. Consistently, TGF- $\beta$  inhibits cell proliferation in human neuroblastoma cell lines expressing type II and III receptors [131] and overexpression of TGFB $\beta$ II suppresses tumorigenesis [132]. TGFB $\beta$ III promotes differentiation and suppresses neuroblastoma proliferation whereas TGFB $\beta$ I only promotes differentiation [132]. Furthermore, evidence that PI3K/Akt negatively regulates SMAD2/4 signaling in neuroblastoma suggests that an imbalance between PI3K/Akt and TGF- $\beta$ /SMAD signaling is a mechanism promoting tumorigenesis in neuroblastoma [133].

**PDGF/PDGF-R and PI3K/Akt and ERK1/2 axis.** PDGF is secreted by endothelial cells [134], preosteoclasts [135], and can interact with neuroblastoma cell lines that express PDGFR. PDGFR activation stimulates migration, invasion and proliferation in PI3K and ERK dependent mechanisms [136].

#### Soluble products secreted by neuroblastoma cells that “educate” TME cells

Much less is known of the soluble products released by neuroblastoma cells that interact and educate TME cells. The contribution of neuroblastoma-derived VEGF to the autocrine (neuroblastoma cells) and paracrine (endothelial cells, MSC) activation of signaling pathways promoting tumor cell growth and angiogenesis is well known and has been discussed previously. Neuroblastoma cells secrete MCP-1/CCL2 that interacts with the CCR2 receptor expressed by type I NKT cells which attracts them in the tumor. The expression of MCP-1 by neuroblastoma cells is downregulated by MYCN thus preventing the recruitment of type I NKT cells and contributing to immune escape [76].

Human neuroblastoma cell lines produce galectin-3 binding protein (Gal-3BP), a sialoglycoprotein also present in neuroblastoma

tumors that interacts with galectin-3 present in TME cells such as TAM and MSC. Gal-3BP interaction with Gal-3 induces the transcriptional activation of IL-6 in a RAS/MEK/ERK-dependent mechanism [137,138].

There is also recent evidence that the secretion of extracellular vesicles including exosomes by tumor cells is a mechanism used to educate TME cells and, for example, to induce the establishment of a pre-metastatic niche [139]. These vesicles contain a large variety of proteins, lipids, metabolites and nucleic acids including regulatory miR that act as shuttles mediating the communication between tumor cells and stromal cells in both directions. The protein content of the cargo of exosomes from several neuroblastoma cells includes, in addition to the exosomal markers (CD63, CD9, CD81, Hsp70, Hsp 90, Alix), GD2 disialoganglioside and proteins involved in tumor progression such as CD147, a multifunctional protein involved in invasion and metastasis, and CD276/B7-H3, an immune checkpoint protein that protects neuroblastoma cells from attack by NK cells [140]. The profile of miR content of exosome-like particles from two MYCN-A neuroblastoma cell lines was also recently reported showing that the exosomal miRNAs are associated with a range of cellular and molecular functions related to cell growth, cancer progression and drug resistance [31,141].

## Therapeutic consideration

With a better knowledge of the contribution of the TME to neuroblastoma progression and of its mechanisms, clinical trials testing agents targeting the TME have been initiated. These trials follow three main strategies including (1) Direct targeting of TME cells that contribute to a pro-tumorigenic environment, (2) Targeting signaling pathways activated by the TME in tumor cells or in TME cells (or both), and (3) Immunotherapy. A complete discussion of these strategies is beyond the scope of this review article but a few illustrative examples of ongoing Phase I/II clinical trials are given in Table 1.

### Strategies targeting TME cells

Targeting osteoclasts with bisphosphonates like zoledronic acid has been tested in patients with bone metastasis and the results of a Phase I trial completed by the New Advances in Neuroblastoma Therapy (NANT) consortium demonstrated the safety and efficacy of zoledronic acid [142]. This agent is now tested with cyclophosphamide in a Phase I clinical trial by Baylor College of Medicine (NCT00206388) and in combination with Interleukin-2 in

**Table 1**

Registered Phase I/II clinical trials in neuroblastoma that target the TME. The list was generated from data on [clinicaltrials.gov](http://clinicaltrials.gov).

Category	Pathway(s)	Molecular target(s)	Study	Phase	Sponsor	Number of clinical trial
Tumor microenvironment	Osteoclast survival	Farnesyl pyrophosphate synthase	Zoledronic Acid (ZOMETA) With Cyclophosphamide With Neuroblastoma and Cortical Bone Involvement	Phase I	Baylor College of Medicine	<b>NCT00206388</b>
	Osteoclast survival	Farnesyl pyrophosphate synthase	Pilot Study of Zoledronic Acid and Interleukin-2 for Refractory Pediatric Neuroblastoma	Phase I	University of Alabama at Birmingham	<b>NCT01404702</b>
	VEGF signaling and osteoclast survival	VEGF and farnesyl pyrophosphate synthase	N2007-02: Bevacizumab, Cyclophosphamide, & Zoledronic Acid in Patients W/Recurrent or Refractory High-Risk Neuroblastoma	Phase I	New Approaches to Neuroblastoma Therapy Consortium	<b>NCT00885326</b>
Pathways activated by the TME	MAPK and STAT signaling	RAF/MEK/ERK and STAT-3	Sorafenib and Cyclophosphamide/Topotecan in Patients With Relapsed and Refractory Neuroblastoma (N2013-02)	Phase I	New Approaches to Neuroblastoma Therapy Consortium	<b>NCT02298348</b>
	VEGFR and EGFR signaling	VEGFR and EGFR signaling	ZD6474 Alone and in Combination With Retinoic Acid in Pediatric Neuroblastoma	Phase I	M.D. Anderson Cancer Center	<b>NCT00533169</b>
	JAK/STAT and FLT3 signaling	JAK-2, TrkA, TrkB, TrkC,	N2001-03: CEP-701 in Treating Young Patients With Recurrent or Refractory High-Risk Neuroblastoma	Phase I	New Approaches to Neuroblastoma Therapy Consortium	<b>NCT00084422</b>
	MEK/MAPK signaling	Topoisomerase II-β and MEK/MAPK	R(+)-XK469 in Treating Patients With Advanced Neuroblastoma	Phase I	National Cancer Institute	<b>NCT00028522</b>
	AKT signaling	mTOR	Irinotecan Hydrochloride and Temozolomide With Temsirolimus or Dinutuximab in Treating Younger Patients With Refractory or Relapsed Neuroblastoma	Phase II	National Cancer Institute	<b>NCT01767194</b>
	AKT signaling	PI3K and mTOR	SF1126 for Patients With Relapsed for Refractory Neuroblastoma	Phase I	New Approaches to Neuroblastoma Therapy Consortium	<b>NCT02337309</b>
Immunotherapy	AKT signaling and Src family tyrosine kinase	mTOR and BCR/ABL and Src tyrosine kinases	Multimodal Molecular Targeted Therapy to Treat Relapsed or Refractory High-risk Neuroblastoma	Phase II	University of Regensburg	<b>NCT01467986</b>
	GD2	GD2	Monoclonal Antibody 3F8 and Sargramostim in Treating Patients With Neuroblastoma	Phase II	Memorial Sloan Kettering Cancer Center	<b>NCT00072358</b>
	GD2	GD2	Monoclonal Antibody 3F8 and GM-CSF in Treating Young Patients With High-Risk, Refractory or Relapsed Neuroblastoma	Phase I	Memorial Sloan Kettering Cancer Center	<b>NCT00450307</b>
	GD2	GD2	Activated T Cells Armed With GD2 Bispecific Antibody in Children and Young Adults With Neuroblastoma and Osteosarcoma	Phase II	Barbara Ann Karmanos Cancer Institute	<b>NCT02173093</b>

refractory neuroblastoma by University of Alabama at Birmingham (NCT01404702).

Targeting endothelial cells in neuroblastoma has also been tested and a Phase I trial with bevacizumab, cyclophosphamide and zoledronic acid in patients with recurrent or refractory high-risk neuroblastoma has been recently completed by the NANT consortium (NCT00885326).

#### *Strategies targeting pathways activated by the TME*

These strategies typically combine a small molecule inhibitor of a signaling pathway with standard therapy. For example, sorafenib, a broad spectrum kinase inhibitor with pre-clinical activity in neuroblastoma [143,144], is presently tested in Phase I in combination with cyclophosphamide and topotecan in patients with relapsed and refractory neuroblastoma by NANT (NCT02298348). ZD6474, an inhibitor of VEGFR and EGFR, is also tested in Phase I alone and in combination with retinoic acid in neuroblastoma by M.D. Anderson Cancer Center (NCT00533169). Lestaurtinib (CEP-701), an inhibitor of JAK-2, TrkA, TrkB and TrkC, is actually tested in Phase I in young patients with recurrent or refractory high-risk neuroblastoma by NANT (NCT00084422). R(+)-XK469, an inhibitor of topoisomerase II- $\beta$  and MEK/MAPK signaling kinases, is used in treating patients with advanced neuroblastoma in Phase I by NCI (NCT00028522). Temsirolimus, a rapamycin analog inhibitor of the Akt pathway, is presently tested in combination with irinotecan and temozolomide in patients with relapsed pediatric solid tumors including neuroblastoma [145] by the NCI (NCT01767194). SF1126, a dual PI3K/Akt and mTOR inhibitor, is tested in patients with refractory/recurrent neuroblastoma (NCT02337309). In addition, a combination of Rapamycin, mTOR inhibitor, with dasatinib is currently tested in patients with relapsed or refractory high-risk Neuroblastoma by the University of Regensburg (NCT01467986).

#### *Immunotherapies*

Whereas the human-mouse chimeric 14:18 anti-GD2 monoclonal antibody is now part of the standard therapy of neuroblastoma [3], other anti-GD2 antibodies are tested. The monoclonal antibody 3F8 is currently tested in a Phase II trial in combination with sargramostim in patients with neuroblastoma (NCT00072358). In addition, another clinical trial sponsored by Memorial Sloan Kettering Cancer Center is testing the antibody 3F8 in combination with GM-CSF (NCT00450307) [146]. The same antibody 3F8 coated in T cells to promote cytotoxicity is also the subject of a Phase I trial. Activated T cells armed with a GD2 bispecific antibody are tested in Phase I in children and young adults with neuroblastoma at the Barbara Ann Karmanos Cancer Institute (NCT02173093). New strategies using immunomodulators like lenalidomide [147], vaccine therapy and engineered T cells and NK cells are planned, often in combination with anti-GD2 immunotherapy, by several groups [148–150]. This is an area of intensive investigation.

#### **Conclusion**

After much focus on genetic aspects of neuroblastoma biology in the late 1990s and early 2000s, it is now clear that neuroblastoma is truly a disease of the seed and the soil, and that the TME significantly contributes in a favorable or unfavorable way to its progression. The observations summarized in this article raised the interesting and unexplored question of the potential interaction between genetic driver events in neuroblastoma and their influence through paracrine mechanisms on the TME. In other words, do genetic alterations in the seeds have the ability to influence the soil in a way that is critical for their development and survival? We have reviewed some evidence, for example, that MYCN and ALK

could exert a paracrine control on angiogenesis. Thus targeting MYCN will have a dual effect on the seed and the soil.

As we better appreciate the tremendous level of complexity in the interactions between neuroblastoma cells and the TME, the challenge will be to distinguish interactions that play a more dominant role affecting both tumor and TME cells from those that have a less important function, to identify effective agents for these pathways and to develop biomarkers to monitor their effects. The study of the TME in neuroblastoma will continue to be an important field of investigation that lead to new therapies.

#### **Acknowledgments**

This article was supported in part by grant U54 CA163117 from the National Institutes of Health and by grant W81XWH-12-1-0571 from the Department of the Army to Y.A. DeClerck. L. Borriello is supported by a fellowship from The Saban Research Institute of Children's Hospital Los Angeles.

#### **Conflict of interest**

None.

#### **References**

- [1] N.K. Cheung, M.A. Dyer, Neuroblastoma: developmental biology, cancer genomics and immunotherapy, *Nat. Rev. Cancer* 13 (2013) 397–411.
- [2] K.K. Matthay, J.G. Villablanca, R.C. Seeger, D.O. Stram, R.E. Harris, N.K. Ramsay, et al., Treatment of high-risk neuroblastoma with intensive chemotherapy, radiotherapy, autologous bone marrow transplantation, and 13-cis-retinoic acid. Children's Cancer Group, *N. Engl. J. Med.* 341 (1999) 1165–1173.
- [3] A.L. Yu, A.L. Gilman, M.F. Ozkaynak, W.B. London, S.G. Kreissman, H.X. Chen, et al., Anti-GD2 antibody with GM-CSF, interleukin-2, and isotretinoin for neuroblastoma, *N. Engl. J. Med.* 363 (2010) 1324–1334.
- [4] M. Schwab, K. Alitalo, K.H. Klempnauer, H.E. Varmus, J.M. Bishop, F. Gilbert, et al., Amplified DNA with limited homology to myc cellular oncogene is shared by human neuroblastoma cell lines and a neuroblastoma tumour, *Nature* 305 (1983) 245–248.
- [5] G.M. Brodeur, R.C. Seeger, M. Schwab, H.E. Varmus, J.M. Bishop, Amplification of N-myc in untreated human neuroblastomas correlates with advanced disease stage, *Science* 224 (1984) 1121–1124.
- [6] R.C. Seeger, G.M. Brodeur, H. Sather, A. Dalton, S.E. Siegel, K.Y. Wong, et al., Association of multiple copies of the N-myc oncogene with rapid progression of neuroblastomas, *N. Engl. J. Med.* 313 (1985) 1111–1116.
- [7] I. Janoueix-Lerosey, D. Lequin, L. Brugieres, A. Ribeiro, L. de Pontual, V. Combaret, et al., Somatic and germline activating mutations of the ALK kinase receptor in neuroblastoma, *Nature* 455 (2008) 967–970.
- [8] D. Trochet, F. Bourdeaut, I. Janoueix-Lerosey, A. Deville, L. de Pontual, G. Schleiermacher, et al., Germline mutations of the paired-like homeobox 2B (PHOX2B) gene in neuroblastoma, *Am. J. Hum. Genet.* 74 (2004) 761–764.
- [9] L.B. Nguyen, S.J. Diskin, M. Capasso, K. Wang, M.A. Diamond, J. Glessner, et al., Phenotype restricted genome-wide association study using a gene-centric approach identifies three low-risk neuroblastoma susceptibility loci, *PLoS Genet.* 7 (2011) e1002026.
- [10] T.J. Pugh, O. Morozova, E.F. Attiyeh, S. Asgharzadeh, J.S. Wei, D. Auclair, et al., The genetic landscape of high-risk neuroblastoma, *Nat. Genet.* 45 (2013) 279–284.
- [11] N.K. Cheung, J. Zhang, C. Lu, M. Parker, A. Bahrami, S.K. Tickoo, et al., Association of age at diagnosis and genetic mutations in patients with neuroblastoma, *JAMA* 307 (2012) 1062–1071.
- [12] L.J. Valentijn, J. Koster, F. Haneveld, R.A. Aissa, P. van Sluis, M.E. Broekmans, et al., Functional MYCN signature predicts outcome of neuroblastoma irrespective of MYCN amplification, *Proc. Natl. Acad. Sci. U.S.A.* 109 (2012) 19190–19195.
- [13] S. Asgharzadeh, J.A. Salo, L. Ji, A. Oberthuer, M. Fischer, F. Berthold, et al., Clinical significance of tumor-associated inflammatory cells in metastatic neuroblastoma, *J. Clin. Oncol.* 30 (2012) 3525–3532.
- [14] K. Larsson, A. Kock, H. Idborg, M. Arsenian Henriksson, T. Martinsson, J.I. Johnsen, et al., COX/mPGES-1/PGE2 pathway depicts an inflammatory-dependent high-risk neuroblastoma subset, *Proc. Natl. Acad. Sci. U.S.A.* 112 (2015) 8070–8075.
- [15] D. Hanahan, R.A. Weinberg, Hallmarks of cancer: the next generation, *Cell* 144 (2011) 646–674.
- [16] D. Hanahan, L.M. Coussens, Accessories to the crime: functions of cells recruited to the tumor microenvironment, *Cancer Cell* 21 (2012) 309–322.
- [17] G.M. Brodeur, Neuroblastoma: the biological insights into a clinical enigma, *Nat. Rev. Cancer* 3 (2003) 203–216.

- [18] G.M. Brodeur, J.E. Minturn, R. Ho, A.M. Simpson, R. Iyer, C.R. Varela, et al., Trk receptor expression and inhibition in neuroblastomas, *Clin. Cancer Res.* 15 (2009) 3244–3250.
- [19] G.M. Brodeur, R. Bagatell, Mechanisms of neuroblastoma regression, *Nat. Rev. Clin. Oncol.* 11 (2014) 704–713.
- [20] I.M. Ambros, A. Zellner, B. Roald, G. Amann, R. Ladenstein, D. Printz, et al., Role of ploidy, chromosome 1p, and Schwann cells in the maturation of neuroblastoma [see comments], *N. Engl. J. Med.* 334 (1996) 1505–1511.
- [21] G.M. Brodeur, Schwann cells as antineuroblastoma agents, *N. Engl. J. Med.* 334 (1996) 1537–1539.
- [22] J.L. Kwiatkowski, J.L. Rutkowski, D.J. Yamashiro, G.I. Tennekoon, G.M. Brodeur, Schwann cell-conditioned medium promotes neuroblastoma survival and differentiation, *Cancer Res.* 58 (1998) 4602–4606.
- [23] T. Ara, L. Song, H. Shimada, N. Keshelava, H.V. Russell, L.S. Metelitsa, et al., Interleukin-6 in the bone marrow microenvironment promotes the growth and survival of neuroblastoma cells, *Cancer Res.* 69 (2009) 329–337.
- [24] T. Ara, R. Nakata, M.A. Sheard, H. Shimada, R. Buettner, S.G. Groshen, et al., Critical role of STAT3 in IL-6-mediated drug resistance in human neuroblastoma, *Cancer Res.* 73 (2013) 3852–3864.
- [25] V.M. Weaver, C.D. Roskelley, Extracellular matrix: the central regulator of cell and tissue homeostasis, *Trends Cell Biol.* 7 (1997) 40–42.
- [26] W.A. Lam, L. Cao, V. Umesh, A.J. Keung, S. Sen, S. Kumar, Extracellular matrix rigidity modulates neuroblastoma cell differentiation and N-myc expression, *Mol. Cancer* 9 (2010) 35.
- [27] D.A. Tweddle, A.D. Pearson, M. Haber, M.D. Norris, C. Xue, C. Flemming, et al., The p53 pathway and its inactivation in neuroblastoma, *Cancer Lett.* 197 (2003) 93–98.
- [28] T. Van Maerken, J. Vandesompele, A. Rihani, A. De Paepe, F. Speleman, Escape from p53-mediated tumor surveillance in neuroblastoma: switching off the p14(ARF)-MDM2-p53 axis, *Cell Death Differ.* 16 (2009) 1563–1572.
- [29] E. Brighenti, C. Calabrese, G. Liguori, F.A. Giannone, D. Tere, L. Montanaro, et al., Interleukin 6 downregulates p53 expression and activity by stimulating ribosome biogenesis: a new pathway connecting inflammation to cancer, *Oncogene* 33 (2014) 4396–4406.
- [30] E. Hiyama, K. Hiyama, T. Yokoyama, Y. Matsuura, M.A. Piatyszek, J.W. Shay, Correlating telomerase activity levels with human neuroblastoma outcomes, *Nat. Med.* 1 (1995) 249–255.
- [31] K.B. Challagundla, P.M. Wise, P. Neviani, H. Chava, M. Murtadha, T. Xu, et al., Exosome-mediated transfer of microRNAs within the tumor microenvironment and neuroblastoma resistance to chemotherapy, *J. Natl Cancer Inst.* 107 (2015).
- [32] S.G. Dubois, Y. Kalika, J.N. Lukens, G.M. Brodeur, R.C. Seeger, J.B. Atkinson, et al., Metastatic sites in stage IV and IVS neuroblastoma correlate with age, tumor biology, and survival, *J. Pediatr. Hematol. Oncol.* 21 (1999) 181–189.
- [33] A.J. Carlisle, C.A. Lyttle, R.Y. Carlisle, J.M. Maris, CXCR4 expression heterogeneity in neuroblastoma cells due to ligand-independent regulation, *Mol. Cancer* 8 (2009) 126.
- [34] J. Liberman, H. Sartelet, M. Flahaut, A. Muhlethaler-Mottet, A. Coulon, C. Nyaland, et al., Involvement of the CXCR7/CXCR4/CXCL12 axis in the malignant progression of human neuroblastoma, *PLoS ONE* 7 (2012) e43665.
- [35] H.V. Russell, J. Hicks, M.F. Okcu, J.G. Nuchtern, CXCR4 expression in neuroblastoma primary tumors is associated with clinical presentation of bone and bone marrow metastases, *J. Pediatr. Surg.* 39 (2004) 1506–1511.
- [36] A. Muhlethaler-Mottet, J. Liberman, K. Ascencio, M. Flahaut, K. Balmas Bourlout, P. Yan, et al., The CXCR4/CXCR7/CXCL12 axis is involved in a secondary but complex control of neuroblastoma metastatic cell homing, *PLoS ONE* 10 (2015) e0125616.
- [37] H. Geminder, O. Sagi-Assif, L. Goldberg, T. Meshel, G. Rechavi, I.P. Witz, et al., A possible role for CXCR4 and its ligand, the CXC chemokine stromal cell-derived factor-1, in the development of bone marrow metastases in neuroblastoma, *J. Immunol.* 167 (2001) 4747–4757.
- [38] M. Ma, J.Y. Ye, R. Deng, C.M. Dee, G.C. Chan, Mesenchymal stromal cells may enhance metastasis of neuroblastoma via SDF-1/CXCR4 and SDF-1/CXCR7 signaling, *Cancer Lett.* 312 (2011) 1–10.
- [39] Y. Sohara, H. Shimada, M. Scadeng, H. Pollack, S. Yamada, W. Ye, et al., Lytic bone lesions in human neuroblastoma xenograft involve osteoclast recruitment and are inhibited by bisphosphonate, *Cancer Res.* 63 (2003) 3026–3031.
- [40] Y. Sohara, H. Shimada, C. Minkin, A. Erdreich-Epstein, J.A. Nolte, Y.A. DeClerck, Bone marrow mesenchymal stem cells provide an alternate pathway of osteoclast activation and bone destruction by cancer cells, *Cancer Res.* 65 (2005) 1129–1135.
- [41] S. Avnet, M. Salerno, G. Quacquarello, D. Granchi, A. Giunti, N. Baldini, IGF2 derived from SH-SY5Y neuroblastoma cells induces the osteoclastogenesis of human monocyte precursors, *Exp. Cell Res.* 317 (2011) 2147–2158.
- [42] C.M. van Golen, T.S. Schwab, B. Kim, M.E. Soules, O.S. Su, K. Fung, et al., Insulin-like growth factor-I receptor expression regulates neuroblastoma metastasis to bone, *Cancer Res.* 66 (2006) 6570–6578.
- [43] D. Granchi, I. Amato, L. Battistelli, S. Avnet, S. Capaccioli, L. Papucci, et al., In vitro blockade of receptor activator of nuclear factor-kappaB ligand prevents osteoclastogenesis induced by neuroblastoma cells, *Int. J. Cancer* 111 (2004) 829–838.
- [44] S. Lee, J. Qiao, P. Paul, K.L. O'Connor, M.B. Evers, D.H. Chung, FAK is a critical regulator of neuroblastoma liver metastasis, *Oncotarget* 3 (2012) 1576–1587.
- [45] A. Chlenski, S. Liu, S.L. Cohn, The regulation of angiogenesis in neuroblastoma, *Cancer Lett.* 197 (2003) 47–52.
- [46] L. Chesler, D.D. Goldenberg, I.T. Seales, R. Satchi-Fainaro, M. Grimmer, R. Collins, et al., Malignant progression and blockade of angiogenesis in a murine transgenic model of neuroblastoma, *Cancer Res.* 67 (2007) 9435–9442.
- [47] T.A. Baudino, C. McKay, H. Pendeville-Samain, J.A. Nilsson, K.H. Maclean, E.L. White, et al., c-Myc is essential for vasculogenesis and angiogenesis during development and tumor progression, *Genes Dev.* 16 (2002) 2530–2543.
- [48] J.R. Whitfield, L. Soucek, Tumor microenvironment: becoming sick of Myc, *Cell. Mol. Life Sci.* 69 (2012) 931–934.
- [49] N.M. Sodik, L.B. Swigart, A.N. Karnezis, D. Hanahan, G.I. Evan, L. Soucek, Endogenous Myc maintains the tumor microenvironment, *Genes Dev.* 25 (2011) 907–916.
- [50] J. Kang, P.G. Rychahou, T.A. Ishola, J.M. Mourot, B.M. Evers, D.H. Chung, N-myc is a novel regulator of PI3K-mediated VEGF expression in neuroblastoma, *Oncogene* 27 (2008) 3999–4007.
- [51] Y.H. Chantry, W.C. Gustafson, M. Itsara, A. Persson, C.S. Hackett, M. Grimmer, et al., Paracrine signaling through MYCN enhances tumor-vascular interactions in neuroblastoma, *Sci. Transl. Med.* 4 (2012) 115ra113.
- [52] D. Di Paolo, C. Ambrogio, F. Pastorino, C. Brignole, C. Martinengo, R. Carosio, et al., Selective therapeutic targeting of the anaplastic lymphoma kinase with liposomal siRNA induces apoptosis and inhibits angiogenesis in neuroblastoma, *Mol. Ther.* 19 (2011) 2201–2212.
- [53] J.H. HaDuong, L. Blavier, S.K. Baniwal, B. Frenkel, J. Malvar, V. Punj, et al., Interaction between bone marrow stromal cells and neuroblastoma cells leads to a VEGFA-mediated osteoblastogenesis, *Int. J. Cancer* 137 (2015) 797–809.
- [54] A. Chlenski, S. Liu, S.E. Crawford, O.V. Volpert, G.H. DeVries, A. Evangelista, et al., SPARC is a key Schwannian-derived inhibitor controlling neuroblastoma tumor angiogenesis, *Cancer Res.* 62 (2002) 7357–7363.
- [55] D. Huang, J.L. Rutkowski, G.M. Brodeur, P.M. Chou, J.L. Kwiatkowski, A. Babbo, et al., Schwann cell-conditioned medium inhibits angiogenesis, *Cancer Res.* 60 (2000) 5966–5971.
- [56] A. Chlenski, S. Liu, L.J. Baker, Q. Yang, Y. Tian, H.R. Salwen, et al., Neuroblastoma angiogenesis is inhibited with a folded synthetic molecule corresponding to the epidermal growth factor-like module of the follistatin domain of SPARC, *Cancer Res.* 64 (2004) 7420–7425.
- [57] R. Zeine, H.R. Salwen, R. Peddinti, Y. Tian, L. Guerrero, Q. Yang, et al., Presence of cancer-associated fibroblasts inversely correlates with Schwannian stroma in neuroblastoma tumors, *Mod. Pathol.* 22 (2009) 950–958.
- [58] S. Jodele, C.F. Chantrain, L. Blavier, C. Lutzko, G.M. Crooks, H. Shimada, et al., The contribution of bone marrow-derived cells to the tumor vasculature in neuroblastoma is matrix metalloproteinase-9 dependent, *Cancer Res.* 65 (2005) 3200–3208.
- [59] C.F. Chantrain, H. Shimada, S. Jodele, S. Groshen, W. Ye, D.R. Shalinsky, et al., Stromal matrix metalloproteinase-9 regulates the vascular architecture in neuroblastoma by promoting pericyte recruitment, *Cancer Res.* 64 (2004) 1675–1686.
- [60] C.F. Chantrain, P. Henriot, S. Jodele, H. Emonard, O. Feron, P.J. Courtoy, et al., Mechanisms of pericyte recruitment in tumour angiogenesis: a new role for metalloproteinases, *Eur. J. Cancer* 42 (2006) 310–318.
- [61] T. Teitz, J.M. Lahti, V.J. Kidd, Aggressive childhood neuroblastomas do not express caspase-8: an important component of programmed cell death, *J. Mol. Med.* 79 (2001) 428–436.
- [62] S. Barbero, A. Mielgo, V. Torres, T. Teitz, D.J. Shields, D. Mikolon, et al., Caspase-8 association with the focal adhesion complex promotes tumor cell migration and metastasis, *Cancer Res.* 69 (2009) 3755–3763.
- [63] T. Khan, J.A. Hixon, J.K. Stauffer, E. Lincoln, T.C. Back, J. Brenner, et al., Therapeutic modulation of Akt activity and antitumor efficacy of interleukin-12 against orthotopic murine neuroblastoma, *J. Natl Cancer Inst.* 98 (2006) 190–202.
- [64] L.A. Lampson, C.A. Fisher, J.P. Whelan, Striking paucity of HLA-A, B, C and beta 2-microglobulin on human neuroblastoma cell lines, *J. Immunol.* 130 (1983) 2471–2478.
- [65] L.A. Lampson, C.A. Fisher, Weak HLA and beta 2-microglobulin expression of neuronal cell lines can be modulated by interferon, *Proc. Natl. Acad. Sci. U.S.A.* 81 (1984) 6476–6480.
- [66] E.K. Main, L.A. Lampson, M.K. Hart, J. Kornbluth, D.B. Wilson, Human neuroblastoma cell lines are susceptible to lysis by natural killer cells but not by cytotoxic T lymphocytes, *J. Immunol.* 135 (1985) 242–246.
- [67] R. Handgretinger, A. Kimmig, P. Lang, B. Daurer, S. Kuci, G. Bruchelt, et al., Interferon-gamma upregulates the susceptibility of human neuroblastoma cells to interleukin-2-activated natural killer cells, *Nat. Immun. Cell Growth Regul.* 8 (1989) 189–196.
- [68] K.W. Pajtler, V. Rebmann, M. Lindemann, J.H. Schulte, S. Schulte, M. Stauder, et al., Expression of NTRK1/TrkA affects immunogenicity of neuroblastoma cells, *Int. J. Cancer* 133 (2013) 908–919.
- [69] R. Bernards, S.K. Dessain, R.A. Weinberg, N-myc amplification causes down-modulation of MHC class I antigen expression in neuroblastoma, *Cell* 47 (1986) 667–674.
- [70] L. Raffaghello, I. Prigione, I. Airoidi, M. Camoriano, I. Levreri, C. Gambini, et al., Downregulation and/or release of NKG2D ligands as immune evasion strategy of human neuroblastoma, *Neoplasia* 6 (2004) 558–568.
- [71] J. Leitner, C. Klausner, W.F. Pickl, J. Stockl, O. Majdic, A.F. Bardet, et al., B7-H3 is a potent inhibitor of human T-cell activation: no evidence for B7-H3 and TREM2 interaction, *Eur. J. Immunol.* 39 (2009) 1754–1764.
- [72] F. Morandi, I. Levreri, P. Bocca, B. Galleni, L. Raffaghello, S. Ferrone, et al., Human neuroblastoma cells trigger an immunosuppressive program in monocytes by stimulating soluble HLA-G release, *Cancer Res.* 67 (2007) 6433–6441.

- [73] L.S. Metelitsa, Anti-tumor potential of type-I NKT cells against CD1d-positive and CD1d-negative tumors in humans, *Clin. Immunol.* 140 (2011) 119–129.
- [74] C. Bottino, A. Dondero, F. Bellora, L. Moretta, F. Locatelli, V. Pistoia, et al., Natural killer cells and neuroblastoma: tumor recognition, escape mechanisms, and possible novel immunotherapeutic approaches, *Front. Immunol.* 5 (2014) 56.
- [75] L. Song, S. Asgharzadeh, J. Salo, K. Engell, H.W. Wu, R. Sposto, et al., Valpha24-invariant NKT cells mediate antitumor activity via killing of tumor-associated macrophages, *J. Clin. Invest.* 119 (2009) 1524–1536.
- [76] L.S. Metelitsa, H.W. Wu, H. Wang, Y. Yang, Z. Warsi, S. Asgharzadeh, et al., Natural killer T cells infiltrate neuroblastomas expressing the chemokine CCL2, *J. Exp. Med.* 199 (2004) 1213–1221.
- [77] L. Song, T. Ara, H.W. Wu, C.W. Woo, C.P. Reynolds, R.C. Seeger, et al., Oncogene MYCN regulates localization of NKT cells to the site of disease in neuroblastoma, *J. Clin. Invest.* 117 (2007) 2702–2712.
- [78] E.L. Williams, S.N. Dunn, S. James, P.W. Johnson, M.S. Cragg, M.J. Glennie, et al., Immunomodulatory monoclonal antibodies combined with peptide vaccination provide potent immunotherapy in an aggressive murine neuroblastoma model, *Clin. Cancer Res.* 19 (2013) 3545–3555.
- [79] M. Boes, F. Meyer-Wentrup, TLR3 triggering regulates PD-L1 (CD274) expression in human neuroblastoma cells, *Cancer Lett.* 361 (2015) 49–56.
- [80] D.J. Smith, L.R. Cossins, I. Hatzinisiiriou, M. Haber, P. Nagley, Lack of correlation between MYCN expression and the Warburg effect in neuroblastoma cell lines, *BMC Cancer* 8 (2008) 259.
- [81] J. Navratilova, T. Hankeova, P. Benes, J. Smarda, Low-glucose conditions of tumor microenvironment enhance cytotoxicity of tetrathiomolybdate to neuroblastoma cells, *Nutr. Cancer* 65 (2013) 702–710.
- [82] G. Lundberg, D. Sehic, J.K. Lansberg, I. Ora, A. Frigyesi, V. Castel, et al., Alternative lengthening of telomeres—an enhanced chromosomal instability in aggressive non-MYCN amplified and telomere elongated neuroblastomas, *Genes Chromosomes Cancer* 50 (2011) 250–262.
- [83] D. Abraham, K. Zins, M. Sioud, T. Lucas, R. Schafer, E.R. Stanley, et al., Stromal cell-derived CSF-1 blockade prolongs xenograft survival of CSF-1-negative neuroblastoma, *Int. J. Cancer* 126 (2010) 1339–1352.
- [84] R.L. Chen, C.P. Reynolds, R.C. Seeger, Neutrophils are cytotoxic and growth-inhibiting for neuroblastoma cells with an anti-GD2 antibody but, without cytotoxicity, can be growth-stimulating, *Cancer Immunol. Immunother.* 48 (2000) 603–612.
- [85] J. Michon, S. Moutel, J. Barbet, J.L. Romet-Lemonne, Y.M. Deo, W.H. Fridman, et al., In vitro killing of neuroblastoma cells by neutrophils derived from granulocyte colony-stimulating factor-treated cancer patients using an anti-disialoganglioside/anti-Fc gamma RI bispecific antibody, *Blood* 86 (1995) 1124–1130.
- [86] N. Schwankhaus, C. Gathmann, D. Wicklein, K. Riecken, U. Schumacher, U. Valentiner, Cell adhesion molecules in metastatic neuroblastoma models, *Clin. Exp. Metastasis* 31 (2014) 483–496.
- [87] H.H. Birdsall, C. Lane, M.N. Ramser, D.C. Anderson, Induction of VCAM-1 and ICAM-1 on human neural cells and mechanisms of mononuclear leukocyte adherence, *J. Immunol.* 148 (1992) 2717–2723.
- [88] H.E. Chuluyan, B.J. Lang, T. Yoshimura, J.S. Kenney, A.C. Issekutz, Chemokine production and adhesion molecule expression by neural cells exposed to IL-1, TNF alpha and interferon gamma, *Life Sci.* 63 (1998) 1939–1952.
- [89] C. Winter, B. Pawel, E. Seiser, H. Zhao, E. Raabe, Q. Wang, et al., Neural cell adhesion molecule (NCAM) isoform expression is associated with neuroblastoma differentiation status, *Pediatr. Blood Cancer* 51 (2008) 10–16.
- [90] E. Phimister, F. Kiely, J.T. Kemshead, K. Patel, Expression of neural cell adhesion molecule (NCAM) isoforms in neuroblastoma, *J. Clin. Pathol.* 44 (1991) 580–585.
- [91] L.L. Lanier, C. Chang, M. Azuma, J.J. Ruitenber, J.J. Hemperly, J.H. Phillips, Molecular and functional analysis of human natural killer cell-associated neural cell adhesion molecule (N-CAM/CD56), *J. Immunol.* 146 (1991) 4421–4426.
- [92] V. Ciccarone, B.A. Spengler, M.B. Meyers, J.L. Biedler, R.A. Ross, Phenotypic diversification in human neuroblastoma cells: expression of distinct neural crest lineages, *Cancer Res.* 49 (1989) 219–225.
- [93] T. Yoshihara, N. Esumi, M.J. Humphries, S. Imashuku, Unique expression of integrin fibronectin receptors in human neuroblastoma cell lines, *Int. J. Cancer* 51 (1992) 620–626.
- [94] A. Meyer, C.M. van Golen, B. Kim, K.L. van Golen, E.L. Feldman, Integrin expression regulates neuroblastoma attachment and migration, *Neoplasia* 6 (2004) 332–342.
- [95] R. Judware, L.A. Culp, Over-expression of transfected N-myc oncogene in human SKNSH neuroblastoma cells down-regulates expression of beta 1 integrin subunit, *Oncogene* 11 (1995) 2599–2607.
- [96] R. Judware, R. Lechner, L.A. Culp, Inverse expressions of the N-myc oncogene and beta 1 integrin in human neuroblastoma: relationships to disease progression in a nude mouse model system, *Clin. Exp. Metastasis* 13 (1995) 123–133.
- [97] M.C. Favrot, V. Combaret, E. Goillot, P. Lutz, D. Frappaz, P. Thiesse, et al., Expression of integrin receptors on 45 clinical neuroblastoma specimens, *Int. J. Cancer* 49 (1991) 347–355.
- [98] B.E. Smith, A.D. Bradshaw, E.S. Choi, P. Rouselle, E.A. Wayner, D.O. Clegg, Human SY5Y neuroblastoma cell interactions with laminin isoforms: neurite outgrowth on laminin-5 is mediated by integrin alpha 3 beta 1, *Cell Adhes. Commun.* 3 (1996) 451–462.
- [99] K.L. Abbott, K. Troupe, I. Lee, M. Pierce, Integrin-dependent neuroblastoma cell adhesion and migration on laminin is regulated by expression levels of two enzymes in the O-mannosyl-linked glycosylation pathway, PomGnT1 and GnT-Vb, *Exp. Cell Res.* 312 (2006) 2837–2850.
- [100] S.K. Mitra, D.A. Hanson, D.D. Schlaepfer, Focal adhesion kinase: in command and control of cell motility, *Nat. Rev. Mol. Cell Biol.* 6 (2005) 56–68.
- [101] L. Wu, J.A. Bernard-Trifilo, Y. Lim, S.T. Lim, S.K. Mitra, S. Uryu, et al., Distinct FAK-Src activation events promote alpha5beta1 and alpha4beta1 integrin-stimulated neuroblastoma cell motility, *Oncogene* 27 (2008) 1439–1448.
- [102] S. Cursi, A. Rufini, V. Stagni, I. Condo, V. Matafora, A. Bachi, et al., Src kinase phosphorylates Caspase-8 on Tyr380: a novel mechanism of apoptosis suppression, *EMBO J.* 25 (2006) 1895–1905.
- [103] B. Helfer, B.C. Boswell, D. Finlay, A. Cipres, K. Vuori, T. Bong Kang, et al., Caspase-8 promotes cell motility and calpain activity under nonapoptotic conditions, *Cancer Res.* 66 (2006) 4273–4278.
- [104] E. Hulleman, J.J. Bijvelt, A.J. Verkleij, C.T. Verrips, J. Boonstra, Integrin signaling at the M/G1 transition induces expression of cyclin E, *Exp. Cell Res.* 253 (1999) 422–431.
- [105] S.A. Young, K.E. McCabe, A. Bartakova, J. Delaney, D.P. Pizzo, R.O. Newbury, et al., Integrin alpha4 enhances metastasis and may be associated with poor prognosis in MYCN low neuroblastoma, *PLoS ONE* 10 (2015) e0120815.
- [106] V. Combaret, N. Gross, C. Lasset, D. Frappaz, C. Beretta-Brogna, T. Philip, et al., Clinical relevance of CD44 cell surface expression and MYCN gene amplification in neuroblastoma, *Eur. J. Cancer* 33 (1997) 2101–2105.
- [107] K. Kramer, N.K. Cheung, W.L. Gerald, M. LaQuaglia, B.H. Kushner, J.M. LeClerc, et al., Correlation of MYCN amplification, Trk-A and CD44 expression with clinical stage in 250 patients with neuroblastoma, *Eur. J. Cancer* 33 (1997) 2098–2100.
- [108] N. Gross, K. Balmas, C.B. Brogna, Absence of functional CD44 hyaluronan receptor on human NMYC-amplified neuroblastoma cells, *Cancer Res.* 57 (1997) 1387–1393.
- [109] Z.L. Wu, E. Schwartz, R. Seeger, S. Ladisch, Expression of GD2 ganglioside by untreated primary human neuroblastomas, *Cancer Res.* 46 (1986) 440–443.
- [110] T. Kazarian, A.A. Jabbar, F.Q. Wen, D.A. Patel, L.A. Valentino, Gangliosides regulate tumor cell adhesion to collagen, *Clin. Exp. Metastasis* 20 (2003) 311–319.
- [111] D.A. Cheresch, M.D. Pierschbacher, M.A. Herzig, K. Mujoo, Disialogangliosides GD2 and GD3 are involved in the attachment of human melanoma and neuroblastoma cells to extracellular matrix proteins, *J. Cell Biol.* 102 (1986) 688–696.
- [112] A. Kowalczyk, M. Gil, I. Horwacik, Z. Odrowaz, D. Kozbor, H. Rokita, The GD2-specific 14G2a monoclonal antibody induces apoptosis and enhances cytotoxicity of chemotherapeutic drugs in IMR-32 human neuroblastoma cells, *Cancer Lett.* 281 (2009) 171–182.
- [113] W.T. Arscott, A.E. LaBauve, V. May, U.V. Wesley, Suppression of neuroblastoma growth by dipeptidyl peptidase IV: relevance of chemokine regulation and caspase activation, *Oncogene* 28 (2009) 479–491.
- [114] B. Meister, F. Grünebach, F. Bautz, W. Brügger, F.M. Fink, L. Kanz, et al., Expression of vascular endothelial growth factor (VEGF) and its receptors in human neuroblastoma, *Eur. J. Cancer* 35 (1999) 445–449.
- [115] E.A. Beierle, W. Dai, M.R. Langham Jr., E.M. Copeland 3rd, M.K. Chen, Expression of VEGF receptors in cocultured neuroblastoma cells, *J. Surg. Res.* 119 (2004) 56–65.
- [116] M. Fakhari, D. Pullirsch, D. Abraham, K. Paya, R. Hofbauer, P. Holzfeind, et al., Selective upregulation of vascular endothelial growth factor receptors neuropilin-1 and -2 in human neuroblastoma, *Cancer* 94 (2002) 258–263.
- [117] M. Fakhari, D. Pullirsch, K. Paya, D. Abraham, R. Hofbauer, S. Aharinejad, Upregulation of vascular endothelial growth factor receptors is associated with advanced neuroblastoma, *J. Pediatr. Surg.* 37 (2002) 582–587.
- [118] E.A. Beierle, A. Nagaram, W. Dai, M. Iyengar, M.K. Chen, VEGF-mediated survivin expression in neuroblastoma cells, *J. Surg. Res.* 127 (2005) 21–28.
- [119] B. Das, H. Yeger, R. Tsuchida, R. Torkin, M.F. Gee, P.S. Thorne, et al., A hypoxia-driven vascular endothelial growth factor/Flt1 autocrine loop interacts with hypoxia-inducible factor-1alpha through mitogen-activated protein kinase/extracellular signal-regulated kinase 1/2 pathway in neuroblastoma, *Cancer Res.* 65 (2005) 7267–7275.
- [120] G.D. Roodman, Role of stromal-derived cytokines and growth factors in bone metastasis, *Cancer* 97 (2003) 733–738.
- [121] J. Wang, Y. Tang, W. Zhang, H. Zhao, R. Wang, Y. Yan, et al., Insulin-like growth factor-1 secreted by brain microvascular endothelial cells attenuates neuron injury upon ischemia, *FEBS J.* 280 (2013) 3658–3668.
- [122] B.F. Boyce, T. Yoneda, T.A. Guise, Factors regulating the growth of metastatic cancer in bone, *Endocr. Relat. Cancer* 6 (1999) 333–347.
- [123] B. Kim, C.M. van Golen, E.L. Feldman, Insulin-like growth factor-I signaling in human neuroblastoma cells, *Oncogene* 23 (2004) 130–141.
- [124] A. Puglianiello, D. Germani, P. Rossi, S. Cianfanari, IGF-1 stimulates chemotaxis of human neuroblasts. Involvement of type 1 IGF receptor, IGF binding proteins, phosphatidylinositol-3 kinase pathway and plasmin system, *J. Endocrinol.* 165 (2000) 123–131.
- [125] G.E. Meyer, E. Shelden, B. Kim, E.L. Feldman, Insulin-like growth factor I stimulates motility in human neuroblastoma cells, *Oncogene* 20 (2001) 7542–7550.
- [126] C.M. van Golen, V.P. Castle, E.L. Feldman, IGF-1 receptor activation and BCL-2 overexpression prevent early apoptotic events in human neuroblastoma, *Cell Death Differ.* 7 (2000) 654–665.
- [127] D. Chambery, S. Mohseni-Zadeh, B. De Galle, S. Babajko, N-myc regulation of type I insulin-like growth factor receptor in a human neuroblastoma cell line, *Cancer Res.* 59 (1999) 2898–2902.

- [128] R.K. Assoian, B.E. Fleurdelys, H.C. Stevenson, P.J. Miller, D.K. Madtes, E.W. Raines, et al., Expression and secretion of type beta transforming growth factor by activated human macrophages, *Proc. Natl. Acad. Sci. U.S.A.* 84 (1987) 6020–6024.
- [129] S.M. Wahl, N. McCartney-Francis, J.B. Allen, E.B. Dougherty, S.F. Dougherty, Macrophage production of TGF-beta and regulation by TGF-beta, *Ann. N. Y. Acad. Sci.* 593 (1990) 188–196.
- [130] J.L. Crane, X. Cao, Bone marrow mesenchymal stem cells and TGF-beta signaling in bone remodeling, *J. Clin. Invest.* 124 (2014) 466–472.
- [131] S. Scarpa, A. Coppa, M. Ragano-Caracciolo, G. Mincione, A. Giuffrida, A. Modesti, et al., Transforming growth factor beta regulates differentiation and proliferation of human neuroblastoma, *Exp. Cell Res.* 229 (1996) 147–154.
- [132] A. Turco, S. Scarpa, A. Coppa, G. Baccheschi, C. Palumbo, C. Leonetti, et al., Increased TGFbeta type II receptor expression suppresses the malignant phenotype and induces differentiation of human neuroblastoma cells, *Exp. Cell Res.* 255 (2000) 77–85.
- [133] J. Lynch, J. Fay, M. Meehan, K. Bryan, K.M. Watters, D.M. Murphy, et al., MiRNA-335 suppresses neuroblastoma cell invasiveness by direct targeting of multiple genes from the non-canonical TGF-beta signalling pathway, *Carcinogenesis* 33 (2012) 976–985.
- [134] A. Abramsson, P. Lindblom, C. Betsholtz, Endothelial and nonendothelial sources of PDGF-B regulate pericyte recruitment and influence vascular pattern formation in tumors, *J. Clin. Invest.* 112 (2003) 1142–1151.
- [135] H. Xie, Z. Cui, L. Wang, Z. Xia, Y. Hu, L. Xian, et al., PDGF-BB secreted by preosteoclasts induces angiogenesis during coupling with osteogenesis, *Nat. Med.* 20 (2014) 1270–1278.
- [136] T. Matsui, K. Sano, T. Tsukamoto, M. Ito, T. Takaishi, H. Nakata, et al., Human neuroblastoma cells express alpha and beta platelet-derived growth factor receptors coupling with neurotrophic and chemotactic signaling, *J. Clin. Invest.* 92 (1993) 1153–1160.
- [137] Y. Fukaya, H. Shimada, L.C. Wang, E. Zandi, Y.A. DeClerck, Identification of Gal-3 binding protein as a factor secreted by tumor cells that stimulates interleukin-6 expression in the bone marrow stroma, *J. Biol. Chem.* 283 (2008) 18573–18581.
- [138] A.M. Silverman, R. Nakata, H. Shimada, R. Sposto, Y.A. DeClerck, A galectin-3-dependent pathway upregulates interleukin-6 in the microenvironment of human neuroblastoma, *Cancer Res.* 72 (2012) 2228–2238.
- [139] H. Peinado, M. Aleckovic, S. Lavotshkin, I. Matei, B. Costa-Silva, G. Moreno-Bueno, et al., Melanoma exosomes educate bone marrow progenitor cells toward a pro-metastatic phenotype through MET, *Nat. Med.* 18 (2012) 883–891.
- [140] D. Marimpietri, A. Petretto, L. Raffaghello, A. Pezzolo, C. Gagliani, C. Tacchetti, et al., Proteome profiling of neuroblastoma-derived exosomes reveal the expression of proteins potentially involved in tumor progression, *PLoS ONE* 8 (2013) e75054.
- [141] B.H. Haug, O.H. Hald, P. Utne, S.A. Roth, C. Lokke, T. Flaegstad, et al., Exosome-like extracellular vesicles from MYCN-amplified neuroblastoma cells contain oncogenic miRNAs, *Anticancer Res.* 35 (2015) 2521–2530.
- [142] H.V. Russell, S.G. Groshen, T. Ara, Y.A. DeClerck, R. Hawkins, H.A. Jackson, et al., A phase I study of zoledronic acid and low-dose cyclophosphamide in recurrent/refractory neuroblastoma: a new approaches to neuroblastoma therapy (NANT) study, *Pediatr. Blood Cancer* 57 (2011) 275–282.
- [143] H. Chai, A.Z. Luo, P. Weerasinghe, R.E. Brown, Sorafenib downregulates ERK/Akt and STAT3 survival pathways and induces apoptosis in a human neuroblastoma cell line, *Int. J. Clin. Exp. Pathol.* 3 (2010) 408–415.
- [144] F. Yang, V. Jove, R. Buettner, H. Xin, J. Wu, Y. Wang, et al., Sorafenib inhibits endogenous and IL-6/S1P induced JAK2-STAT3 signaling in human neuroblastoma, associated with growth suppression and apoptosis, *Cancer Biol. Ther.* 13 (2012) 534–541.
- [145] B. Georger, M.W. Kieran, S. Grupp, D. Perek, J. Clancy, M. Krygowski, et al., Phase II trial of temsirolimus in children with high-grade glioma, neuroblastoma and rhabdomyosarcoma, *Eur. J. Cancer* 48 (2012) 253–262.
- [146] B.H. Kushner, K. Kramer, S. Modak, N.K. Cheung, Successful multifold dose escalation of anti-GD2 monoclonal antibody 3F8 in patients with neuroblastoma: a phase I study, *J. Clin. Oncol.* 29 (2011) 1168–1174.
- [147] Y. Xu, J. Sun, M.A. Sheard, H.C. Tran, Z. Wan, W.Y. Liu, et al., Lenalidomide overcomes suppression of human natural killer cell anti-tumor functions by neuroblastoma microenvironment-associated IL-6 and TGFbeta1, *Cancer Immunol. Immunother.* 62 (2013) 1637–1648.
- [148] C.U. Louis, B. Savoldo, G. Dotti, M. Pule, E. Yvon, G.D. Myers, et al., Antitumor activity and long-term fate of chimeric antigen receptor-positive T cells in patients with neuroblastoma, *Blood* 118 (2011) 6050–6056.
- [149] Y. Liu, H.W. Wu, M.A. Sheard, R. Sposto, S.S. Somanchi, L.J. Cooper, et al., Growth and activation of natural killer cells ex vivo from children with neuroblastoma for adoptive cell therapy, *Clin. Cancer Res.* 19 (2013) 2132–2143.
- [150] R. Esser, T. Muller, D. Stefes, S. Kloess, D. Seidel, S.D. Gillies, et al., NK cells engineered to express a GD2-specific antigen receptor display built-in ADCC-like activity against tumour cells of neuroectodermal origin, *J. Cell. Mol. Med.* 16 (2012) 569–581.

**Tumor-associated macrophages activate STAT3 and MYC in neuroblastomas  
independently of IL6**

Michael D. Hadjidaniel<sup>1</sup>, Sakunthala Muthugounder<sup>1</sup>, Long Hung<sup>1</sup>, Soheila Shirinbak<sup>1</sup>, Randall Chan<sup>1,4,5</sup>, Rie Nakata<sup>1</sup>, Lucia Borriello<sup>1</sup>, Rebekah J. Kennedy<sup>1</sup>, Michael Sheard<sup>1</sup>, Hiroshi Iwakura<sup>2</sup>, Takashi Akamizu<sup>3</sup>, Hiroyuki Shimada<sup>1,4</sup>, Richard Sposto<sup>1,4</sup>, Yves A. DeClerck<sup>1,4</sup>,  
Shahab Asgharzadeh<sup>1,4,#</sup>

1. Children's Hospital Los Angeles and The Saban Research Institute, Los Angeles, CA;
2. Medical Innovation Center, Kyoto University Graduate School of Medicine, Kyoto, Japan;
3. The First Department of Medicine, Wakayama Medical University, Wakayama, Japan
4. Keck School of Medicine, University of Southern California, Los Angeles, CA;
5. Los Angeles County + University of Southern California Medical Center, Los Angeles, CA

# Corresponding Author

Shahab Asgharzadeh, MD

4650 Sunset Boulevard, MS 57

Los Angeles, CA 90027

Tel. 323-361-8643, Fax. 323-361-4902

[sasgharzadeh@chla.usc.edu](mailto:sasgharzadeh@chla.usc.edu)

**Acknowledgment of Research Support:** This work was supported by a grant to SA from the Department of Defense (CDMRP10669916), and in part by support from the Martell Foundation, Norris Foundation, and Nautica Malibu Triathlon; and grants to YDC and SA from Department of Defense (W81XWH-12-1-0571) and NIH U54 (5U54CA163117).

**Running Title:** Tumor-Associated Macrophages in Murine Neuroblastoma

**Abstract (150 words)**

Inflammation has pro-tumor effects in cancer through crosstalk between immune, vascular, and tumor cells, and has emerged as important factor governing the biology of cancer. Factors released by tumor-associated macrophages (TAM), including interleukin-6 (IL6) that activates Signal Transduction and Activator of Transcription (STAT3), are among the prototypical mediators in the tumor microenvironment (TME). Here, we demonstrate, in the context of neuroblastoma (NBL), that STAT3 and MYC are critical downstream factors activated by TAM through redundant pathways in the absence of IL6. MYC expression correlates with markers of TAM infiltration in human tumors. Mechanistically, macrophage-tumor interaction leads to increased STAT3 activation and upregulation of MYC in tumor cells, phenomena recapitulated with macrophages and mice lacking IL6. In contrast to IL6 suppression, blocking STAT3 inhibited macrophage-mediated tumor proliferation and growth in part through MYC downregulation, demonstrating the importance of this axis in NBL TME.

**Significance:** The role of TME in adult and pediatric cancers is being increasingly appreciated. We show that TAM are essential for promoting tumor proliferation and growth through STAT3 activation and upregulation of MYC, which can occur through redundant mechanisms in the absence of IL6. Our findings support the notion of targeting TAM and STAT3 rather than upstream ligand-receptors.

## Introduction

The role of inflammation in promoting tumor growth and immune response in the tumor microenvironment (TME) has emerged as an important characteristic of cancer (1). Tumor-associated macrophages (TAM), which most closely resemble M2-polarized macrophages, are major contributors to the TME, and are found in tumors from a variety of human cancers (2, 3). The presence of TAM and high levels of specific chemokines and cytokines, including interleukin 6 (IL6), are associated with lower survival rates in patients with several tumors including neuroblastoma (4-10). IL6 is considered a mediator of monocyte-mediated proliferation of tumor cells through its binding to the IL6 receptor (IL6R). Several ligands can activate IL6R, and its downstream activation of the JAK-STAT signaling plays significant role in proliferation, survival, invasion and immunosuppression of cancers (11-14).

Neuroblastomas (NBL) lacking MYCN amplification are known to recruit monocytes through expression of chemokine (C-C motif) ligand 2 (CCL2; aka Monocyte chemotactic protein 1), and promote their polarization to M2-like TAM, in part through the CCL2-CCR2 axis (15, 16). The presence of TAM correlates with NBL disease stage, with greater infiltration observed in children with metastatic disease. Expression of inflammation-associated genes, including IL6R, also plays an important role in determining outcome in children with high-risk disease whose survival remains poor (5). This raises the prospect that targeting the TME and associated biologic pathways such as the IL6/IL6R and STAT3 pathway, as evaluated in adult cancers (17), may be an important therapeutic approach in children with NBL.

In this study, we focused on the role of TAM and IL6 in NBL and its TME. While TAM are observed in primary tumors of children with high-risk disease, the mechanism of their contribution to tumor growth and the role of IL6 are not clearly understood. Here, we elucidate

the functional and biologic roles of TAM using pharmacologic and genetic approaches, corroborated by gene expression data from a large cohort of NBL tumors. Our findings reveal novel insights about the mechanisms of IL6 and MYC expression, and identify STAT3 as potential target for NBL therapy.

## **Results**

### **Tumor-associated Macrophages Enhance Tumor Proliferation and Growth via MYC Upregulation**

To better understand the relationship of tumor growth to proliferation in the context of tumor-TAM interactions, we utilized a previously described transgenic murine NBL model (NB-Tag) (18). Although, this model was initially reported to express MYCN at the RNA level, our extensive characterization by gene expression, DNA copy number, and immunohistochemistry demonstrated that this model closely resembles human tumors lacking MYCN amplification (Supplemental Figure 1). The reproducible growth characteristics of NB-Tag tumors allowed us to examine the development of the TME over time. We observed significant increase in infiltration of macrophages in NB-Tag tumors over time compared to control adrenal glands (Figure 1A). The macrophage infiltration was prominent around 12-13 weeks of age prior to tumors becoming visible by magnetic resonance imaging (MRI) (Figure 1A and Supplemental Figure 1A), and coincided with an increase in CCL2 expression in tumors (Figure 1B). We previously only observed CCL2 expression in human MYCN non-amplified tumors (15). The fact that CCL2 is expressed by NB-Tag tumors further supports that this model is the murine counterpart of tumors lacking MYCN amplification.

To investigate the effects of macrophages on NBL cell proliferation and growth, we co-cultured NB-Tag-derived mouse cell line (NBT2) with peritoneal-derived macrophages, and measured S-

phase changes by BrdU labeling and flow cytometry. A significant increase in tumor cell proliferation by up to 70% over the basal rate was observed when cells were in direct contact and by up to 55% increase when using the transwell system (Figure 1C). *In vivo*, peritoneal macrophages conditioned by NBT2 cells for 24 hours prior to injection in ??? mice also significantly enhanced subcutaneous tumor growth compared to NBT2 tumor cells alone ( $p < 0.001$ , Figure 1D).

Gene expression analyses of macrophages prior to and after co-cultures (Figure 1E) revealed that expression of CXCL10, CCR7, and NOS2 (iNOS), which are known to be associated with M1 polarization was downregulated, while expression of CCL2, CCL7 (another member of the MCP family) and CCL5, known to be expressed in TAM, were upregulated (16, 19). Expression of CCL2 also increased in NBT2 cells, suggesting autocrine and paracrine activation of the CCL2-CCR2 axis for further recruitment and polarization of macrophages to an M2-like TAM phenotype (16). Interestingly, we also observed an increase in the expression of the *MYC* gene (*c-MYC*) in NBT2 cells after co-cultures. The two-fold upregulation of *c-MYC* mRNA was associated with a similar increase in the level of protein expression after 24 hours of co-culture with peritoneal macrophages (Figure 1F).

The proliferative effect of macrophages on tumor cells was also observed in co-cultures of human macrophages with a MYCN non-amplified cell line (LAN6; Figure 2A). Two additional human cell lines with overexpression of MYC (CHLA-255) or with amplification of MYCN (LAN5) also showed similar effects (Supplemental Figure 2). All cell lines showed a significant increase in S-phase (range 1.2-1.5 fold increase,  $p < 0.05$ ) and a significant decrease in sub-G1 phase (average decrease of 10 fold,  $p < 0.0005$ ; Figure 2B and Supplemental Figure 2). The decrease

in sub-G1 phase could not be observed in the murine NBT2 cells given the high viability of these cells in culture (Supplemental Figure 2B).

We next analyzed the expression profiles of 249 primary human NBL tumor samples from the TARGET project to assess a potential association between MYC expression and the CCL2-CCR2 axis. We found a high correlation between CCL2, CCR2 and the macrophage markers CD163 and CD14, and MYC (0.65, 0.32, 0.44, and 0.53, respectively, all  $p < 0.01$ ), while negative correlation was obtained with MYCN expression (Figure 2C). Overall, our data suggest that NBL tumor cells recruit and polarize macrophages to an M2-like phenotype, which in turn enhance tumor proliferation and growth through upregulation of the MYC protein.

### **Tumor-macrophage Co-culture is Associated with IL6 Expression, but Tumor Proliferation and Growth do not Require IL6**

IL6 and IL6R have been shown to promote tumor growth, and IL6R expression was identified as one of the inflammation-related genes in a 14-gene prognostic signature in children with high-risk tumors lacking MYCN amplification (5). We analyzed expression of IL6 over time in tumor samples and plasma from NB-Tag mice, and noted that its increase correlated with the time of highest macrophage infiltration in the tumors, i.e., >12 weeks of age (Figure 3A). The myeloid cells within the tumors (CD11b<sup>+</sup>/F4-80<sup>+</sup> and CD11b<sup>+</sup>/F4-80<sup>-</sup>) and circulating monocytes (CD11b<sup>+</sup>) in the blood were identified as the predominant cells producing IL6 with minimal contribution from tumor cells and none from CD11<sup>-</sup> immune cells (Figure 3B-D). Considering the well-known effect of IL6 on STAT3 activation and the presence of IL6 in our tumor model, we asked whether IL6 produced by TAM contributes to the proliferative advantage provided by macrophages in our co-culture system. To our surprise, neutralizing IL6 in the co-culture media

with maximal levels of anti-IL6 antibodies did not significantly decrease proliferation of NBT2 cells (3.5% and 7.3% in direct and transwell systems, respectively  $p=???$ ) (Figure 1C).

To assess the role of IL6 in NB-Tag tumor development, we generated IL6-deficient double transgenic mice (NB-Tag/IL6<sup>KO</sup>), and studied the tumor growth kinetics. Supporting our co-culture findings, there was no difference in the growth patterns between NB-Tag/IL6<sup>KO</sup> and NB-Tag control mice (Figure 3E). Furthermore, peritoneal macrophages obtained from the NB-Tag/IL6<sup>KO</sup> mice replicated the growth-promoting effects on NBT2 cells *in vitro* just as well as their wildtype counterpart (Figure 3G) despite their inability to produce any IL6 (Supplemental Figure 2C).

### **Macrophages can induce pSTAT3 in NBL independently of IL6**

As IL6 is known to activate STAT3 in the TME, we evaluated STAT3 activation (assessed by phosphorylation of STAT3) in co-culture of NBT2 cells and macrophages. We observed a strong increase in phosphorylation of STAT3 (pSTAT3) in NBT2 cells cultured with macrophages, which started approximately 6 hours after co-culture (Figure 4A), and occurred approximately 18 hours prior to the increase in tumor MYC levels. We observed similar pattern of expression using macrophages obtained from NB-Tag/IL6<sup>KO</sup> mice (data not shown), and more importantly observed similar STAT3 activation in the tumors of these mice compared to NB-Tag mice (Figure 4C).

To determine whether the IL6R was functional in NBT2 cells, we tested the activation of STAT3 in cells treated with IL6 in the presence of sIL6R, the mediator of IL6 *trans* signaling. These experiments demonstrated that pSTAT3 was elevated after 30 minutes of treatment with recombinant IL6 (10ng/ml) and sIL6R (25ng/ml), and that addition of neutralizing anti-IL6

antibody blocked this activation. Likewise, conditioned media (CM) from NBT2 cells co-cultured with macrophages activated STAT3; however, this effect could not be blocked by anti-IL6, suggesting that other secreted factors can contribute to STAT3 activation (Figure 4B). Experiments conducted using the human CHLA255 cell line replicated our findings in the murine system, showing that IL6 is not the only factor involved in STAT3 activation. Moreover, tumors obtained from NB-Tag/IL6<sup>KO</sup> mice showed similar levels of STAT3 phosphorylation by western blot or IHC analyses (Figure 4). These data suggest that alternative mechanisms of STAT3 phosphorylation could play a role in NBL-TAM cell interaction.

### **STAT3 inhibition decreases macrophage-induced expression of MYC in tumor cells and reverses the proliferative effects of macrophages**

To assess the importance of STAT3 signaling on macrophage-induced tumor cell proliferation, we used two potent STAT3 inhibitors, AZD1480 and Ruxolitinib, to block STAT3 phosphorylation via inhibition of the Jak2 kinase pathway, which is downstream of IL6R. Both Ruxolitinib and AZD1480 significantly reduced NBT2 proliferation by an average of 40% ( $p < 0.05$ , and  $p < 0.001$ , respectively; Figure 5A). Proliferation of NBT2 co-cultured with macrophages was significantly reduced by Ruxolitinib ( $p < 0.001$ ) while it was not altered by AZD1480 (Figure 5 A). Ruxolitinib was more effective than AZD1480 at blocking the macrophage-dependent STAT3 phosphorylation in NBT2 cells (Figure 5B). Interestingly, inhibition of pSTAT3 also led to a decrease in MYC protein levels, suggesting regulation of MYC by macrophages is IL6 independent and STAT3 dependent. *In vitro* proliferation studies showed both AZD1480 and Ruxolitinib also significantly reduced pSTAT3 in NB-Tag tumors (Figure 5C).

We next assessed the effect of Ruxolitinib on growth of NBT2 tumors with and without co-injections of tumor-conditioned macrophages. Ruxolitinib treatment effectively blocked the proliferation advantage provided by macrophages to NBT2 cell lines (ANOVA  $p < 0.001$ , Figure 5C). Tumor lysates at the end of the experiment showed strong inhibition of pSTAT3 in tumors treated with Ruxolitinib (Figure 5D).

## **Discussion**

Utilizing a murine model of NBL characterized as lacking MYCN amplification and with reproducible growth pattern, we were able to study the development of the NBL TME and assess the role and significance of TAM. We demonstrated that tumor cells recruit macrophages, which in turn facilitate tumor proliferation and increase MYC expression through a STAT3-dependent mechanism. Although IL6 expression was elevated in both the human and murine systems and IL6 was produced by macrophages co-cultured with tumor cells, we discovered that macrophages genetically deficient in IL6 were still able to activate STAT3 in tumor cells, upregulate MYC and promote tumor proliferation.

TAM are known to promote tumor progression via multiple mechanisms including effects on tumor cell growth, survival, invasion, metastasis, angiogenesis, inflammation, and immune regulation (2, 20). The presence of TAM has been described in many adult malignancies (21) and recently reported in both neuroblastomas and medulloblastomas (5, 22). In children with high-risk NBL lacking MYCN amplification, increased TAM infiltration and expression of inflammation-related genes associated with M2-like macrophage phenotype was associated with poor outcome (5). Recently, a MYC-expressing class of neuroblastomas has been described as highly aggressive and conferring poor outcome to children bearing these tumors, in par with that of children whose tumors harbor MYCN amplification (23). Our gene expression

analyses of a large cohort of high-risk NBL tumors demonstrated a positive association between expression of genes related to TAM and MYC, an observation that we confirmed experimentally using the murine NBL-macrophage co-culture experiments.

Our previous work attributed the monocyte/macrophage-induced proliferative effect to activation of the IL6 pathway (24). An IL6-rich TME leads to STAT3 activation and promotion of tumor growth (6, 11, 25-27). Persistently active STAT3 can function as a master regulator of molecular and biological events that promote tumorigenesis (14, 26, 28). In NB-Tag mice, macrophage infiltration in the TME coincided with increased IL6 mRNA expression in tumors and increased IL6 levels in the sera, findings also observed in children with NBL (29). TAM were the predominant source of IL6 production, yet despite expectations, our *in vitro* and *in vivo* data illustrate that these cells can promote tumor cell proliferation even in the absence of IL6. Indeed, STAT3 can be activated by several other cytokines and growth factors, including epidermal growth factor, platelet-derived growth factor, and oncogenic proteins including Src and Ras (30). The majority of these ligands bind to gp130 that signals through the Janus-activated kinases (JAK) pathway to phosphorylate STAT3. In our study, we illustrated the *in vitro* and *in vivo* usefulness of STAT3 inhibition via JAK2 inhibitors that abolished the macrophage-induced tumor proliferative effects.

The increase of MYC protein expression in NBL tumors after co-culture with macrophages in a STAT3 dependent-manner is novel , and demonstrates that TAM and the pathways they activate are important therapeutic targets in NBL. Persistent expression of activated STAT3 in fibroblasts induces transformation have been shown to increase MYC expression by 2-3 fold (26), and the mechanism of its activation is via direct binding to the E2F binding site of the MYC promoter (31). We postulate that any members of the IL6 family of cytokines such as ciliary

nerve trophic factor, leukemia inhibitory factor, oncostatin M, IL-11, cardiotrophin-1, or IL6 itself may be involved in activation of STAT3 depending on the tumor type and its underlying cell of origin.

Here, we characterized the TME of a novel murine model of MYCN non-amplified NBL, revealing infiltration of IL6-producing TAM in early phases of tumor growth. Tumor-macrophage interaction leads to tumor proliferation in a STAT3-dependent MYC activation, which can be induced in the absence of IL6.

## Methods

**NB-Tag murine model:** All experimental procedures were approved by the Children's Hospital Los Angeles Institutional Animal Care and Use Committee. Transgenic mice carrying the SV40 large T-antigen gene (NB-Tag) have been described earlier (18). NB-Tag tumor was characterized as neuroblastoma by tyrosine hydroxylase (TH) immunohistochemistry, and further classified as undifferentiated neuroblastoma with high mitosis-karyorrhexis index by a pathologist (Dr. Shimada). MYCN gene amplification status in the NB-Tag tumors was determined by comparative genomic hybridization assay (CGH) using Nimblegen murine 385K aCGH arrays and comparing tumor DNA against control (liver) DNA per the manufacturer's instructions (MOgene, St. Louis, MO). Double transgenic NB-Tag/IL6<sup>KO</sup> mice were produced by crossing NB-Tag male mice with IL6 knockout female mice (B6.129S2-*Il6*<sup>tm1Kopf</sup>/J, Jackson Laboratory, Bar Harbor, Maine). NB-Tag tumors were monitored by magnetic resonance imaging (MRI) on a Biospin preclinical MRI platform after injection with 30 $\mu$ L of Magnevist (Bayer Pharmaceuticals, Leverkusen, Germany). Images were analyzed using the ImageJ program (National Institutes of Health). Tumors were measured in two dimensions and tumor volume was estimated with the formula, volume = 0.5 x length x width<sup>2</sup> (23). Subcutaneous

tumor measurements were performed with calipers in two dimensions and tumor volume was estimated using the same formula. The murine NBT2 neuroblastoma cell line was established from the adrenal tumor of a 16-week old NB-Tag mouse. Its neuroblastoma identity was validated by RT-PCR for the TH gene, while its tumorigenic character was validated by subcutaneous tumorigenicity studies in NSG and C57/BL6 mice. Human NBL cell lines used (CHLA-255, LAN-6 and LAN-5) have been previously described (32).

**RNA and Protein Analyses:** Total RNA was isolated using the STAT-60 RNA reagent and cleaned by passing through RNeasy columns (Qiagen, Valencia, CA), Gene expression was quantified by the Nanostring nCounter Analysis System (Nanostring Technologies, Seattle, WA) or by RT-PCR. For RT-PCR assays, clean RNA was used as template for cDNA transcription using SuperScript® III Reverse Transcriptase (Life Technologies, Grand Island, NY), and this was used as template for real time PCR using mouse immune Taqman Low Density Arrays (Life Technologies) or pre-designed gene specific primer probe sets. Total RNA was also used to obtain expression of genes with the Nanostring nCounter Mouse Inflammation Kit (Nanostring Technologies). For immunohistochemistry analyses, adrenal gland or tumor from 4-, 8-, 12- and 16-week old WT and NB-Tag mice were fixed and embedded with 4% paraformaldehyde and paraffin wax. Macrophages, TH levels and pSTAT3 were detected using rat anti-mouse F4/80 (Invitrogen: MF48000), rabbit polyclonal anti-mouse Tyrosine hydroxylase (Abcam: ab112) and rabbit pSTAT3 (Cell signaling: Tyr (705) (D3A7)). Serum IL6 levels were quantified for animals of different ages using the Luminex assay and the MILLIPLEX MAP Mouse Cytokine/Chemokine - Premixed 32 Plex kit (Millipore, Temecula, CA). IL6 released in culture media during co-culture experiments was quantified using the DuoSet mouse IL6 Elisa kit (R&D systems, Minneapolis, MN) according to the manufacturer's protocols. Western blots were probed with rabbit polyclonal antibodies for pSTAT3 (Tyr705)(D3A7), pSTAT3 (Ser727), STAT3

(79D7) (Cell signaling) or cMYC–Y69 (Abcam), and detected using donkey anti-rabbit IRDye fluorescent labeled secondary antibody (LI-COR Biosciences, Lincoln, NE). The detection and quantification were conducted using the Odyssey Infrared Imaging Systems (LI-COR Biosciences).

**Macrophage isolation and co-culture experiments:** Mouse macrophage cells were isolated from peritoneal cavity cell populations by positive selection with F4/80-APC antibody (Ab) and APC microbeads (Miltenyi Biotec, Auburn, CA). Isolation of peritoneal cavity cells was conducted as previously described, but without the use of thioglycate (33). Briefly, peritoneal washings were obtained from 10-12 week old mice using ice-cold MACS buffer (0.5% BSA and 2mM EDTA in PBS) and cells were labeled with the F4/80-APC antibody. These were then incubated with APC microbeads and passed through a MACS separator column as per the manufacturer's protocol. The phenotype and purity of macrophages were assessed using flow cytometry and monoclonal antibodies for F4/80-APC and CD11b-PE (eBioscience, San Diego, CA). F4/80+ cells isolated as above were co-cultured with NBT2 ( $1 \times 10^5$  cells/well; 1:1 ratio) cells in 12-well dishes in IMDM, 2% FBS for 36 hours. For transwell co-cultures, F4/80+ cells were plated in transwell inserts (0.4 $\mu$ m, Costar) at a density of  $1 \times 10^5$  cells per insert with NBT2 cells at the bottom of the 12-well plates. For determining proliferation, cells were pulsed with BrdU for 45 minutes before being harvested with Accumax (Millipore, Hayward, CA), followed by staining with anti-CD45-APC antibody, fixation, permeabilization, and staining with anti-BrdU-FITC and 7-amino actinomycin D (7AAD) counterstain (BD Biosciences, San Jose, CA) according to the manufacturer's instructions. Staining with fluorescently labeled anti-CD45 was used to discriminate between NBL cells and macrophages. NBL cells in the S-phase of the cell cycle were identified as BrdU positive events, after excluding the CD45+ population, using FCS Express 3 (De Novo Software, Los Angeles, CA). Co-cultured cells were separated into NBL

and immune cell fractions for RNA and protein extraction using CD45-APC staining and magnetic bead isolation (Miltenyi Biotec). To evaluate the growth promoting effect of macrophages on NBT2 cells *in vivo*, eight-week old NSG mice were inoculated subcutaneously with  $1 \times 10^6$  NBT2 cells. One shoulder of the mice was co-injected with macrophages while the other shoulder was injected with NBT2 cells only. For co-injections, F4/80+ macrophages were isolated from WT mice as described above, conditioned for 36 hours in plates containing NBT2 cells in a transwell insert. The conditioned F4/80+ macrophages were co-injected with equal numbers of naive NBT2 cells. This tumor implant model was used to test the efficacy of JAK inhibitor ruxolitinib in inhibiting macrophage-induced tumor growth *in vivo*. Luciferase expressing NBT3L cells were used instead of NBT2 cells to track tumor growth by xenogen imaging. The mice were randomized into two different treatment arms. A stock solution of ruxolitinib was prepared in dimethyl sulphoxide (DMSO) and diluted in vehicle (Saline) prior to treatment. Mice were treated daily twice by oral gavage with vehicle or ruxolitinib (60 mg/kg) from the 2<sup>nd</sup> day of tumor injection continuously for 3 weeks. The primary endpoint for the study was achievement of 500 mm<sup>3</sup> tumor volume.

For human system experiments, peripheral blood mononuclear cells (PBMCs) were freshly isolated by Ficoll-Paque gradient centrifugation from discarded leukocyte filters obtained during platelet collection from healthy adults at the Children's Hospital Los Angeles Blood Collection Center. Monocytes were selected using the Monocyte Isolation Kit II (Miltenyi Biotec, Auburn, CA), and differentiated to M2-like macrophages by culturing in IMDM, 10% FBS supplemented with 10ng/ml MCSF-1 for seven days as described earlier (34). These macrophages were co-cultured with human neuroblastoma cell lines in IMDM 3% FBS for 48 hours. Cell proliferation was determined by flow cytometry as described for NBT2 cells earlier.

**Flow cytometry Analyses:** Mouse tumors were excised and dissociated using a gentleMACS™ dissociator (Miltenyi Biotec) according to the manufacturer's protocol. Peripheral blood was collected in tubes containing 2% EDTA solution (Sigma-Aldrich, MO) to get single cell suspension. Brefeldine, a protein transport inhibitor (BD Biosciences) was used in all pre-fix permeabilization buffers. Cells were surface-stained with a pre-mixed fluorescence-conjugated monoclonal antibody cocktail or isotype controls for 45 minutes at 4°C in the dark. The cocktails were prepared in 5 different combinations [(1) CD45, CD11b, Ly6G (2) CD45, CD11b, F4/80 (3) CD45, CD11b, B220 (4) CD45, CD11b, CD8a (5) CD45, CD8a, CD4]. Blood samples (25-35µl per tube) were stained with the antibody cocktails, and RBCs were removed after surface staining using BD Pharm Lyse (BD Biosciences) according to manufacturer's protocols. For intracellular staining, samples already stained for surface antigens were fixed with 0.128% formaldehyde for 10 min at 37°C. Fixed cells were washed with staining buffer and permeabilized by washing twice with BD Perm/Wash buffer (BD Biosciences). Permeabilized cells were incubated with anti-IL6-FITC antibody (eBioscience) for 45 minutes at 4°C, subsequently washed twice with BD Perm/Wash and analyzed by flow cytometry. DAPI (0.5ng/ml final concentration) was added to all samples, and data were acquired on a LSR-II four-laser flow cytometer (BD Biosciences) using a UV laser to excite DAPI. Analysis was performed using BD FACSDiva software v. 6.0 and FlowJo 10.0.6 (Tree Star, Inc, Ashland, OR). Antibodies and fluorochromes included Anti-Mouse CD45-APC-Cyanine7, Anti-Mouse CD4-FITC, Anti-Mouse F4/80-Percp-Cy5.5, Anti-Mouse F4/80-APC, Anti-Mouse Ly6G-APC (Biolegend, San Diego, CA) as well as Anti-Mouse CD4-APC-H7, Anti-Mouse CD19-PerCP-Cyanine5.5, Anti-Mouse CD11b-PE, Anti-Mouse B220-PE (BD Biosciences) and corresponding isotype controls.

**STAT3 inhibition experiments:** NBT2 cells were cultured with and without macrophages in the presence of STAT3 inhibitors AZD1480 or Ruxolitinib (Selleckchem, Houston, TX). At different time points, NBT2 cells were collected and protein was used to evaluate the STAT3 phosphorylation by western blotting. For the *in vivo* study, tumor cells from NB-Tag mice or those used for the study were treated with ruxolitinib twice daily for at least one week and tumor dissected 1 hour after the last inhibitor dose to assess the status of pSTAT3.

**Statistical analysis:** All statistical analyses were performed using R version 3 (The R Project for Statistical Computing). Differences in means were determined with the Student's t-test, not assuming equal variances; the Wilcoxon rank test was substituted where indicated for non-normal data. *In vivo* co-culture growth analysis was performed using linear regression with group as the independent variable. A *p*-value of 0.05 was used as the cutoff for statistical significance.

### **Author Contributions**

**Conception and design:** M. Hadjidaniel, S. Muthugounder, L. Hung, Y.A. DeClerck, S. Asgharzadeh

**Development of methodology:** M. Hadjidaniel, S. Muthugounder, L. Hung, S. Asgharzadeh

**Acquisition of data (provided animals, acquired and managed patients, provided facilities, etc.):** M. Hadjidaniel, S. Muthugounder, L. Hung, L. Borriello, R. Nakata, H. Iwakura, T. Akamizu,

**Analysis and interpretation of data (e.g., statistical analysis, biostatistics, computational analysis):** M. Hadjidaniel, S. Muthugounder, L. Hung, H. Shimada, R. Chan, M. Sheard, R. Spoto, R. Kennedy, S. Asgharzadeh

**Writing, review, and/or revision of the manuscript:** M. Hadjidaniel, S. Muthugounder, S. Shirinbak, L. Hung, R.Chan, Y.A. DeClerck, S. Asgharzadeh

**Study supervision:** S. Asgharzadeh

### **Acknowledgements**

The authors would like to acknowledge Tsen-Yin Lin at the CHLA's flow cytometry core for helping with the flow analyses, Ira Harutyunyan at Small Animal Imaging Facility for doing MRI, Esteban Fernandez for his assistance in photomicroscopy. The authors would also like to thank Dr. Martine Torres for editing and critical review of the manuscript.

## Reference List

1. Hanahan D, Weinberg RA. Hallmarks of cancer: the next generation. *Cell*. 2011;144:646-74.
2. Pollard JW. Tumour-educated macrophages promote tumour progression and metastasis. *Nat Rev Cancer*. 2004;4:71-8.
3. Santoni M, Massari F, Amantini C, Nabissi M, Maines F, Burattini L, et al. Emerging role of tumor-associated macrophages as therapeutic targets in patients with metastatic renal cell carcinoma. *Cancer Immunology, Immunotherapy*. 2013;62:1757-68.
4. Asgharzadeh S, Pique-Regi R, Sposto R, Wang H, Yang Y, Shimada H, et al. Prognostic Significance of Gene Expression Profiles of Metastatic Neuroblastomas Lacking MYCN Gene Amplification. *JNCI Journal of the National Cancer Institute*. 2006;98:1193-203.
5. Asgharzadeh S, Salo JA, Ji L, Oberthuer A, Fischer M, Berthold F, et al. Clinical Significance of Tumor-Associated Inflammatory Cells in Metastatic Neuroblastoma. *Journal of Clinical Oncology*. 2012;30:3525-32.
6. Ara T, DeClerck YA. Interleukin-6 in bone metastasis and cancer progression. *European Journal of Cancer*. 2010;46:1223-31.
7. DeNardo DG, Brennan DJ, Rexhepaj E, Ruffell B, Shiao SL, Madden SF, et al. Leukocyte Complexity Predicts Breast Cancer Survival and Functionally Regulates Response to Chemotherapy. *Cancer Discovery*. 2011;1:54-67.
8. Song L, Asgharzadeh S, Salo J, Engell K, Wu H-w, Sposto R, et al. V $\alpha$ 24-invariant NKT cells mediate antitumor activity via killing of tumor-associated macrophages. *Journal of Clinical Investigation*. 2009;119:1524-36.

9. Coward J, Kulbe H, Chakravarty P, Leader D, Vassileva V, Leinster DA, et al. Interleukin-6 as a therapeutic target in human ovarian cancer. *Clinical cancer research : an official journal of the American Association for Cancer Research*. 2011;17:6083-96.
10. Knupfer H, Preiss R. Significance of interleukin-6 (IL-6) in breast cancer (review). *Breast cancer research and treatment*. 2007;102:129-35.
11. Chang Q, Bournazou E, Sansone P, Berishaj M, Gao SP, Daly L, et al. The IL-6/JAK/Stat3 Feed-Forward Loop Drives Tumorigenesis and Metastasis. *Neoplasia*. 2013;15:848-IN45.
12. Chang Q, Daly L, Bromberg J. The IL-6 feed-forward loop: A driver of tumorigenesis. *Seminars in Immunology*. 2014;26:48-53.
13. Hodge DR, Hurt EM, Farrar WL. The role of IL-6 and STAT3 in inflammation and cancer. *European Journal of Cancer*. 2005;41:2502-12.
14. Yu H, Lee H, Herrmann A, Buettner R, Jove R. Revisiting STAT3 signalling in cancer: new and unexpected biological functions. *Nat Rev Cancer*. 2014;14:736-46.
15. Song L, Ara T, Wu HW, Woo CW, Reynolds CP, Seeger RC, et al. Oncogene MYCN regulates localization of NKT cells to the site of disease in neuroblastoma. *J Clin Invest*. 2007;117:2702-12.
16. Sierra-Filardi E, Nieto C, Dominguez-Soto A, Barroso R, Sanchez-Mateos P, Puig-Kroger A, et al. CCL2 shapes macrophage polarization by GM-CSF and M-CSF: identification of CCL2/CCR2-dependent gene expression profile. *Journal of immunology*. 2014;192:3858-67.
17. Voorhees PM, Manges RF, Sonneveld P, Jagannath S, Somlo G, Krishnan A, et al. A phase 2 multicentre study of siltuximab, an anti-interleukin-6 monoclonal antibody, in patients with relapsed or refractory multiple myeloma. *British journal of haematology*. 2013;161:357-66.
18. Iwakura H, Ariyasu H, Kanamoto N, Hosoda K, Nakao K, Kangawa K, et al. Establishment of a novel neuroblastoma mouse model. *Int J Oncol*. 2008;33:1195-9.

19. Fujimoto H, Sangai T, Ishii G, Ikehara A, Nagashima T, Miyazaki M, et al. Stromal MCP-1 in mammary tumors induces tumor-associated macrophage infiltration and contributes to tumor progression. *International journal of cancer Journal international du cancer*. 2009;125:1276-84.
20. Candido J, Hagemann T. Cancer-related inflammation. *Journal of clinical immunology*. 2013;33 Suppl 1:S79-84.
21. Noy R, Pollard JW. Tumor-associated macrophages: from mechanisms to therapy. *Immunity*. 2014;41:49-61.
22. Margol AS, Robison NJ, Gnanachandran J, Hung LT, Kennedy RJ, Vali M, et al. Tumor-associated macrophages in SHH subgroup of medulloblastomas. *Clinical cancer research : an official journal of the American Association for Cancer Research*. 2015;21:1457-65.
23. Wang LL, Teshiba R, Ikegaki N, Tang XX, Naranjo A, London WB, et al. Augmented expression of MYC and/or MYCN protein defines highly aggressive MYC-driven neuroblastoma: a Children's Oncology Group study. *British journal of cancer*. 2015;113:57-63.
24. Song L, Asgharzadeh S, Salo J, Engell K, Wu HW, Sposto R, et al. Valpha24-invariant NKT cells mediate antitumor activity via killing of tumor-associated macrophages. *J Clin Invest*. 2009.
25. Borriello L, Seeger RC, Asgharzadeh S, DeClerck YA. More than the genes, the tumor microenvironment in neuroblastoma. *Cancer letters*. 2015.
26. Bromberg JF, Wrzeszczynska MH, Devgan G, Zhao Y, Pestell RG, Albanese C, et al. Stat3 as an Oncogene. *Cell*. 1999;98:295-303.
27. Ara T, Nakata R, Sheard MA, Shimada H, Buettner R, Groshen SG, et al. Critical Role of STAT3 in IL-6-Mediated Drug Resistance in Human Neuroblastoma. *Cancer Research*. 2013;73:3852-64.
28. Darnell JE. Validating Stat3 in cancer therapy. *Nature Medicine*. 2005;11:595-6.

29. Russell HV, Groshen SG, Ara T, DeClerck YA, Hawkins R, Jackson HA, et al. A phase I study of zoledronic acid and low-dose cyclophosphamide in recurrent/refractory neuroblastoma: a new approaches to neuroblastoma therapy (NANT) study. *Pediatric blood & cancer*. 2011;57:275-82.
30. Aggarwal BB, Kunnumakkara AB, Harikumar KB, Gupta SR, Tharakan ST, Koca C, et al. Signal Transducer and Activator of Transcription-3, Inflammation, and Cancer: How Intimate Is the Relationship? *Annals of the New York Academy of Sciences*. 2009;1171:59-76.
31. Kiuchi N, Nakajima K, Ichiba M, Fukada T, Narimatsu M, Mizuno K, et al. STAT3 is required for the gp130-mediated full activation of the c-myc gene. *The Journal of experimental medicine*. 1999;189:63-73.
32. Wada RK, Seeger RC, Brodeur GM, Einhorn PA, Rayner SA, Tomayko MM, et al. Human neuroblastoma cell lines that express N-myc without gene amplification. *Cancer*. 1993;72:3346-54.
33. Ray A, Dittel BN. Isolation of mouse peritoneal cavity cells. *Journal of visualized experiments : JoVE*. 2010.
34. Geissmann F, Manz MG, Jung S, Sieweke MH, Merad M, Ley K. Development of Monocytes, Macrophages, and Dendritic Cells. *Science*. 2010;327:656-61.

## Figure Legends

**Figure 1.** TAM infiltration in NB-Tag tumors is associated with tumor proliferation and induction of MYC expression. **A)** Left: Representative Immunohistochemical analysis comparing macrophages (detected using anti-F4/80 antibody) in the adrenal medulla of WT mice to tumors arising from adrenal glands of NB-Tag mice of various ages (magnification x400). Macrophage counting (F4/80+ cells) from IHC images of mice >12 weeks of age compared to age-matched adrenal medulla sections (At least 5 tiles from each tumor or adrenal gland section were analyzed, 4-6 tissues per group); **B)** CCL2 gene expression levels comparing tumors versus WT adrenal glands in mice <12 weeks of age and >12 weeks of age (n=6 per group); **C)** Left: Tumor proliferation analysis by BrdU incorporation comparing fold-change alteration to baseline NBT2 proliferation rate in tumor-macrophage co-culture experiments (direct and transwell) with and without anti-IL6 neutralizing antibody. Data were compiled from at least 3 independent experiments in triplicates. Right: Representative flow cytometry profile of incorporation of BrDU in NBT2 cells in various experimental designs; **D)** Tumor growth in mice injected with  $1 \times 10^6$  tumor cells alone in one shoulder or co-injected with equal number of macrophages in the opposite shoulder (macrophages were conditioned for 24-36 hours with NBT2 cells in the transwell system) (n=3-4 mice per group, ANOVA p=0.03); **E)** Differential gene expression analysis between freshly obtained peritoneal macrophages versus macrophages co-cultured with NBT2 tumor cells for 36 hours, and NBT2 cells cultured with and without macrophages; **F)** Expression levels of MYC in protein lysates of NBT2 cells cultured with (in transwell system) and without macrophages analyzed by Western blotting (\*\* p<0.005).

**Figure 2.** MYC upregulation in human NBL associated with presence of macrophages. **A)** NBL tumor cells (LAN-6) co-cultured with macrophages polarized to M2 (4:1 ratio) showed significant increase in BrdU incorporation by flow cytometry and reduction in the percentage of cells in Sub-G phase (direct co-culture system with macrophages separated by anti-CD45 antibody); **B)** Two-fold increase in MYC protein expression in NBL cells was observed after 36 hours of co-culture of LAN-6 cells and M2 macrophages in the a transwell culture system; **C)** Pearson correlation analysis of MYC, MYCN, CCL2, and CD14 expression levels (log2 base) based on microarray data from 249 primary NBL tumors.

**Figure 3.** Evidence of macrophage-induced tumor proliferation independent of IL6. **A)** Left: IL6 gene expression levels comparing tumors versus WT adrenal glands in mice <12 weeks of age and >12 weeks of age (n=6 per group). Right: Plasma IL6 concentration, as measured by the Luminex assay, comparing tumor-bearing NB-Tag mice with clearly visible tumor by MRI ( $\geq 15$  weeks of age) to NB-Tag <15 weeks of age and their age-matched wild-type controls (WT n=19, NB-Tag n =20); **B-D)** Representative flow cytometry dot plots illustrating intracellular IL6 expression in circulating and tumor infiltrating CD45+ immune cell subsets, and tumor cells (CD45-) in a 24-week old NB-Tag mouse. Clear histograms represent isotype control antibodies. Monocytic lineage cells (CD11b+) are separated into F4/80 positive and negative populations; **E)** Tumor size measurement by MRI of NB-Tag and NB-Tag-IL6<sup>KO</sup> in mice of various ages (n=3-4 in each group), and representative MRI images (16-week old mice); **F)** BrdU incorporation comparing fold-change alteration in NBT2 cells directly co-cultured with WT macrophages (M $\phi$ ) to macrophages obtained from IL6<sup>KO</sup> animals. (\*  $p < 0.05$ ; \*\*  $p < 0.005$ ; \*\*\*  $p < 0.0005$ ).

**Figure 4.** STAT3 activation in tumor cells by macrophages does not require IL6. **A)** STAT3 expression and phosphorylated STAT3 (pSTAT3) levels over time in protein lysates of NBT2 cells cultured in transwells with and without macrophages. GAPDH is used as control for protein loading; **B)** STAT3 and pSTAT3 levels in NBT2 (murine) and CHLA255 (human) NBL cells at basal level, and in the presence of IL6 (10ng/ml) or sIL6R (25ng/ml) either alone or with macrophages previously conditioned with tumor cell media, and incubated with IgG (control) or species-specific neutralizing anti-IL6 (at 1 and 5  $\mu\text{g/ml}$ ); **C)** STAT3 expression and pSTAT3 levels assessed by Western blot analysis from protein lysates of adrenal glands of WT, NB-Tag, and NB-Tag-IL6<sup>KO</sup> mice (14-22 weeks of age); **D)** Examples of pSTAT3 IHC in tumors of NB-Tag and NB-Tag-IL6<sup>KO</sup> mice (inset: WT adrenal gland).

**Figure 5.** Macrophage-mediated proliferation of NBT2 cells is dependent on STAT3 phosphorylation. **A)** Differential effects of pSTAT3 inhibitors AZD1480 (5 $\mu\text{M}$ ) and Ruxolitinib (1 $\mu\text{M}$ ) on proliferation of NBT2 cells in co-culture with macrophages. Ruxolitinib showed significant inhibitory effect on both NBT2 cells alone and co-cultured with macrophages. Bar graphs represents S phase fold change measured as percent BrdU incorporation relative to no drug treatment; **B)** Expression of STAT3 and MYC, and pSTAT3 levels in protein lysates of NBT2 cells after 6 and 24 hours co-cultures with macrophages and in presence of AZD1480 (5 $\mu\text{M}$ ) or Ruxolitinib (1 $\mu\text{M}$ ); **C)** Tumor growth in mice injected with  $1 \times 10^6$  tumor cells alone in

one shoulder or co-injected with equal number of macrophages in the opposite shoulder (macrophages were conditioned for 24-36 hours with tumor cells in the transwell system). Animals were administered Ruxolitinib (60mg/kg) or drug vehicle by oral gavage twice daily for 3 weeks (ANOVA  $p < 0.005$  in untreated, and NS in treated group); **D**) Expression of STAT3 and pSTAT3 levels in protein lysates from tumors of NB-Tag or subcutaneous tumors (Sub-Q) treated with ruxolitinib for one week.

**Supplemental Figure 1.** *NB-Tag is an immunocompetent murine model of human high-risk MYCN non-amplified neuroblastomas.* **A**) Representative MRI images of tumor growth in the bilateral adrenal glands (white arrows) in NB-Tag mice at different ages; **B**) MRI image of liver metastasis in NB-Tag mice, typically evident around 22 weeks of age; **C**) Survival analysis of NB-Tag mice (n=16) shows 100% penetrance and lethality of the disease; **D**) H&E analysis of normal adrenal gland (left picture; C-Cortex; M-Medulla) and of tumor (right) showing undifferentiated small blue round tumor cells with high MKI; **E**) Immunohistochemical (IHC) staining for tyrosine hydroxylase (TH) of 12-week old NB-Tag tumor compared to normal adrenal gland (magnification x200); **F**) Reproducible growth pattern of NB-Tag tumors at 12, 14, and 16 weeks (n=5-6 mice per group) as assessed by MRI images and compared to the size of WT adrenal gland (n=7); **G**) Comparative Genomic Hybridization plot of chromosome 12 region, which harbors the mouse MYCN gene (red dashed lines), for a NB-Tag tumor. The Y-axis indicates the log<sub>2</sub> ratio for each probe set (log<sub>2</sub> ratio of 0 indicates normal copy number), a positive log<sub>2</sub> ratio indicates amplification, while a negative log<sub>2</sub> ratio indicates deletion; **H**) Principal Component analysis of microarray expression profiles comparing orthologous genes between NB-Tag tumors and human cancer samples, i.e., colon cancer (purple), breast cancer (green), pituitary adenoma (orange), neuroblastoma stage 4 MYCN non-amplified (blue), neuroblastoma stage 4 MYCN amplified (brown) and NB-Tag neuroblastoma tumors (red).

**Supplemental Figure 2.** **A**) NBL human tumor cells (CHLA255 or LAN5) co-cultured with human macrophages polarized to M2 (at a 4:1 ratio) showed significant increase in BrdU incorporation by flow cytometry and reduction in percentage of cells in Sub-G phase; **B**) The decrease in apoptosis rate (as measured by percent of cells in SubG1 phase) was not observed in human NBL cell lines due to the high viability (>98%) of NBT2 cells; **C**) IL6 levels as measured by ELISA in NBT2 cells cultured for 48 hours alone or with peritoneal macrophages collected from WT or IL6<sup>KO</sup> mice.

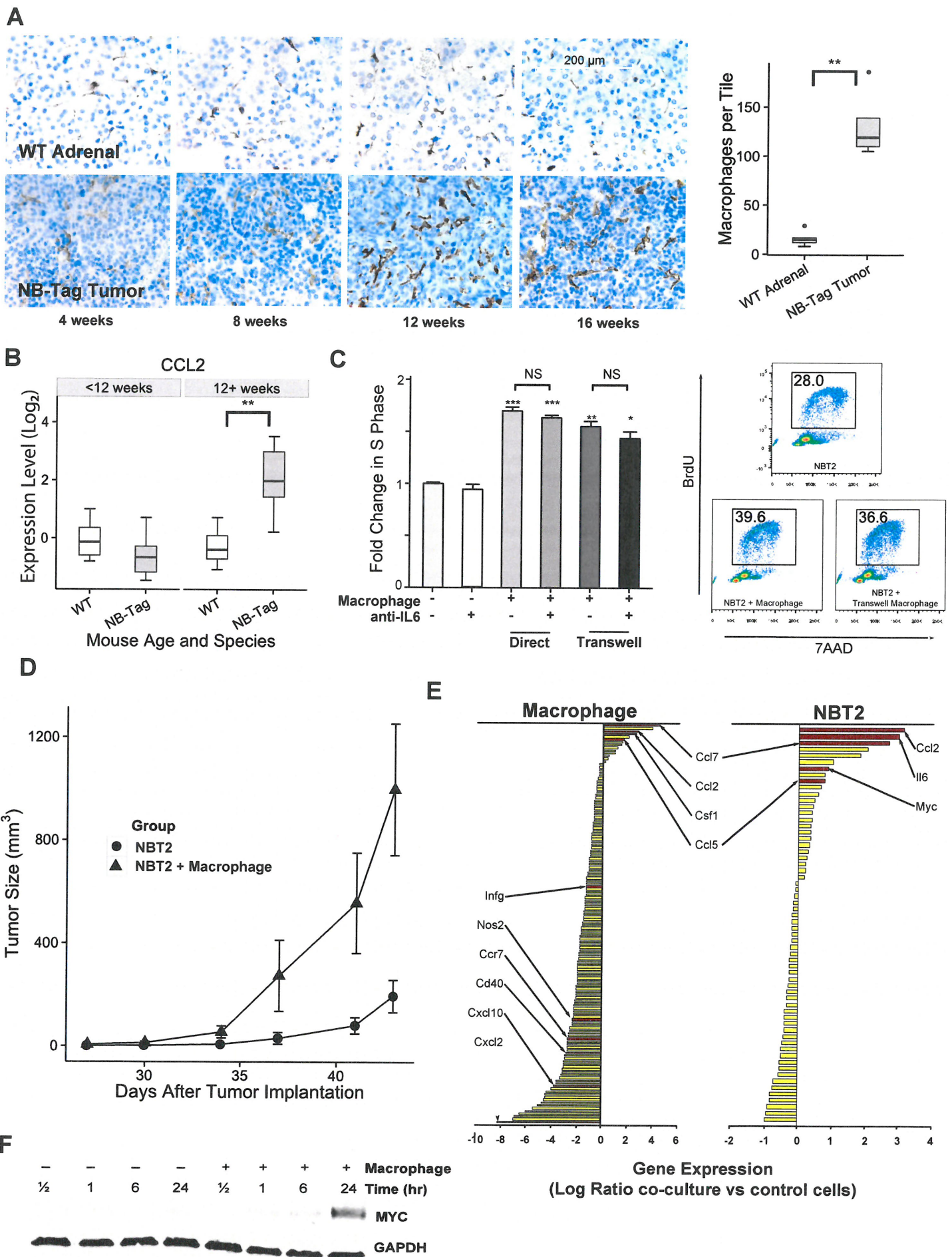
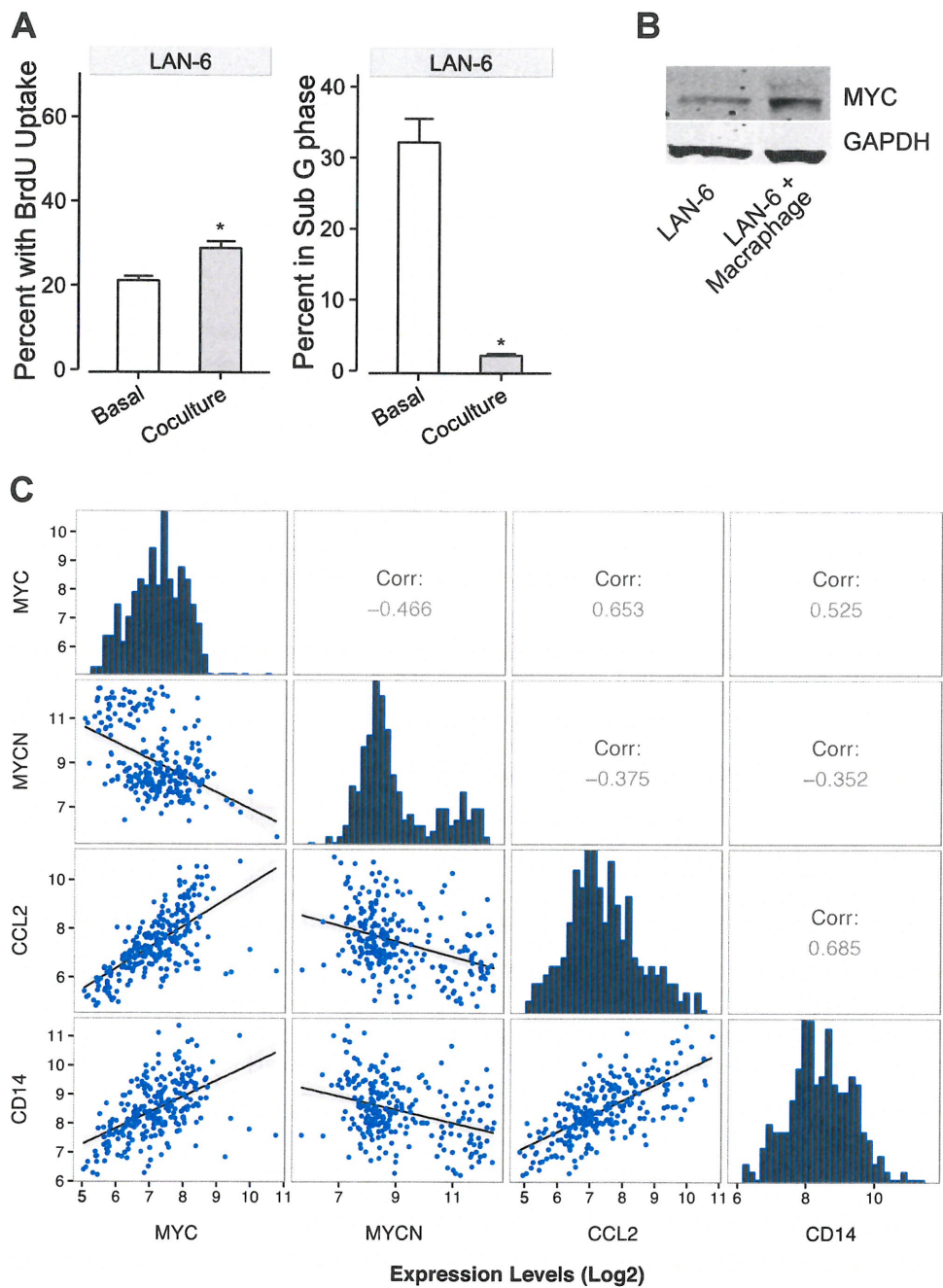
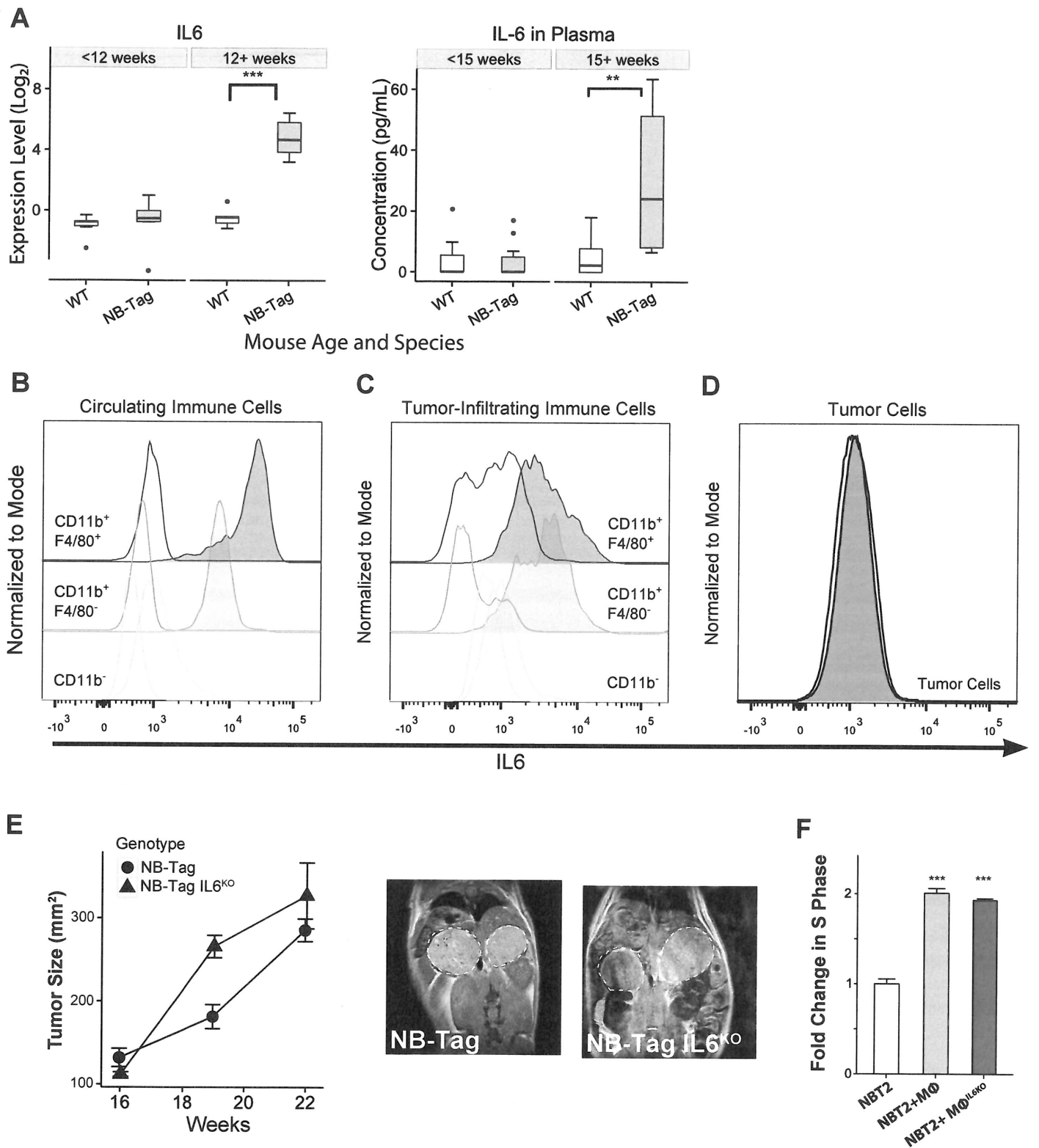


Figure 1



**Figure 2**



**Figure 3**

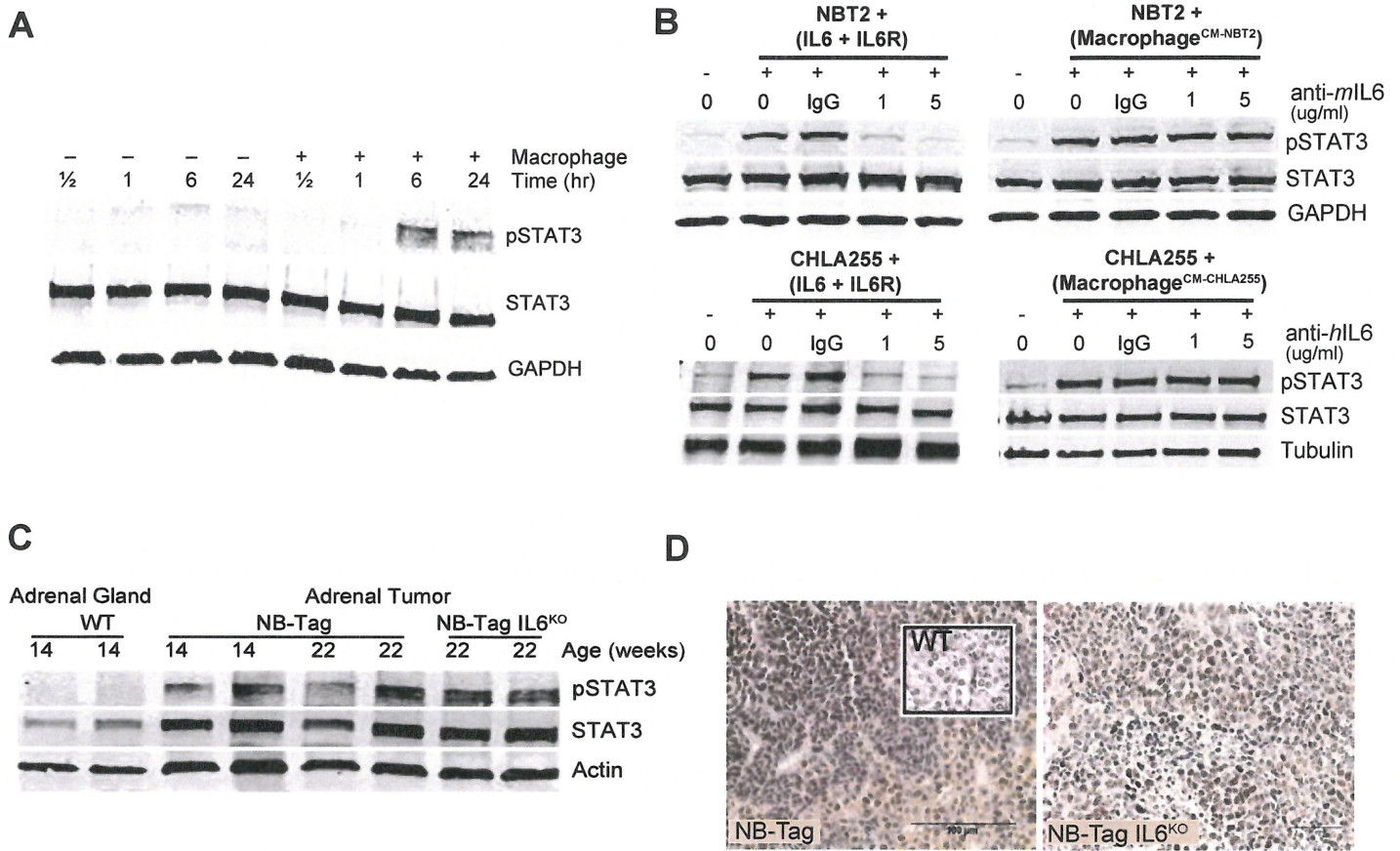
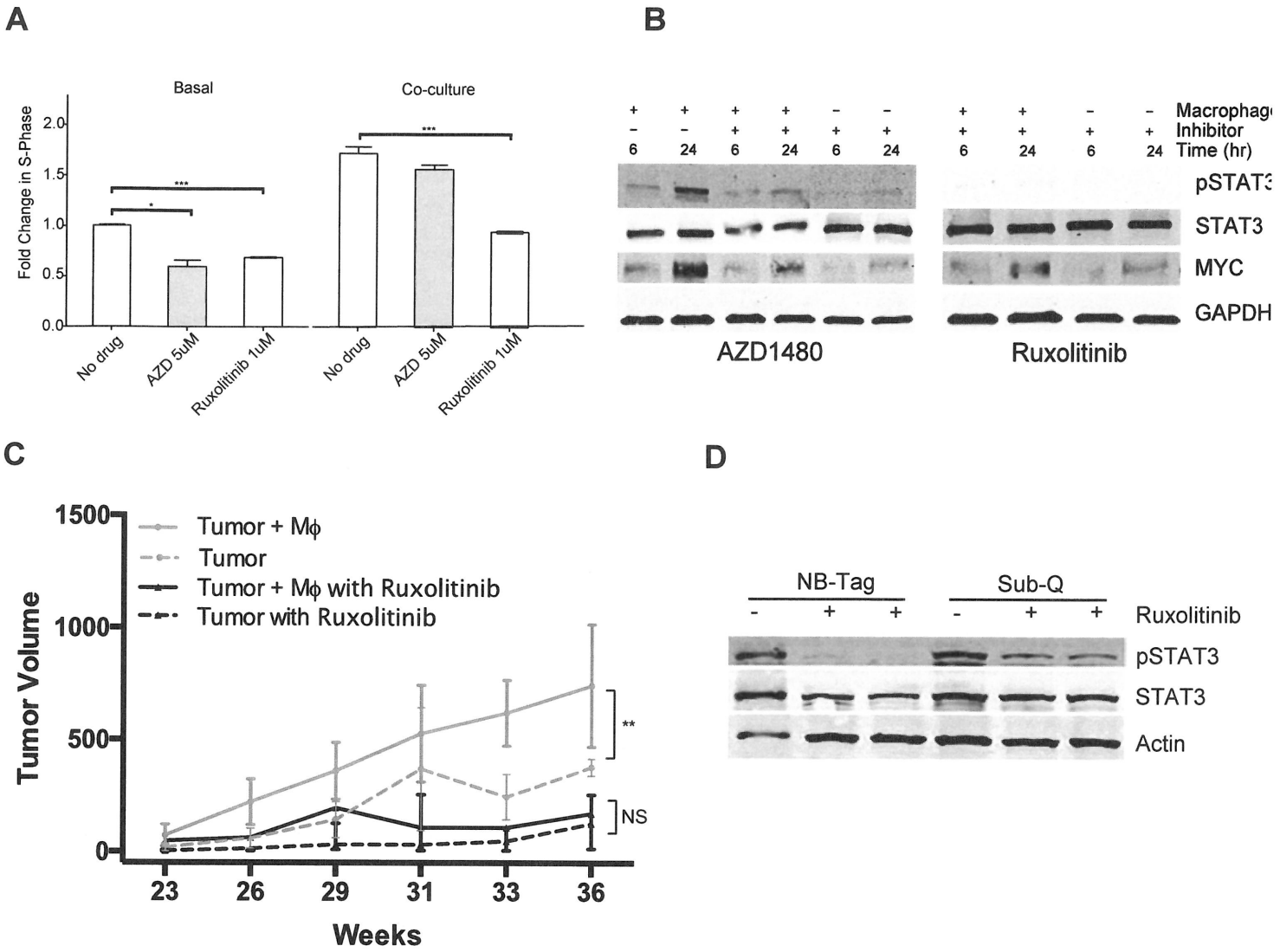
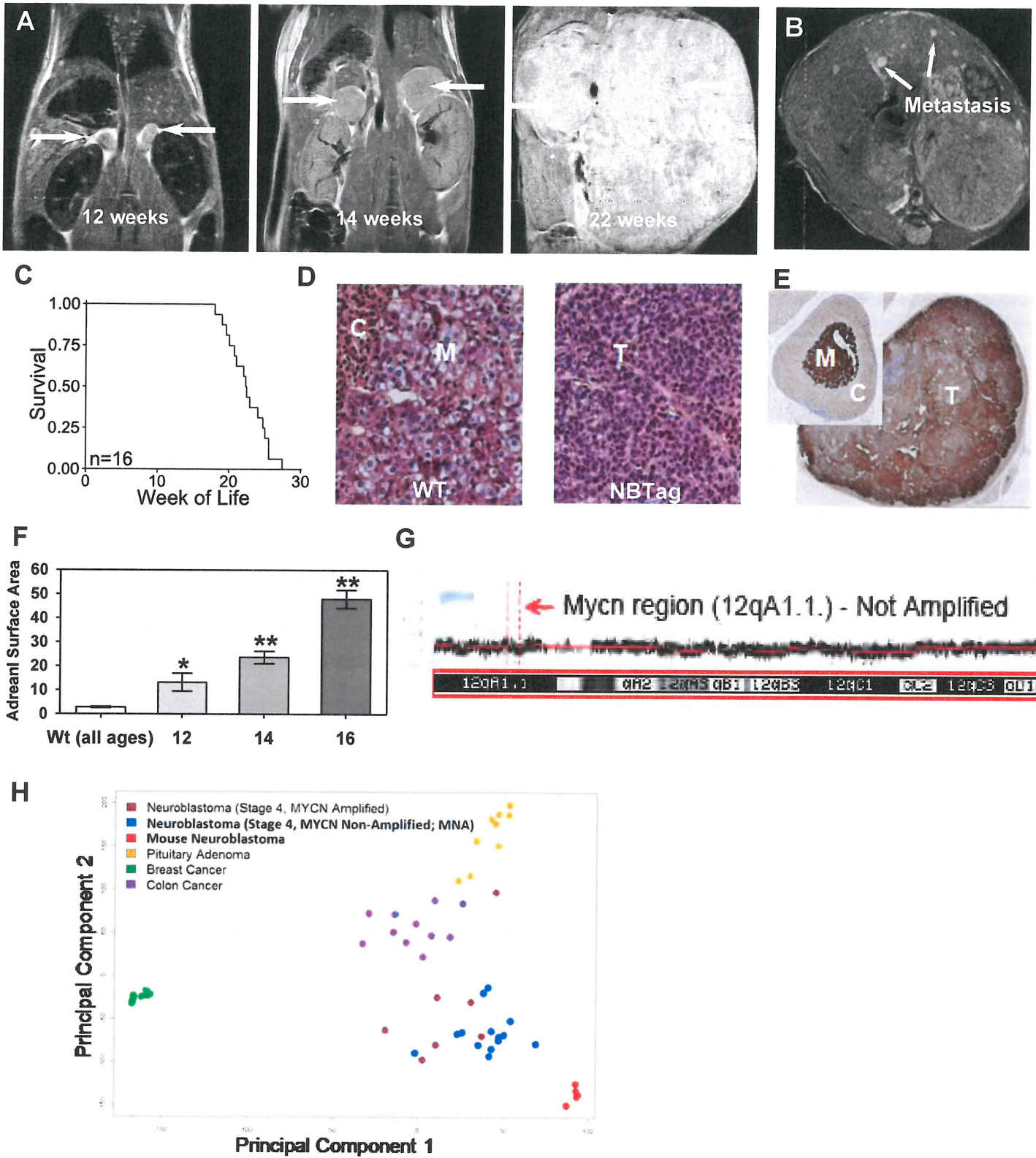


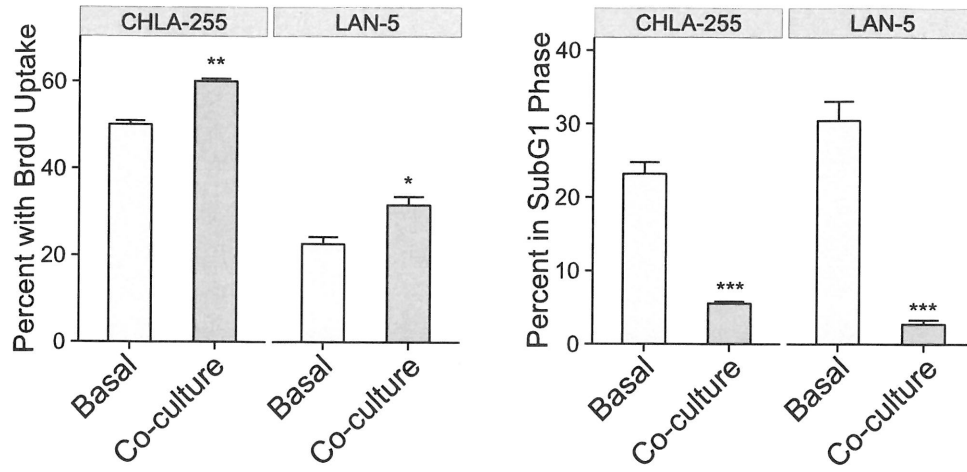
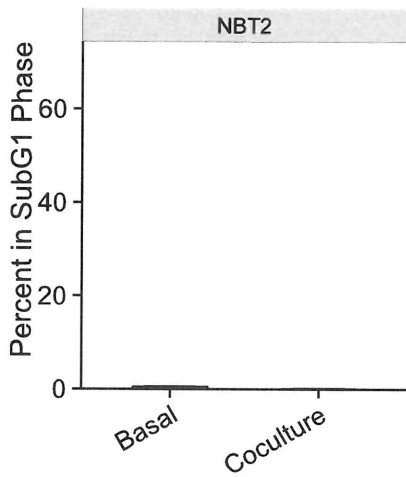
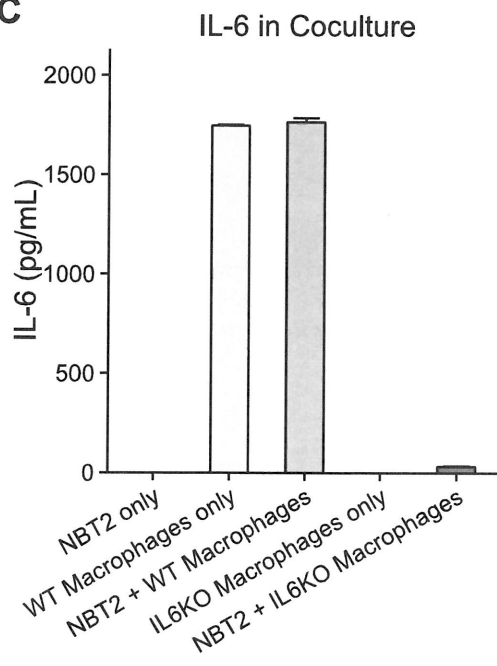
Figure 4



**Figure 5**



Supplemental Figure 1

**A****B****C****Supplemental Figure 2**